UNIVERSITA' DEGLI STUDI DI NAPOLI
FEDERICO II

FACOLTA' DI SCIENZE MATEMATICHE, FISICHE E NATURALI
DOTTORATO DI RICERCA IN SCIENZE CHIMICHE
XX CICLO

STRUCTURAL STUDY OF LIPOPOLYSACCHARIDES AND THEIR INTERACTION WITH CAPSULAR POLYSACCHARIDES RESPONSIBLE FOR THE VIRULENCE OF GRAM-NEGATIVE BACTERIA

GIUSEPPINA PIERETTI

Tutore
Ch.ma Prof.ssa Maria Michela Corsaro

Relatore
Ch.mo Prof. Pietro Pucci

Coordinatore
Ch.mo Prof. Aldo Vitagliano

Anno accademico 2006-2007

INDEX

Achronims.

AcOH: acetic acid.	Gal*p*NAcA: *N*-acetyl galacturonopyranos acid
Ag_2CO_3: argentum carbonate.	GC-MS: gas chromatography-mass spectrometry
CH_3CN: acetonitril	GlcN: glucosamine
COSY: correlation spectroscopy	GlcNAc: *N*-acetylglucosamine
CPS: capsular polysaccharides	Glc*p*A: glucuronopyranosyl acid.
CSD: capillary skimmer dissociation	GPG:1,2-diacylglycero-3-phosphoryl-glycerol
DAEC: diffusely adherent	HF: hydrofluoric acid
DOC: sodium deoxycholate	HMBC: heteronuclear multibond correlation
DPG: cardiolipin.	HPAEC: high pressure anion exchange chromatography
DQF-COSY: double quantum filtered COSY	HSQC-DEPT: heteronuclear single quantum correlation. with distortionless enhancement by polarization transfer
EAEC: enteroaggregative	IM: inner membrane
EDTA: ethylenediaminetetraacetic acid.	Ino: inositole
ESI: electrospray ionization	I. S.: internal standard
EHEC: enterohaemorrhagic	Kdo: 3-deoxy-D-*manno*-oct-2-ulosonic acid
EIEC: enteroinvasive	KOH: potassium hydroxide
E.L.I.S.A.: enzyme linked immuno-sorbent assay	LBP: LPS binding protein
EPEC: enteropathogenic	L,D-Hep: L-*glicero*-D-*manno*-heptose
ETC**:** extracellular toxic complex.	LPS: lipopolysaccharide
ETEC: enterotoxigenic	MALDI: matrix assisted laser desorption ionization
FT-ICR MS: Fourier Transform Ion Cyclotron Resonance Mass Spectrometry	MS: mass spectrometry
Gal: galactose	NMR: nuclear magnetic resonance

GalA: galacturonic acid	
NOESY: nuclear Overhauser effect spectroscopy.	QuiN: quinovosamine
orf10: open reading frame 10	Rha: rhamnose
OM: outer membrane	SDS: sodium dodecyl sulfate
OS: oligosaccharide	SDS-PAGE: SDS-polyacrylamide gel electrphoresis.
PEA: 1,2 diacylglycero-3-phosphoryl ethanolamine	TFA: trifluoroacetic acid.
PCP: phenol, chloroform, petroleum ether	THF: tetrahydrofuran
PG: peptidoglycan	TLR4: toll-like receptor 4.
PS: polysaccharide.	TOCSY: total correlation spectroscopy.
PSD: post source decay	TOF: time of flight.
PW: phenol-water	TRIS: $C_4H_{11}NO_3$

Abstract.

Several human pathogens belong to Gram-negative bacteria. They possess a cell wall, whose components enable them to adhere to the host cell surface and to colonize and infect the organism.

Lipopolysaccharides (LPS) constitute 75% of the Gram-negative bacteria outer membrane. Their structure can be divided in three regions: Lipid A, core oligosaccharide and O-specific chain (Mayer *et al*. 1989; Raetz and Whitfield, 2002; Yethon and Whitfield, 2001), which show differences in their structure and biosynthesis pathways (Raetz and Whitfield, 2002; Yethon and Whitfield, 2001). The lipid A constitutes the glycolipid portion of the LPS and it anchors the molecule in the OM. Its highly conserved structure is recognized by TLR4, an ancient receptor of the innate immune system. This is the first step of the host organism innate immune response against Gram-negative bacteria. The core oligosaccharide can be divided in two different regions: the inner and the outer core. The former one, spatially closer to the lipid A, is more conserved and comprises peculiar sugars such as Kdo (3-deoxy-D-*manno*-oct-2-ulosonic acid) and L,D-Hep (L-*glicero*-D-*manno*-heptose). The outer core usually contains more common monosaccharides and shows higher heterogeneity. The O-specific chain polysaccharide (O-antigen) is the most variable portion of the LPS. It can be an homopolymer, formed by a repeating monosaccharide or an heteropolymer, composed by a variable number (up to 40) of repeating units, each one containing up to 10 sugars.

One of the most important virulence determinant of Gram-negative bacteria is the capsular polysaccharide (CPS). It encompasses the whole cell protecting the bacterium from the innate immune response. At the same time, together with the O-antigen, it is able to elicit the type-specific protective immune response. Nevertheless some particularly virulent strains of *E. coli* possess K1 CPS, which is not immunogenic and then able to elude the adaptative immune response.

Very little is known about the mechanism of capsule association to the cell surface. As in several pathogen bacteria the capsule has been described as the major virulence determinant, we started to study the mechanism of capsule association to the cell surface, which is the mandatory starting point for the development of new antibiotics.

The work borned in collaboration with the group of professors Juan Tomàs and Miguel Reguè, belonging to the Microbiology Department of Barcelona University. In particular, my work aimed at the elucidation, on chemical basis, of the genes involved in the core oligosaccharide biosynthesis of LPS from *Klebsiella pneumoniae* and *Escherichia coli*, and their involvement in the interaction between the core oligosaccharide and the capsule.

The structures of LPS from several mutants from *Klebsiella pneumoniae* and *Escherichia coli*, which showed a decrease in the capsule association, were analysed.

Klebsiella pneumonieae is an important nosocomial opportunistic pathogen, of which, almost all clinical isolate are capsulate. Recently it has been demonstrated that in *Klebsiella pneumoniae* 52145 strain the K2 CPS is associated to the cell surface through an ionic interaction, between the acidic residues present both in the CPS and in the LPS core region, mediated by divalent cations (Fresno *et al.*, 2006).

Despite the presence of two GalA residues in the core region (Reguè et al., 2005; Vinogradov *et al.*, 2001), only one Galacturonosyl transferase was identified (WabG; Izquierdo *et al*., 2003). Since it was observed a decrease in the cell bound capsule in a mutant lacking the unknown *orf10* gene, we hypothesized that it could encode a second GalA transferase. In order to prove it, the structure of the core oligosaccharide of the LPS from the Δ*waaL* Δ*orf10* double mutant was elucidated. The structure was inferred by MS and NMR analysis of the products obtained by both mild acid and strong alkaline degradation of the LPS.

The core oligosaccharide belonging to the Δ*waaL*-Δ*orf10* mutant lacked in the *t*-GalA (terminal-galacturonic acid) residue respect to the wild type core structure, confirming that *orf10* gene encodes for a galacturonosyltransferase (Fresno *et al*., 2007).

Moreover, transmission electron microscopy experiments, carried out in Spanish laboratories showed a drastic reduction in the amount of cell-bound capsule for the *Klebsiella pneumoniae* 52145 Δ*wabO* mutant in comparison to wild type cells. A similar result was obtained using the double mutant Δ*waaL*-Δ*wabO* cells versus Δ*waaL*. As expected, introduction of *wabO* gene restored wild type levels of cell surface associated K2 capsule.

Confirmation of the presence of an ionic interaction between the core oligosaccharide and the K2 capsular polysaccharide in *Klebsiella pneumoniae* 52145 was obtained after co-extraction of the two components and their separation on a Sephacryl S-200 column in denaturing conditions, as previously reported (Fresno *et al*., 2006).

YibD protein of *E. coli* showed high similarity with the WabO and contained a conserved domain, typically observed in glycosyltransferases. These data suggested that, even if the *yibD* gene is located upstream of the *waa* cluster of the genes involved in the core biosynthesis of *E. coli*, YibD could be involved in the transfer of a glycosidic residue to the core oligosaccharide. Moreover a mutant, which presented deletion in the *yibD* gene, showed a decrease in the amount of capsule attached to the cell surface.

On the basis of these data, we decided to look for structural modification in the core oligosaccharide in the *yibD* mutant of *E. coli*.

In order to simplify this analysis two mutants were constructed for *E. coli* O16:K1 (K-12 core type). The Δ*waaL* mutant and the double non-polar Δ*waaL*-Δ*yibD* mutants. Since the function of the *waaL* gene is known to be involved in the O-antigen linkage to the core-lipid A, both the mutants possessed a rough type LPS.

The *O*-deacylated LPS (LPS-OH) were analysed by ESI mass spectrometry. The analysis of the spectra suggested that the difference between the LPS-OH$_{waaL}$ and LPS-OH$_{waaL\text{-}yibD}$ resides in the inner core and in particular in the third Kdo residue, which was absent in the LPS$_{waaL\text{-}yibD}$. To confirm these results, ESI-MS analysis was performed on mutants with an high truncated core too (LPS$_{waaF}$ and LPS$_{waaF\text{-}yibD}$).

Thus we determined the function of the *yibD* gene which resulted to be responsible of the transfer of the third Kdo residue in the inner core of *E. coli* O16:K1 (K-12 core type). The lack of the negatively charged Kdo residue leads to a decrease in the cell bound capsule. These data suggested that also in this case, as for *Klebsiella pneumoniae*, an ionic interaction could contribute to the association of the negatively charged K-1 CPS to the cell wall. Nevertheless the small amount of CPS produced by this strain of *E. coli* made not possible to directly prove it.

During the second year of my PhD, in collaboration with the professor O. Holst from the Borstel Research Centre in Germany, the structure of the LPS core from the haloalkaliphilic bacterium *Halomonas pantelleriensis* was investigated.

Several haloalkaliphilic bacteria are able to thrive in alkaline hyper-saline environments thanks to their ability to maintain a lower salt concentration and a lower pH inside the cell. The mechanisms on the basis of this phenomenon are far from being elucidated. The main research in this field is aimed at the study of the cell wall components and differences in the outer membrane lipid composition have been found.

The lipopolysaccharides are supposed to play a crucial role in the outer membrane permeability properties. Nevertheless, few data are available about LPS structure from haloalkaliphilic microorganisms (de Castro *et al.*, 2003), even if the determination of the LPS primary structure is the mandatory starting point for the comprehension of the biological role played by these molecules.

Recently it was determined the O-chain repeating unit structure of the LPS of *Halomonas pantelleriensis* which is constituted by the highly charged tetrasaccharidic repeating unit →4)-β-D-Glc*p*A-(1→4)-α-D-Gal*p*NAcA-(1→3)-β-L-Qui*p*NAc-(1→2)-β-D-[4-*O*-(*S*)-1-carboxyethyl]-Glc*p*A-(1→ (Corsaro *et al.*, 2006).

The core structure has been elucidated by using ESI ICR-FT MS and NMR spectroscopy (Pieretti *et al*., 2007).

The products obtained after both mild acid hydrolysis and strong alkaline treatment of the LPS were analyzed and this allowed the identification of two main core oligosaccharides for *Halomonas pantelleriensis*, which differ for one heptose unit. Moreover, the presence of 4-linked uronic acids in the O-chain polysaccharide allowed the isolation of a tridecasaccharide containing the full core oligosaccharide and two residues belonging to the O-chain repeating unit, which revealed the linkage between the core region and the O-chain, allowing the identification of the biological O-chain repeating unit.

Chapter 1

Introduction

1.1 Bacteria.

Bacteria are unicellular microorganisms found in every habitat on Earth, growing in soil, acidic hot springs, radioactive waste, seawater, and deep in the Earth's crust. Bacteria are prokaryotes and, unlike animal cells and other eukaryotes, do not contain a nucleus and rarely harbor membrane-bound organelles. Prokaryotic cells are about 10 times smaller than eukaryotic cells and are typically 0.5–5.0 micrometers in length. Their small size is very important because it confers a large surface area-to-volume ratio allowing a rapid uptake and intracellular distribution of nutrients and excretion of wastes.

Bacterial cells display a wide diversity of shapes and sizes (Figure 1.1), generally characteristic of a given bacterial species. Most bacterial species are either spherical, called cocci or rod-shaped, called bacilli. Some rod-shaped bacteria, called vibrio, are slightly curved or comma-shaped; others, can be spiral-shaped, called spirilla, or tightly coiled, called spirochetes. A small number of species even have tetrahedral or cuboidal shapes. This wide variety of shapes is determined by the bacterial cell wall and cytoskeleton, and is important because it can influence the ability of bacteria to acquire nutrients, attach to surfaces, swim through liquids and escape from predators (Cabeen and Jacobs-Wagner, 2005; Young, 2006).

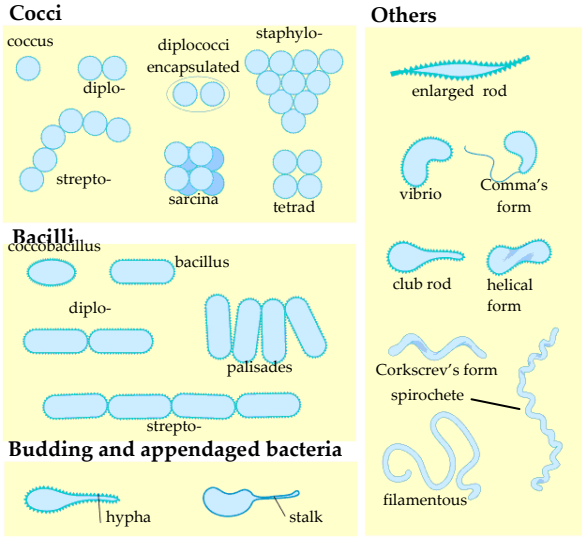

Fig. 1.1. Bacteria shape.

Bacteria are grouped in several families, which include various genera, on the basis of cell structure, cellular metabolism or differences in cell components, such as DNA, fatty acids, pigments, antigens and quinones. Among a genus, several species can be found, which, in turn, comprise different strains.

Sometimes, closely related bacteria can show differences in morphology and metabolism, due to lateral gene transfer. To overcome uncertainties, modern bacterial classification emphasizes molecular systematics, using genetic techniques such as guanine-cytosine ratio determination, genome-genome hybridization, as well as sequencing conserved genes, such as the 16s rDNA gene.

Bacteria are classified in two broad groups, **Gram-negative** and **Gram-positive** bacteria depending on their response to a colorimetric assay developed by Christian Gram in 1884. The different reaction in the Gram assay reflects the structural diversity and the different behaviours of bacteria against several antibiotics. The main

difference found between Gram-negative and Gram-positive bacteria regards the cell envelope and, in particular, the size of the peptidoglycan (PG) layer, that is much thicker in Gram-positive bacteria. Furthermore, Gram-negative bacteria possess an outer membrane, external to their peptidoglycan layer, that is not present in their Gram-positive counterparts (Beveridge and Graham, 1991). In contrast to the thickness of the PG layer, Gram-negative bacteria show much more resistance against antibacterial compounds. The explanation of this phenomenon has been found in the porosity of the PG layer that, despite its mechanical resistance, is not able to resist the diffusion of small molecules like antibiotics (Demchick and Koch, 1996; Pink *et al.*, 2000).

This means that Gram-negative bacteria Outer Membrane is more selective in the diffusion of molecules from the environment into the cell.

Among Gram-negative bacteria, the *Enterobacteriaceae* constitute a large family, which comprises many familiar pathogens such as *Escherichia coli* and *Klebsiella pneumoniae.* Members of this family are generally rod-shaped. Many of them are commonly found in the gut flora of humans and other animals, while others are found in water or soil or are parasites on a variety of different animals and plants.

Klebsiella pneumoniae.

Klebsiella pneumoniae is a non motile and usually capsulated Gram-negative bacillus belonging to *Enterobacteriaceae* family. It was isolated for the first time in the XIX century from the german bacteriologist Edwin Klebs. *Klebsiella* species have been isolated from environment (water, soil, industrial effluent) as well as from healthy humans and animals. Its ability to cause diseases was first recognised in 1882 by Frideländer, who isolated *Klebsiella pneumoniae* from the lungs of patients with pneumonia.

Actually, *Klebsiella pneumonieae* is an important nosocomial opportunistic pathogen (Williams and Tomàs, 1990) causing infections that may occur at almost all body sites, with highest incidence in the urinary and respiratory tracts. It is second only to *Escherichia coli* as the most common cause of Gram-negative sepsis. The main populations at risk are neonates, immunocompromised hosts, and patients predisposed by surgery, diabetes, malignancy, etc.

Almost all clinical isolate from *Klebsiella pneumoniae* are capsulate and although not all capsulate strains are virulent, the K-antigen has long been considered as the major virulence determinant in *Klebsiella pneumoniae.* In particular it has been reported that various strains of *Klebsiella pneumoniae* are able to produce an extracellular toxic complex (ETC) that is responsible for virulence. This complex is reported to be composed of 63% of capsular polysaccharide (CPS), 30% of LPS and 7% of proteins. It was demonstrated that the ETC toxicity depends on the LPS, but this one, alone, is decidely less toxic than the entire complex (Straus, 1987).

Escherichia coli.

Escherichia coli was discovered in 1885 by Theodor Escherich, a German pediatrician and bacteriologist. It is the predominant facultative anaerobe of the gut flora. *E. coli* is able to colonizes the infant gastro-intestinal tract within hours after birth. Afterwards *E. coli* and the host organism derive mutual benefit for the rest of the host's life. In fact *E. coli* assists with waste processing, vitamin K production, and food absorption.

Nevetheless, certain strains have acquired virulence factors and may cause a variety of infections in humans and in animals. There are three clinical syndromes caused by *E. coli*: (i) sepsis/meningitis; (ii) urinary tract infection and (iii) diarrhoea.

Among the *E. coli* causing intestinal diseases, there are six well-described "pathotypes": enteropathogenic (EPEC), enterotoxigenic (ETEC), enteroinvasive (EIEC), enterohaemorrhagic (EHEC), enteroaggregative (EAEC) and diffusely adherent (DAEC) *E. coli*. These pathotypes have virulence attributes that help bacteria to cause diseases by different mechanisms (Nataro and Kaper, 1998; Kaper et al., 2004).

1.2 Gram-negative bacteria cell envelope.

Bacteria possess a cell envelope that protects them from the environment and from its potential harmful influences (Figure 1.2). Moreover it enables the bacteria to transport substances and informations from inside to outside and to communicate with the environment.

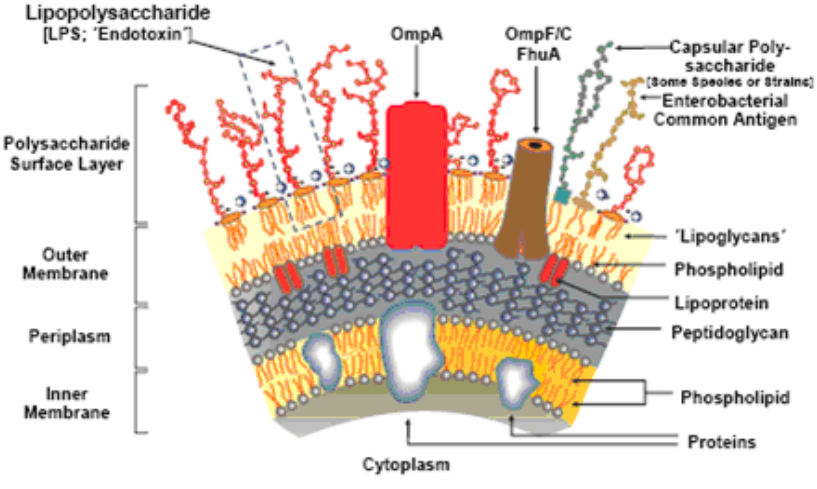

Fig 1.2. Gram negative bacteria cell envelope

The cell envelope of Gram-negative bacteria is constituted by a cytoplasmic or inner membrane (IM), which is a phospholipid bilayer, and an asymmetrical outer membrane (OM), which holds phospholipids and lipopolysaccharides in its inner and

outer leaflet, respectively. Moreover, the OM comprises several kind of proteins with different functions. These proteins, together with lipopolysaccharides, are responsible of the particular membrane permeability properties.

Periplasm, which comprises peptidoglycan and lipoproteins, is located between the inner and the outer membranes.

1.3 Lipopolysaccharide: structure and biosynthesis.

In Gram-negative bacteria, lipopolysaccharides (LPS) constitute 75% of the outer membrane. LPS molecules can be divided in three regions (Figure 1.3): lipid A, core oligosaccharide and O-specific chain (Mayer *et al*. 1989; Raetz and Whitfield, 2002; Yethon and Whitfield, 2001). The three regions are different in structure, with highly characteristic constituents and in their biosynthetic pathways (Raetz and Whitfield, 2002; Yethon and Whitfield, 2001).

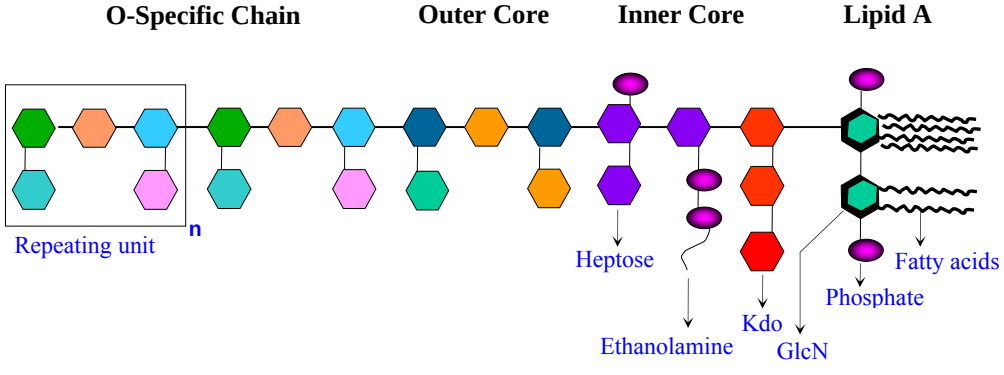

Fig 1.3. LPS structure.

Due to the presence of a relative high number of saturated fatty acids in the lipid A and to the formation of salt bridges between different LPS molecules, mediated by divalent cations, lipopolysaccharides confer rigidity to the OM. This give an explanation to the resistance of the Gram-negative bacteria to a series of antibiotics.

1.3.1 The lipid A.

1.3.1.1 Structure.

Lipid A is the glycolipid portion of the LPS and anchors the molecule in the OM (Figure 1.4). Its structure is highly conserved and is constituted by a 1,4′ bis-phosphorylated β-1,6-D-glucosaminyl-D-glucosamine disaccharide. Position 2, 2′ and 3, 3′ of the glucosamine residues are substituted by primary fatty acids, usually hydroxylated, linked as amide or ester respectively. Secondary substitution by α-hydroxylated or saturated fatty acid chains can occur. The fatty acid chains can vary in length from 10 to 20 carbon atoms (Mayer *et al.*, 1989).

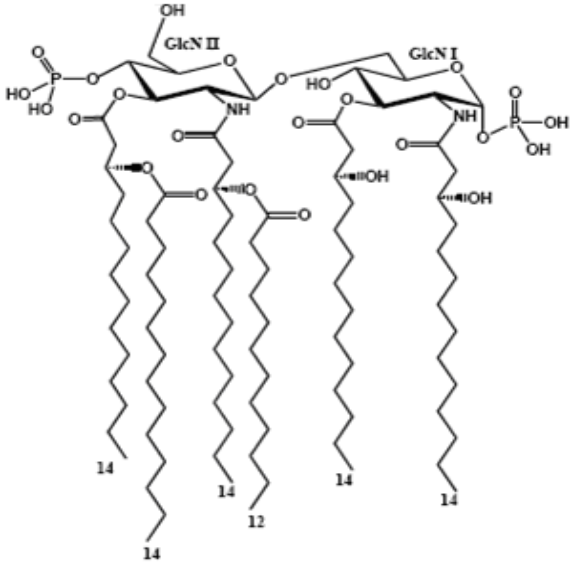

Fig. 1.4. Lipid A structure from *E. coli*.

1.3.1.2 Biosynthesis.

The three regions of the LPS are synthesised through different biosynthetical pathways. The mechanism for lipid A biosynthesis (Figure 1.5) starts from UDP-GlcNAc and the first step consists of one fatty acid addition at position O-3 of the GlcNAc catalyzed by the LpxA enzyme. Then a step of de-*N*-acetylation occurs, which

is catalyzed by the LpxC de-acetylase. Afterwards a second fatty acid chain is transferred to the free nitrogen at position 2. Some UDP-2,3-diacyl-glucosamine molecules are cleaved at the pyrophosphate linkage giving the lipid X, which links its precursor molecule to form a tetraacyl-disaccharide, the precursor of the lipid IV_A (Raetz and Whitfield, 2002; Yethon and Whitfield, 2001; Trent, 2004).

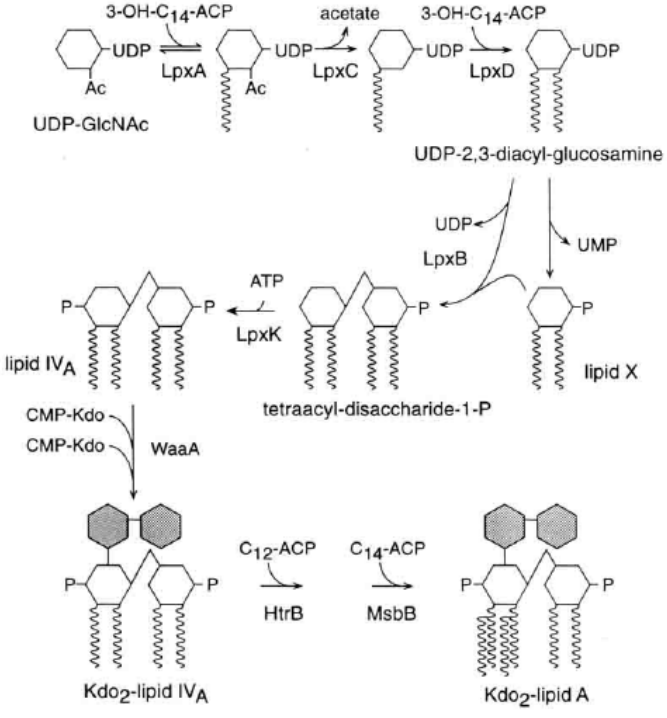

Fig.1.5. Scheme for the biosynthesis of the lipid A in *E. coli*

In *E. coli* the transfer of the Kdo residue to the lipid A is catalyzed by the bifunctional WaaA glycosyltransferase before the completion of the lipid A biosynthesis. The lipid A is known as the real bacterial endotoxin. It has been reported that the synthetic *E. coli* lipid A itself causes a spectrum of effects, when injected into animals, similar to those provoked by the whole LPS.

1.3.2 The core oligosaccharide.

1.3.2.1 Structure.

The core oligosaccharide can be divided in two different regions: the inner and the outer core. The former one, spatially closer to the lipid A, is more conserved and comprises peculiar sugars such as Kdo (3-deoxy-D-*manno*-oct-2-ulosonic acid) and L,D-Hep (L-*glicero*-D-*manno*-heptose). The outer core usually contains more common monosaccharides and shows higher heterogeneity. This is not surprising since this region is more exposed to the environment and has to evade recognition by the host (Mayer *et al*. 1989; Yethon and Whitfield, 2001).

1.3.2.2 Core structure in *Enterobacteriaceae*.

Bacteria belonging to the *Enterobacteriaceae* family share the same inner core structural element (Figure1.6). It comprises two Kdo residues linked through an α-(2→4) linkage (Frirdich and Whitfield, 2005). The reducing residue of the disaccharide is linked to the lipid A and substituted at position O-5 by a trisaccharide, which in turn is constituted by three heptose units.

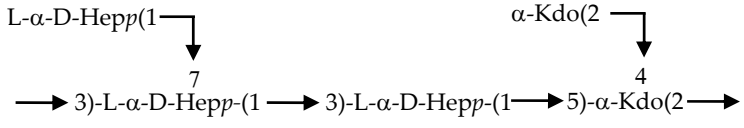

Fig. 1.6. Common structural element in the inner core of *Enterobacteriaceae*.

The presence of non stoichiometric phosphoryl substituents can be found. This yield to heterogeneous extracts. In many cases, only the structure of the predominant carbohydrate backbone is known for a given core oligosaccharide and the extent of phosphorylation is unknown. This is a reflection of the difficulties encountered in structural analysis.

Five core types from *E. coli* are currently known (Figure 1.7), and all of them have been found among commensal isolates (Amor *et al.*, 2000). R1 core type dominates among strains that cause extra-intestinal infections, while the R3 core type has been found in verotoxigenic isolates. The differences between the five core types of *E. coli* are located in the outer core region and in the non stoichiometric substitutions of the inner core (Figure 1.7a, 1.7b). In *E. coli*, in fact, the inner core residues can be substituted by charged groups such as phosphates, pyrophosphates, phosphoryl-ethanolamine or pyrophosphoryl-ethanolamine. Moreover, rhamnose (Rha), galactose (Gal), *N*-acetylglucosamine (GlcNAc) and glucosamine (GlcN) can also be found. For instance, *E. coli* K-12 core type usually contains a Rha residue and a third Kdo unit linked at positions O-4 and O-5 of the second Kdo, respectively.

Only two core types have been characterized in *Klebsiella pneumoniae* LPS (Vinogradov *et al.*, 2001; Vinogradov *et al.*, 2002; Regue *et al.*, 2005 (b)). Both lack phosphoryl substituents. But, alternatively, they possess charged monosaccharides in the outer core. The two core types share the inner core structure and the outer-core-proximal disaccharide GlcN-(1→4)-GalA. In core type 1, the glucosamine residue is substituted at position O-6 by the disaccharide α-Hep*p*-(1→4)-α-Kdo-(2→ or by a Kdo (Vinogradov *et al.*, 2001). In core type 2, the glucosamine is substituted at position O-4 by the disaccharide α-Glc*p*-(1→6)-β-Glc*p*-(1→ (Regue *et al.*, 2005 (b); Figure 1.8).

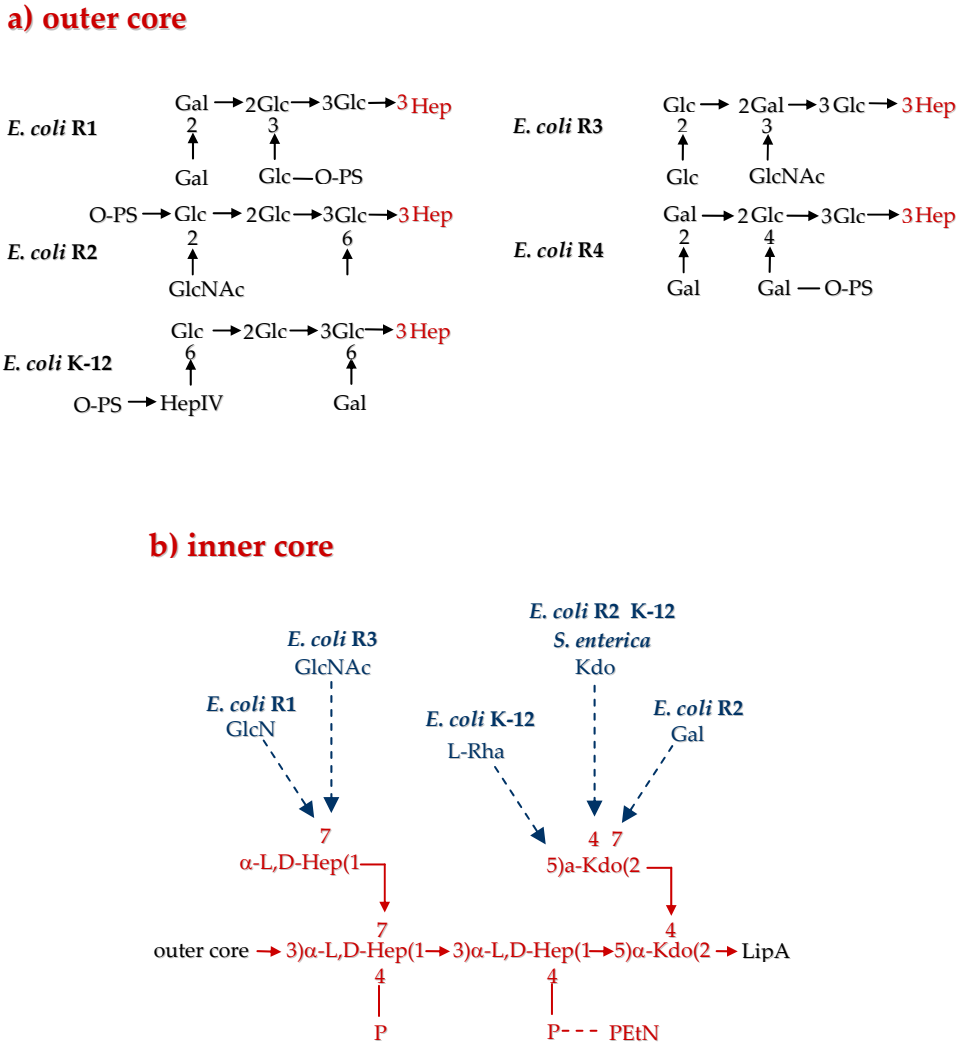

Fig. 1.7 a) Structures of core oligosaccharides from *E. coli*. The outer cores are shown, together with one heptose residue of the inner core. The ligation sites for O polysaccharides (O-PS) are indicated where known. **b)** Conserved base structure of the inner core. Type-specific nonstoichiometric additions to the inner core are identified by dotted lines.

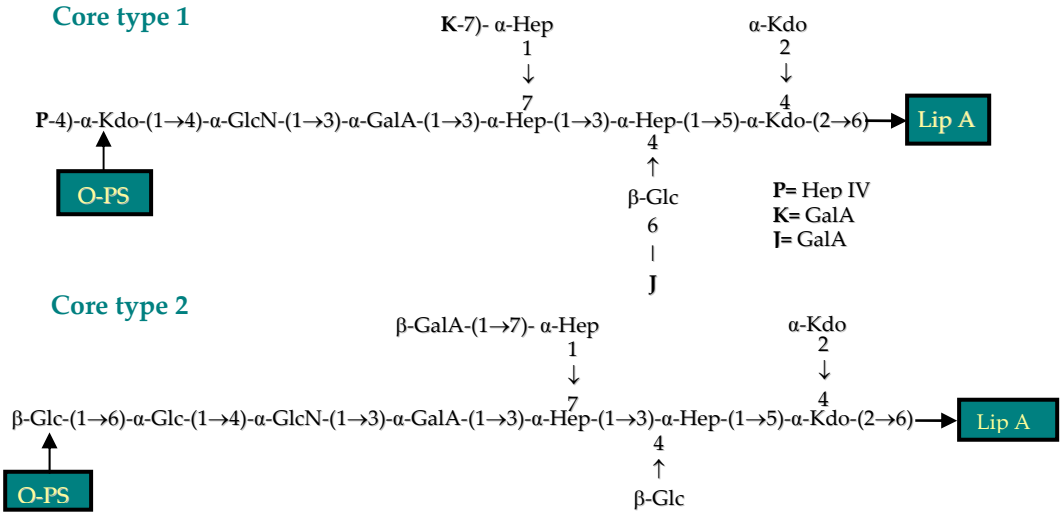

Fig. 1.8 Structure of the two currently known core oligosaccharides from *Klebsiella pneumoniae*.

1.3.2.3 Biosynthesis and genetic organization.

Once the biosynthesis of the Kdo_2-lipid A is completed the molecule serves as acceptor on which the core oligosaccharide is assembled. Core biosynthesis occurs via sequential glycosyl transfers, which are catalysed by specific glycosyltransferases. (Raetz and Whitfield, 2002; Yethon and Whitfield, 2001)

In the *Enterobacteriaceae* family, the genes responsible for the core oligosaccharide biosynthesis are generally located in the *waa* cluster. It is divided in different operons, each one identified by the first gene of the transcriptional unit.

1.3.2.4 The *waa* cluster in *Enterobacteriaceae*.

The *waa* cluster in Enterobacteria can be usually divided in three operons: the *gmhD (hldD)*, the *waaQ* and the *waaA* operons.

In *E. coli*, genes present in the *gmhD* operon are involved in the inner core biosynthesis. In particular, the *gmhD* participates in the biosynthesis of L,D-heptoses (Raetz and Whitfield, 2002).

The *waaQ* operon comprises genes involved in the outer core biosynthesis and in the inner core decorations. The *waaA* gene has been described as a bifunctional Kdo transferase in *E. coli*, which acts during the lipid A biosynthesis transferring the first Kdo residue to the position O-6 of the non reducing glucosamine of the lipid A and then a second Kdo to the position O-4 of the Kdo I (Belunis *et al.*, 1995).

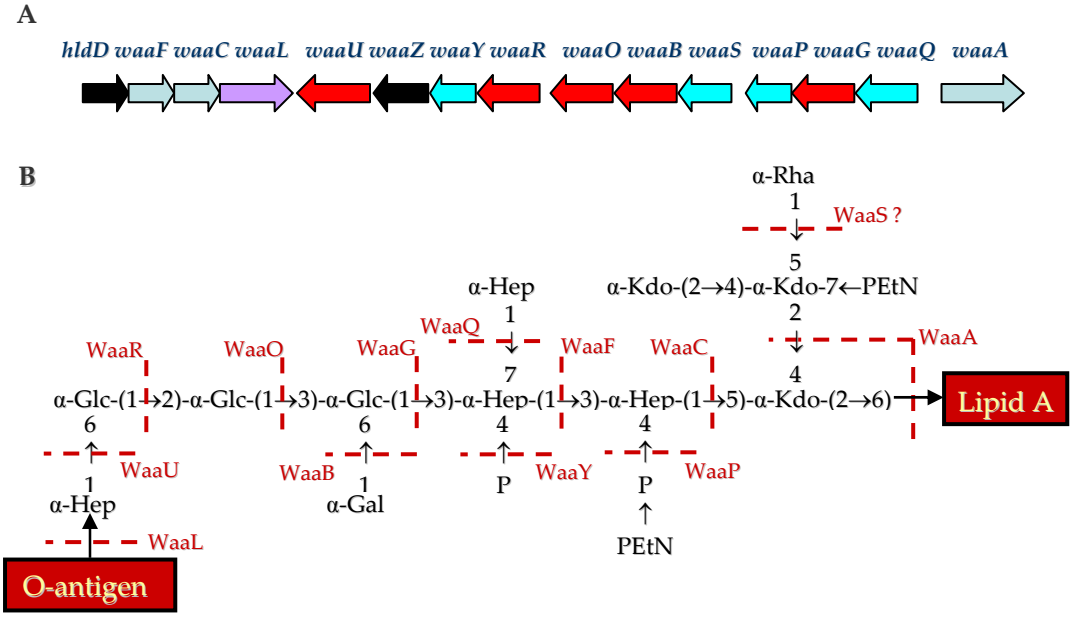

Fig.1.9. (A) Cluster *waa* of the genes involved in the core OS biosynthesis of *E. coli* K-12. **(B)** Structure of the *E. coli* K-12 core OS. Dashed arrows indicate nonstoichiometric substitutions. Dotted lines identify the known or predicted genetic determinants involved in the indicated linkages.

As *Escherichia coli* is one of the best studied microorganisms, the function of almost all the encoded products by genes belonging to its *waa* cluster have been already characterized (Raetz and Whitfield, 2002; Figure 1.9). The *waaZ* gene has been

recently suggested to be a regulator of the Kdo III glycosyltransferase (Frirdrich *et al.* 2003). Homologs of the WaaZ are encoded by the *waa* gene cluster of *S. enterica* and *E. coli* K-12 and R2 core types. The core regions from these bacteria are characterized by the non stoichiometric addition of Kdo III to Kdo II. It has been reported that over-expression of the *waaZ* gene in a strain of *E. coli* with R1 core type, resulted in a truncation of the outer core and in the presence of the Kdo III in the inner core, which normally is not present in the R1 core type. Since no evidences were found, that indicated the WaaZ as a glycosyltransferase, those results suggested that the *waaZ* gene was simply a regulator of the Kdo III transferase and the gene that should codify for this enzyme remained still unknown.

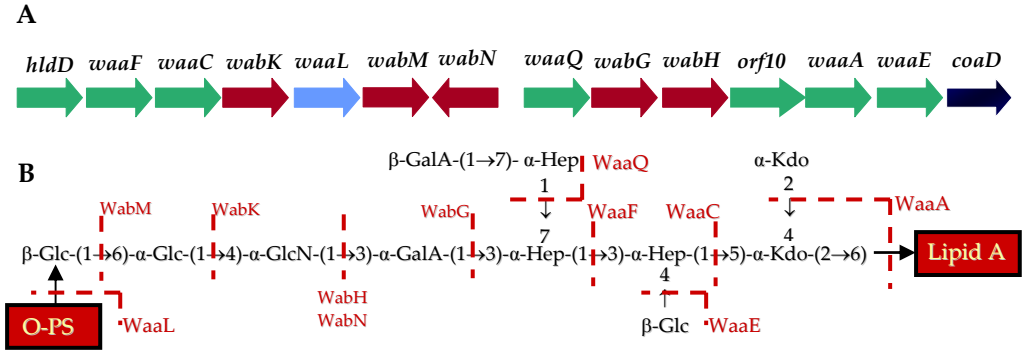

Fig.1.10. (A) Cluster *waa* of the genes involved in the core OS biosynthesis of *Klebsiella pneumoniae* 52145. **(B)** Structure of the core OS from *Klebsiella pneumoniae* 52145. Dotted lines identify the known or predicted genetic determinants involved in the indicated linkages.

Klebsiella pneumoniae waa cluster also comprises the *waaA,* the *waaQ* and *hldD* operons, but it shows some differences compared to *E. coli* (Figure 1.10). In fact, in *Klebsiella pneumoniae* the *waaA* operon comprises also the *waaE* gene (Izquierdo *et al*., 2002), which is involved in the addition of the inner core glucose. Moreover upstream of the *waaQ* operon an independent gene was found, the *wabN*, which is responsible for glucosamine de-acetylation (Regué, 2005 (a)). In fact, the addition of GlcN in the type 2

core of *Klebsiella pneumoniae* requires two enzymatic steps. First, the WabH catalyzes the addition of *N*-acetyl-glucosamine at position O-4 of the GalA residue and then a de-acetylation step occurs, catalysed by the WabN enzyme (Regué, 2005 (a)). However, the *waa* gene cluster characterization in *Klebsiella pneumoniae* was not completed, as no function was assigned to the *orf10* gene.

1.3.2.5 Core oligosaccharide negative charges and their role in outer membrane stability.

Among Enterobacteria, the presence of negative charges in the LPS core region is a very important structural feature. There are strong evidences that charged groups are necessary for cell viability. It had been suggested that, between different negatively charged LPS molecules, the formation of salt bridges, mediated by divalent cations, can occur providing an ordered and resistant protective barrier.

Mutants of *E. coli* and *Salmonella* with high truncated core oligosaccharides, which lacked the inner core heptose region, displayed a deep-rough phenotype. It is characterized by a decrease in the content of OM proteins and, correspondingly, an increase in the amount of phospholipids, which appear also in the outer leaflet of the OM. This causes higher permeability of the OM, that increased the sensitivity of this mutants to hydrophobic compounds. Moreover, the release of periplasmic enzymes and the loss of surface organelles, like pili and flagella, were observed. These changes reflect the increased susceptibility of bacteria to phagocytosis by macrophages. (Raetz and Whitfield, 2002).

Afterward, it was reported that the *waaP* gene in *E. coli* was involved in Hep I phosphorylation (Parker *et al.*, 1992; Yethon *et al.*, 1998). Moreover, the *waaP* mutant showed a truncation of the core. In fact, the addition of the phosphate group at Hep I is strictly required for the transfer of the Hep III to the inner core by WaaQ enzyme,

which in turn is required for the Hep II phosphorylation by WaaY. Nevertheless, only the mutation in the *waaP* gene resulted in a deep-rough phenotype, showing an increased sensitivity to hydrophobic compounds, noviobiocin and sodium dodecyl sulfate. These data suggested that only the complete loss of phosphoryl substituents from the heptose region leads to the deep-rough phenotype. Moreover, when the *waaP* gene was mutated in *Salmonella enterica*, the mutant showed characteristics of a deep-rough phenotype even if it expressed a smooth lipopolysaccharide. This result clearly demonstrated that the deep-rough phenotype is caused by the lack of phosphates and not by a truncation in the core region (Yethon *et al*., 2000).

As stated above two core types are currently known for *Klebsiella pneumoniae* and both show the lack of phosphoryl substituents in the inner core region. Nevertheless, they contain two GalA residues that contribute to the maintenance of the OM. It has been reported (Frirdich *et al*., 2005) that a mutant lacking both galacturonic acids (after deletion of the UDP-galacturonic acid precursor) showed characteristics of a deep-rough phenotype. These results indicated that, in maintaining outer membrane integrity, the carboxyl groups of galacturonic acids play a role which is equivalent to the phosphoryl substituents in *E. coli*. Moreover, it has been proposed that the presence of galacturonic acids instead of phosphates could provide certain advantages for the bacterium in habitats that are low in phosphates and in divalent cations involved in cross-linking adiacent LPS molecules, because the carboxyl groups become more easily protonated decreasing the repulsion between adjacent LPS molecules (Frirdich *et al.* 2005; Nikaido, 2003).

1.3.3 The O-chain polysaccharide.

1.3.3.1 Structure.

The O-specific chain polysaccharide is the most variable portion of the LPS. It can be an homopolymer, formed by a repeating monosaccharide or an heteropolymer, composed by a variable number (up to 40) of repeating units, each one containing up to 10 sugars. The O-antigen can also contain other substituents, like acetyl groups, hydroxybutirryl groups, etc. that can be often found in non stoichiometrically amount in the repetitive unit. Furthermore, in several cases non-usual sugars have been found in O-chain polysaccharides from various genera of bacteria, contributing to the high structural variability of the O-antigen.

As example in *Burkholderia caryophylli* the 3,6,10-trideoxy-4-C-[(R)-1-hydroxyethyl]-d-erythro-d-gulo-decose (caryophyllose, Figure 1.11(A)) was found (Adinolfi *et al.* 1995; De Castro *et al.* 2001), while in the phitopathogen *Pseudomonas corrugata* a 5,7-diamino-5,7,9-trideoxynon-2-ulosonic acid was found (Corsaro *et al.* 2002, Figure 1.11(B)).

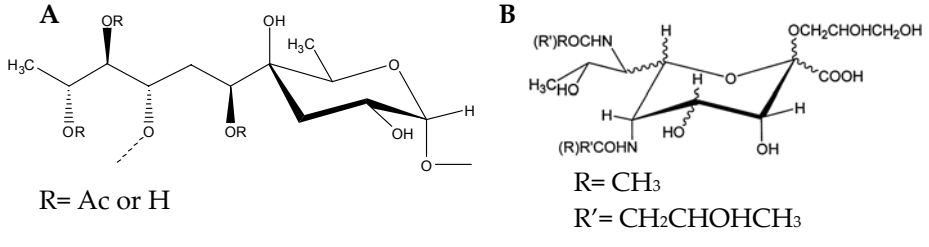

Fig. 1.11. Unusual sugars belonging to the O-chain of (**A**) *Burkholderia caryophylli* and (**B**) *Pseudomonas corrugata*.

1.3.3.2 Biosynthesis.

The O-antigen biosynthesis can occur by three different pathways (Figure 1.12; Raetz and Whitfield, 2002). It involves a first activation step which consists in the transfer of a sugar phosphate residue onto a lipid carrier, called undecaprenol

phosphate, embedded in the plasma membrane. The chain elongation can occur by one of the three mechanisms. In the case of heteropolymers or branched polysaccharides, the synthesis occur by a Wzy dependent pathway. A single repeating unit is synthesized in the cytoplasm by sequential action of specific glycosyltransferases and then the repeating unit is translocated to the periplasm. The nascent chain is added to the new translocated repeating unit by the Wzy O-antigen polymerase. The formation of homopolysaccharide chain occurs by a second mechanism, in which the chain elongation occurs totally in the cytoplasm. The polymer is translocated into the periplasmic side of the membrane via the action of an ATP-binding cassette-transporter. The third pathway has been observed only in the case of *S. enterica* serovar Borreze O:54, whose O-antigen was an homopolymer of *N*-acetylmannosammine. The proposed mechanism suggested the presence of an integral membrane protein with a double function. It could act both as a glycosyltransferase and as an exit pore for the newly formed polymer. This means that the sugars addition to the growing end of the chain extrudes the polymer from the cytoplasm to the periplasm.

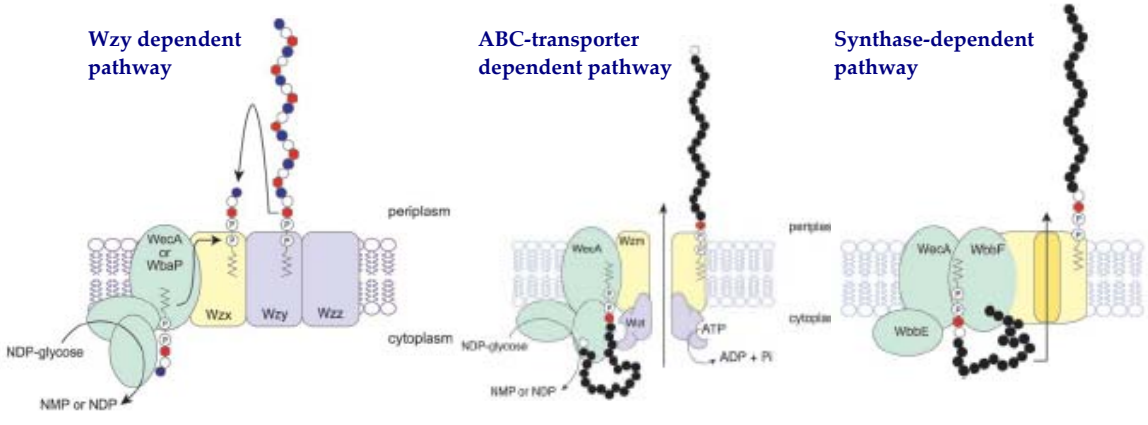

Fig. 1.12. O-chain polysaccharide biosynthesis pathways.

Independently from the mechanism, once the undecaprenol-linked O-antigen is translocated to the periplasm, the O-chain is linked to the preformed lipid A-core by the action of the WaaL ligase, concluding the LPS biosynthesis.

The minimum structure for cell viability of LPS found to date, in the majority of Gram-negative bacteria, is constituted by the lipid A and at least one Kdo residue. The LPS can be found as Smooth type LPS, containing the O-antigen linked to the lipid A-core, or as Rough LPS, that only contains the core linked to the lipid A. The explanation for these different phenotypes is the fact that the loss of the highly hydrated O-chain polysaccharide from the cell surface results in a drier and hence rougher-looking colony morphology.

1.4 Capsular polysaccharide: structure and functions.

The surface of many Gram-positive and Gram-negative bacteria is covered by several kind of polysaccharides, such as capsular polysaccharides (Figure 1.13). A number of possible functions were suggested for these molecules. For instance, being highly hydrated (95 % of water), they are able to protect the cell against desiccation. They are also supposed to promote the adherence of bacteria to the host surface and to each other, facilitating the colonization of various biological niches.

Capsular polysaccharides can be homo- or hetero-polymers containing different kind of sugars. In most cases they contain acidic monosaccharides and additional substituents that contribute to structural diversity. They are divided in four groups on the basis of their biological and chemical properties. Despite the high number of capsular polysaccharide structures characterized and their importance in pathogenicity, the mechanism of their association to the cell membrane is not yet well understood.

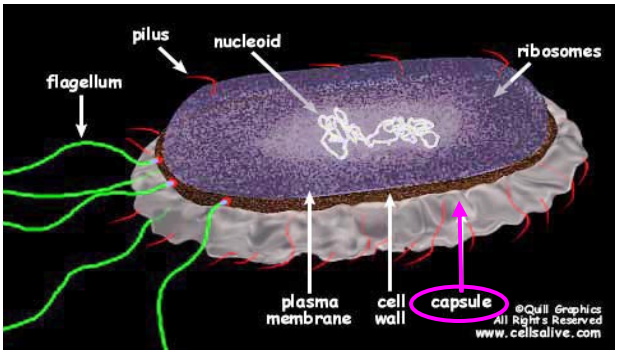

Fig. 1.13. Bacterial cell.The capsular polysaccharide forms a layer that encompasses the whole cell.

It has been reported that in *E. coli* O9:K30 (group I K antigen) and O8:K40:H9 (group II K antigen) capsule association occurs through the lipid A-core portion of the LPS. In the first case, in particular, only K30 oligosaccharides resulted to be covalently linked to the lipid A-core region, while no suggestions were reported for the association of the high molecular mass K30 CPS to the cell surface (MacLachlan *et al.*, 1993). As for K40 CPS, belonging to group II K antigen, long chains of CPS resulted to be linked to the Lipid A-core LPS (Jann *et al.*, 1992). Group II and III capsular polysaccharides were found in *E. coli* isolates that cause extra-intestinal infections. For *E. coli* K92 CPS it was suggested that the polysaccharide was linked to a diacylglycerophosphate through a phosphodiester linkage although an unequivocal determination of the linkage was not possible (Gotschlich *et al.*, 1981). In *E. coli* K12 and K82 CPSs preliminary evidences suggested that the linkage with the diacylglycerophosphate moiety is mediated by a Kdo residue (Whitfield, 2006).

Recently it has been demonstrated that in *Klebsiella pneumoniae* 52145 the K2 CPS, which belongs to group I (Corsaro *et al.*, 2005), is linked to the core region through an ionic interaction mediated by calcium ions in which the GalA residues of the core region were supposed to play a crucial role (Fresno *et al.*, 2006). Considering

that most of the capsular polysaccharides show the presence of acidic units, this mechanism of association seems to be extendible to other bacteria.

1.5 Pathogenicity of Gram-negative bacteria.

Gram-negative bacteria share common pathogenesis mechanism in terms of the phases which precede infection. They posses adhesins, which are involved in the first step of colonization of the host cells, enabling the binding to the host cell surface. Once the pathogen adhers to the host cell surface, it can invade the cell extra- or intra-cellularly by secreting several toxins.

The immunity response of the host organism can be divided in two phases.

1. innate immune response
2. adaptative immune response

In particular the lipid A domain in LPS is a highly specific marker of infection by Gram-negative bacteria. Lipid A molecules are detected in the order of picomolar levels by an ancient receptor of the innate immune system present on macrophages, the TLR4 (Toll-like receptor 4), a membrane–spanning protein. This recognition is mediated by an initial interaction of the LPS with a special lipid transfer protein, LBP (LPS binding protein).

Then the LPS-LBP complex is recognized by the CD14 receptor, which is located on the surface of specific immune cells, like macrophages, and allows LPS to interact with TLR4. This interaction activates a signal transmission to the cell nuclei that leads to the expression of genes involved in the biosynthesis of cytokines (cell inflammation mediators, Figure 1.14). High levels of LPS cause excessive release of inflammatory mediators, that can damage small blood vessels causing the septic shock syndrome (Raetz and Whitfield, 2002).

An important role in the early host defence mechanisms is played by the complement system, which is constituted of a series of glycoproteins that are normally found in the blood in an inactive form. It can be activated both with or without intervention of antibodies and it implies the formation of a proteic complex on the bacterial cell wall, which leads to cell lysis. Gram-negative bacteria activate complement by molecules located on the bacterial cell surface, like LPS. In particular it has been reported that the lipid A induced the highest complement activation (Münstermann *et al.*, 1999).

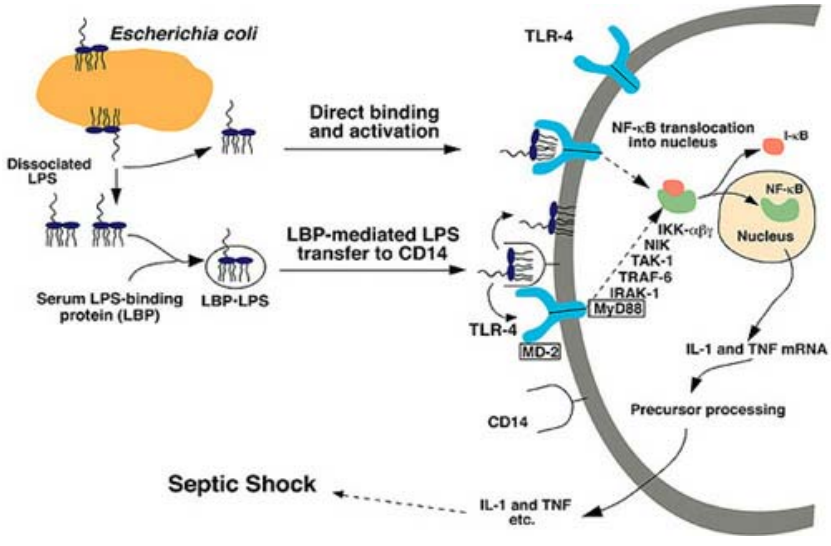

Fig. 1.14. Detection of the lipid A by the TLR4 innate immunity receptor of animal cells.

Bacteria have to protect from the host immune system. For this reason some bacteria overproduce and excrete copious amount of high molecular weight polysaccharides, which encompass the whole cell forming a protective capsule. This structure in fact protects the bacteria from the host inflammatory response. In particular, it gives protection from the complement activation and from phagocytosis

impeding the opsonizing antibody to be recognized by macrophages and neutrophils, that conseguently produce more inflammatory cytokine, causing an increased tissue damage.

In mammals, the innate immunity response induces the activation of adaptative, highly specific, immune response. In this phase specific antibodies are produced, that are frequently directed against epitopes of the polysaccharidic portion of the LPS, or other bacterial antigens. This justifies the high structural variability of the LPS O-antigen respect to the core and lipid A regions. Moreover, the presence of the CPS on the cell wall hides the O-antigens and does not allow the antibody to recognize it.

CPS can also induce the formation of anti-capsular antibodies of the specific immune response, that are active in the host protection from infections. Capsular-specific antibodies are formed at a late stage of infection and overcome the protective action of capsules. Nevertheless, some capsules are not recognised as foreign by the host, so antibodies are not produced and bacteria is able to escape from the host immune recognition. For instance, CPS K1 from *E. coli*, a poly (α-2→8)-sialic acid, is non-immunogenic, because it has the same structure as a terminal sialic acid residue of a mammalian glycoprotein, the n-CAM (neural Cell Adhesion Molecule; Mushtaq, 2004; Troy, 1992).

In conclusion, a lot of information are available about the lipid A function in the establishing of infection. It activates the innate immune response in the host organism. It is also known the role of the O- and K-antigens in the antibody recognition by the host and the protective function of the capsular polysaccharide. Nevertheless, the role of the core oligosaccharide in these mechanisms is still far from being elucidated.

1.6. Aims of the work.

As stated above the capsular polysaccharides are able to elicit the type-specific protective immune response and to protect bacterial cell from the innate immune response. For this reason, it has long been considered as one of the major virulence determinant in Gram-negative bacteria, especially when it is not immunogenic and then able to elude the adaptative immune response. This is the case of *E. coli* K1. Very little is known about the mechanism of capsule association to the cell surface. Nevertheless it has been reported that the pathogenicity of *Klebsiella pneumoniae* is related to the formation of a complex constituted by LPS, CPS and proteins (Straus, 1987).

On this basis we started to study the mechanism of capsule association to the cell wall in Gram-negative bacteria.

The work borned in collaboration with the group of professors Juan Tomàs and Miguel Reguè, belonging to the Microbiology Department of Barcelona University. In particular, my work aimed at the elucidation, on chemical basis, of the genes involved in the core oligosaccharide biosynthesis of LPS from *Klebsiella pneumoniae* and *Escherichia coli*, and their involvement in the interaction between the core oligosaccharide and the capsule.

The structures of LPS from several mutants from *Klebsiella pneumoniae* and *Escherichia coli*, which showed a decrease in the capsule association, were analysed.

As in several pathogen bacteria the capsule has been described as the major virulence determinant, the study of the capsule association to the cell surface is the mandatory starting point for the development of new antibiotics.

Chapter 2

Methods for the Structural Characterization of Lipooligo-/lipopolysaccharides

2.1 Extraction and purification of lipooligo-/lipopolysaccharides.

The lipopolysaccharides isolation from the dried bacterial cells is usually performed following two different standardized procedures.

The classical phenol-water (PW) method had been widely used for lipopolysaccharides extraction (Westphal and Jann, 1965). It uses a mixture of phenol and water (1:1, v/v) at 68°C (at this temperature the mixture appears as a mono-phase system). After centrifugation at 26°C, the two components are separated. The LPS molecules are generally recovered from the water phase together with nucleic acids, while the phenol phase generally contains proteins. In order to remove nucleic acids from the water extract, an enzymatic treatment, with RNase, DNase and protease, is necessary.

The PCP method (Galanos *et al*., 1969) uses a mixture of phenol, chloroform and petroleum ether (2:5:8, v:v:v), which allows to extract the more lipophilic lipopolysaccharides molecules, such as the Rough type lipopolysaccharides, constituted by the lipid A-core portions, or those molecules comprising only a small number of O-chain repeating units. This procedure is more selective than the previous one and allows to obtain a sample almost free from nucleic acids contaminations.

2.2 Electrophoresis analysis.

The electrophoresis analysis is the first step in the analysis of an unknown LPS, because it can rapidly show the size of the extracted LPS molecules.

Typically, because of the wide molecular mass range of LPS molecules biosynthesized by a bacterium, the electrophoresis profile of an LPS shows a ladder like pattern.

The LPSs are amphiphilic molecules, able to form big size micelles. The denaturing agents generally used to perform the analysis are sodium dodecyl sulfate (SDS) and sodium deoxycholate (DOC). The latter gives a better resolution for low molecular mass molecules (Komuro and Galanos, 1988). Nevertheless the best resolution in this range can be achieved by using tricine-SDS-PAGE.

For visualization of lipopolysaccharides the mostly used method is the silver staining (Tsai and Frasch, 1982).

2.3 GC-MS methods for sugar analysis.

The identification of the monosaccharides present in the LPS is carried out by GC-MS analysis. The LPS samples can be hydrolyzed using several reaction conditions, depending on the nature of the sample. Usually the LPS sugar analysis is carried out by derivatization of monosaccharides as acetylated methyl glycosides or as alditol acetates. They are identified both by the retention time and the fragmentation pattern. Generally the fragmentation pattern of a methyl glycoside is more complex respect to the corresponding alditol acetate.

Moreover, using GC-MS, it is possible to obtain the linkage positions of each monosaccharide through the analysis of the partially methylated alditol acetates.

Another important step in the characterization of carbohydrates is the determination of the absolute configuration. In this, GC-MS finds an other application.

The procedure consists in the differentiation of D and L monosaccharides through diastereoisomeric octylglycosides preparation, using (+)-2-octanol. The comparison with the retention times of standard octylglycosides, allows the identification of the absolute configuration of the monosaccharides (Leontein *et al.*, 1978).

2.4 Characterization of the lipooligo-/lipopolysaccharides.

Due to the amphiphilic nature of the LPS, it is difficult to study the molecule without any degradation. It is convenient to separate the lipidic from the saccharidic portion to achieve a better solubility. Two different approaches can be used, which lie in an acid or an alkaline hydrolysis.

2.4.1 Mild acid hydrolysis.

The mild acid treatment exploits the labile glycosidic linkage of the Kdo residue, which links the core region to the lipid A. This kind of procedure allows the isolation of the intact lipid A and of the polysaccharidic portion (Figure 2.1).

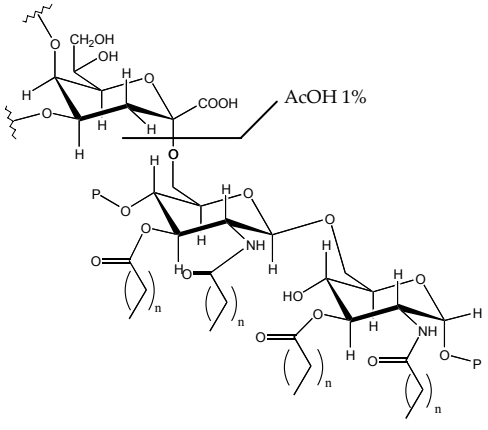

Fig. 2.1. Schematic illustration of the Kdo linkage cleavage during the mild acid treatment.

The reaction conditions lead to dehydration of Kdo with consequent formation of artifacts (Volk *et al*., 1972). This increase the sample heterogeneity and can make difficult the interpretation of NMR spectra, because the artefacts can be present in not negligible amount.

2.4.2 Alkaline hydrolysis.

The alkaline treatment lies in a first *O*-deacylation of the LPS, and a successive *N*-deacylation, which lead to the isolation of a polysaccharide containing the glycosidic portion of the lipid A (Holst, 2000).

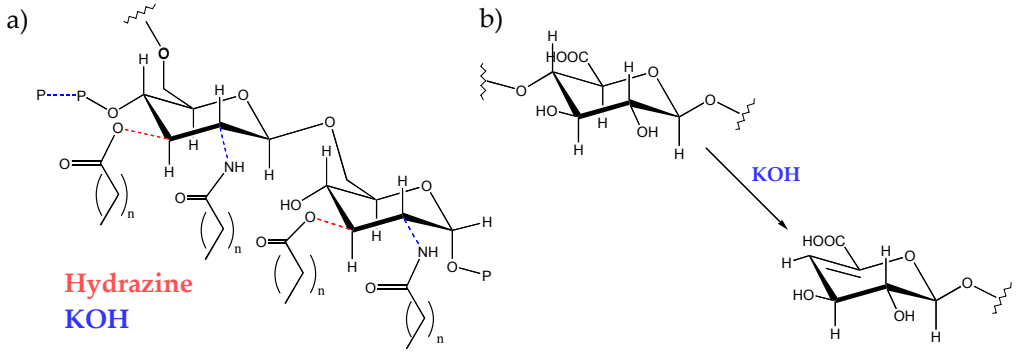

Fig. 2.2. a) Schematic representation of the lipid A. Dotted red and blue lines indicates the linkages hydrolyzed during treatment with hydrazine or KOH, respectively. b) b-elimination reaction on a 4-linked GlcA.

The reaction conditions for the *N*-deacylation are very strong and cause loss of information about the presence of acetyl groups and pyrophosphates substituents (Figure 2.2a). Moreover when 4 linked uronic acids are present, a β-elimination reaction can occur at position 4 (Figure 2.2b).

2.5 Characterization of the saccharidic portion of an LPS.

The LPS produced from bacteria often shows structure heterogeneity. This leads to a glycosidic mixture after both the acid and the alkaline treatments. Mass

spectrometry analysis of the mixture gives important information about the components. Knowing the molecular mass, on the basis of the sugar analysis, it is possible to define the composition of the oligosaccharides. Moreover the Mass spectrum gives information about the heterogeneity of the sample. Afterward, to characterize each glycoform, a separation step is necessary and precludes the study by NMR spectroscopy.

2.5.1 Purification of an oligosaccharides mixture.

Purification of oligosaccharide mixtures is generally achieved by using chromatographic techniques. When the components show high difference in the molecular masses, size-exclusion chromatography is suitable for separation. Different kind of resins are commercially available, with different range of pore sizes. It is possible to elute the sample using water or buffers with high ionic strength.

The best separation can be achieved by high pressure anion exchange chromatography (HPAEC). It is widely used for carbohydrate purification and works at high pH values, at which the oligosaccharides are highly charged. Moreover the oligosaccharides deriving from LPS, often contain phosphoryl substituents, which confer other negative charges. HPAEC allows separation of oligosaccharides with small differences in the molecular mass, of oligosaccharide isomers and, since the retention time depends on the charge to mass ratio, it allows also the separation of oligosaccharides with the same glycosidic backbone, but differing for the phosphate content.

2.5.2 Mass spectrometry of oligosaccharides.

Mass spectrometry is widely applied to carbohydrates structure elucidation. It provides information about the molecular mass of the samples and, in particular cases, information about the sequence of the monosaccharides.

The MALDI and ESI ionization sources are suitable for oligosaccharides structure elucidation. In the standard conditions used to perform the experiments, both the ionization mechanisms do not cause fragmentation of the oligosaccharidic chains. This implies that a MALDI or an ESI mass spectrum can give information about the number of species present in the sample. The main difference between the spectra obtained by the two ionization techniques is that the ESI spectrum can show the presence of multicharged ions.

Among mass analyzers, the FT-ICR gives the best resolving power. In fact, depending on the magnetic field strength, it can achieve a mass resolving power higher than 100000 and a mass accuracy less than 1 ppm.

It is usually coupled with an electrospray ionization source and it finds important applications in LPS analysis. In particular it is possible to perform the CSD (Capillary Skimmer Dissociation) experiment, which allows the cleavage of the labile glycosidic linkage between the Kdo and the GlcN4*P* belonging to the lipid A. Thus, analysing the intact LPS, it is possible to obtain information about both the core region and the lipid A. The signals belonging to the core region are, most of the times, easily recognizable, because they are characterized by the loss of 44 u, which is due to the Kdo de-carboxylation (Kondakov and Lindner, 2005) .

Using a MALDI-TOF system, it is possible to analyze the fragment ions generated by the precursor ions in the flight tube, when a higher laser intensity is applied. In the normal conditions, used to perform a MALDI-TOF experiment, these fragments are not detected because they are not correctly focused by the detector. It is

possible to perform a post source decay (PSD) experiment, during which, varying conveniently the detector parameters, those ions can be correctly focused (Spengler, 1997). Moreover, when a spectrometer is equipped with a collision cell, it is possible to perform tandem mass spectrometry experiments, selecting an ion and inducing its fragmentation.

Nevertheless, the interpretation of fragmentation spectra of carbohydrates is not always easy, because fragmentation could not occur at each glycosidic linkage. Moreover different fragment types can be formed, the identification of which is sometimes not immediate.

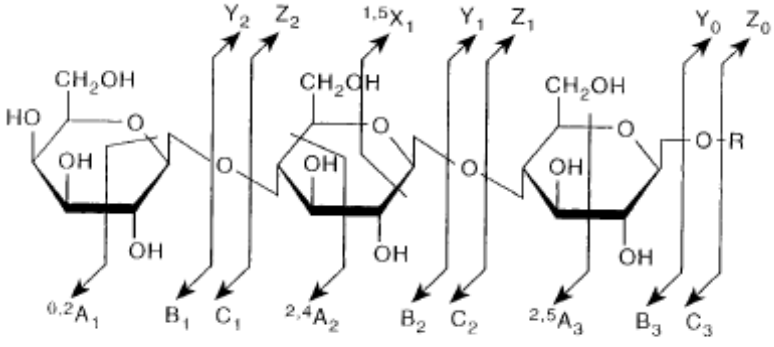

Fig. 2.2. Fragments nomenclature by Domon and Costello.

The nomenclature used for fragment types classification was developed by Domon and Costello in 1988 (Figure 2.2). The cleavage of the glycosidic bond can lead to the formation of B, C, Y and Z fragment types. The fragments which contain the reducing end of the oligosaccharide are named Y and Z, while those containing the non reducing end of the molecule are named B and C fragments. Each fragment is also identified by a number, which indicates the number of monosaccharides present in

the fragment. A type fragments regard internal fragmentation (Domon and Costello, 1988; Spina *et al.*, 2004).

Mass spectrometry alone is not able to give all the necessary informations for the complete characterization of an unknown oligosaccharide. It is fundamental to combine these results with NMR data.

2.5.3 NMR spectroscopy of oligo-polysaccharides.

NMR spectroscopy is fundamental for oligo-polysaccharides characterization. Carbon chemical shifts values for each residue are highly conserved, and there are small differences in the protons chemical shifts respect to the reference methyl glycosides, due to the influence of the neighbour residues.

The region from 4.4 to 5.4 ppm in the ^{1}H-NMR spectrum of an oligosaccharide comprises the anomeric signals. The number of signals in this region gives information on the number of aldopyranoses present in the molecule. The anomeric configuration can be deduced by the chemical shift of the anomeric protons and carbons and by the $^{3}J_{H1,H2}$ and $^{1}J_{C1,H1}$ values (Table 2.1). The carbinolic region (from 3.0 to 4.4 ppm) is more crowded and no information can be obtained using the mono-dimensional NMR spectrum**.**

Table 2.1 Coupling constant values for α and β anomers

anomer	$^{3}J_{H1,H2}$ **(Hz)**	$^{1}J_{C1,H1}$ **(Hz)**
α	2-3	>170
β	8-10	<165

In the high field region of the ^{1}H-NMR spectrum it is possible to find Kdo diagnostic signals, the $H_{3a,b}$, which usually resonate around 2.0 ppm. The methyl groups of 6-deoxysugars are also easily recognizable and are found around 1.0 ppm.

Due to the complexity of the 1D spectrum, it is necessary to study different kind of two-dimensional NMR experiments at the same time, in order to assign the chemical shifts to carbons and protons in an oligosaccharide. The second dimension allows to simplify the most crowded regions of the spectrum. The most used homo-nuclear experiments are COSY, TOCSY and ROESY.

The COSY pulse sequence allows the detection of scalar coupled protons. When the experiment is performed in the phase sensitive mode, the cross peaks appear as multiplets and contain information about the coupling constants. The TOCSY experiment gives correlations between all the protons belonging to a spin system. The pulse sequence comprises a series of soft pulses responsible of magnetization transfer between protons belonging to the same residue. The extent of magnetization transfer depends on the $^{3}J_{H,H}$ coupling constant values therefore, for a monosaccharide having a *gluco* configuration, the TOCSY spectrum will define all the spin system. Nevertheless the lipopolysaccharides contain, in the inner core, peculiar sugars like L-*glicero*-D-*manno*-heptoses. The $^{3}J_{H1,H2}$ in the *manno*-configured sugars is very small and this create an interruption in the magnetization transfer, which makes very difficult the complete assignment.

The linkage positions of the monosaccharides can be determined by the carbons chemical shift values because of the glycosylation shift. The carbons involved in the glycosidic linkage undergo a downfield shift of 8-10 ppm, while the adjacent carbons undergo an upfield shift of 1-3 ppm.

The assignment of the carbons chemical shift is possible using the ^{1}H-^{13}C HSQC, HSQC-TOCSY and HMBC spectra. The first shows the correlations between directly linked carbons and protons. A variant of this experiment combines the HSQC and the TOCSY pulse sequences and leads to a spectrum which shows correlations between one proton and the carbons belonging to its spin system. The HMBC shows

correlations among carbons and protons linked through three bonds. This makes such experiment suitable for the determination of the monosaccharides sequence in the chain.

A ROESY spectrum, which is built up by the NOE effect, also can give useful information about the sequence, but it is based on dipolar interactions between nuclei and then the interpretation of the spectrum is tricky since the cross peaks can be due either to *intra*-molecular or *inter*-molecular couplings.

Chapter 3

Structural Determination of the LPS Core from the Δ*waaL*-Δ*wabO* Mutant of *Klebsiella pneumoniae* and Capsule Association to the Cell Surface

3.1 Background of the work.

Klebsiella pneumonieae is an important nosocomial opportunistic pathogen, of which, almost all clinical isolates are capsulate. Although not all capsulate strain are virulent, the K-antigen has long been considered as the major virulence determinant in *Klebsiella pneumoniae.*

Recently, it has been demonstrated that in *Klebsiella pneumoniae* 52145 strain the K2 CPS is associated to the cell surface through an ionic interaction, between the acidic residues present both in the CPS and in the LPS core region, mediated by divalent cations (Fresno *et al.*, 2006; Figure 3.1).

Despite the presence of two GalA residues in the core region (Reguè et al., 2005; Vinogradov *et al.*, 2001), only one Galacturonosyltransferase was identified. Thus, either the previously identified GalA transferase (WabG; Izquierdo *et al.*, 2003) is bifunctional or a second GalA transferase remains to be identified. The functions of twelve of the thirteen genes in both *wa*$_{C3}$ and *wa*$_{52145}$ clusters were known and since it

was observed a decrease in the cell bound capsule in a mutant lacking the unknown *orf10* gene, we hypothesized that it could encode a second GalA transferase. In order to prove it, the structure of the core oligosaccharide of the LPS from the Δ*waaL*-Δ*orf10* double mutant was elucidated.

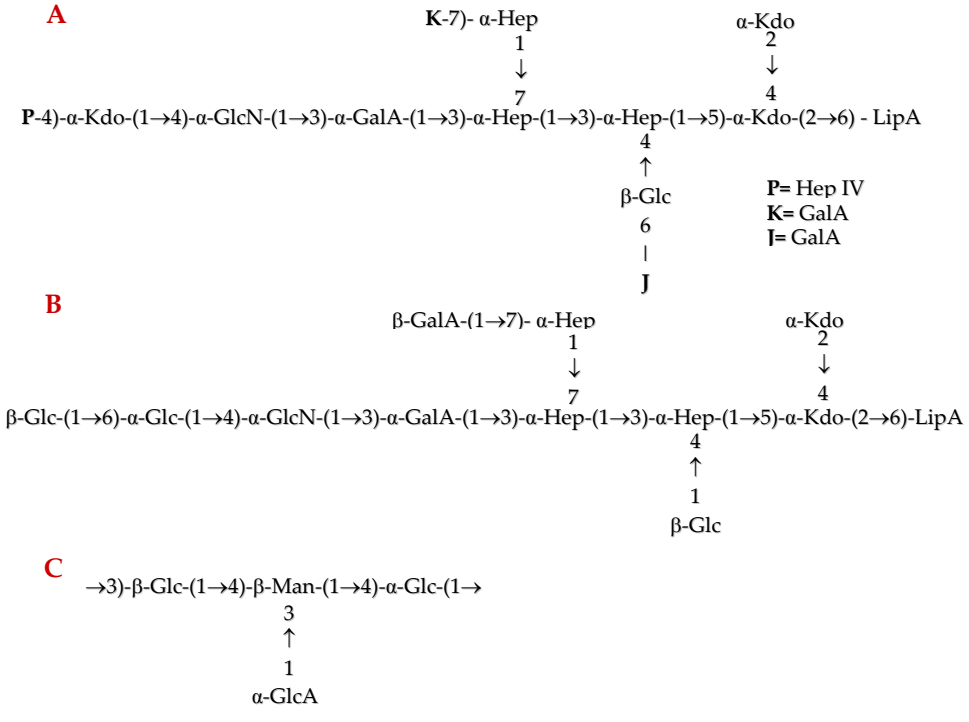

Fig. 3.1 *Klebsiella pneumoniae* type 1 and type 2 core oligosaccharide structures are represented in **A** and **B**, respectively. The repeating unit of the K2 capsular polysaccharide is represented in **C**.

3.2 Results.

3.2.1 Structural characterization of LPS from Δ*waaL*-Δ*wabO* double mutant.

The LPS from *Klebsiella pneumoniae* Δ*waaL*-Δ*wabO* double mutant was isolated from the dried cells by PCP (phenol: chloroform: light petroleum) with a yield of 2.6%**.** The LPS ($LPS_{waaL\text{-}wabO}$) was then analysed by (tricine)-SDS-PAGE together with an LPS sample obtained from *Klebsiella pneumoniae* 52145 (LPS_{52145}; Figure 3.1). As expected $LPS_{waaL\text{-}wabO}$ did not show the typical ladder-like pattern. In addition it migrated slightly faster than the LPS_{52145}, suggesting that a residue is missing in the $LPS_{waaL\text{-}wabO}$ structure.

Fig 3.1. (tricine)-SDS-PAGE LPS from. **A**: *Klebsiella pneumoniae* 52145 wild type and **B**: *Klebsiella pneumoniae* 52145 Δ*waaL*-Δ*orf10* mutant.

The glycosyl analysis of $LPS_{waaL\text{-}wabO}$ together with absolute configuration determination revealed the presence of D-GalA, D-GlcN, D-Glc, L,D-Hep, and Kdo (Figure 3.2).

The core OS structure was obtained by degradation of LPS under both alkaline (OS_{KOH}) and acid conditions (OS_{AcOH}).

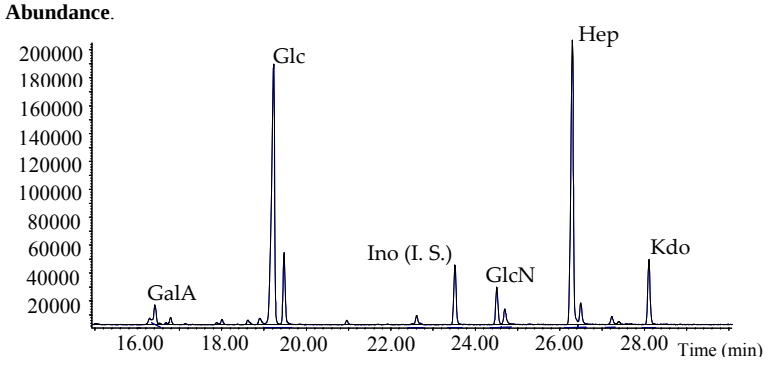

Fig.3.2 GC-MS analysis of acetylated methyl glycosides. Inositol was used as internal standard

3.2.1.1 OS_{KOH} analysis.

The LPS was treated with anhydrous hydrazine, then dephosphorylated using 48% HF and, after reduction of the free reducing glucosamine, a stronger alkaline hydrolysis with 4M KOH was performed. Finally the sample was purified by gel filtration, on a Sephadex G-10 column, to give OS_{KOH}.

3.2.1.1.1 Mass spectrometric analysis of the OS_{KOH}.

The positive ions MALDI-TOF mass spectrum of OS_{KOH} showed a very complex pattern of signals (spectrum not shown) suggesting the presence of a mixture of oligosaccharides. The signal at *m/z* 1679.86 was in agreement with the presence of one hexose, three heptoses, one glucosamine, one glucosaminitol, two Kdo and one hexenuronic unit (calculated average mass $(M+H)^+$=1680.47). The presence of the latter residue was probably due to a β-elimination reaction underwent by a 4-linked Hexuronic acid. Additional peaks in the spectrum could be attributed to molecular species lacking one GlcN, or one Kdo or one hexenuronic unit. The finding of this oligosaccharides mixture could be explained by a partial degradation of the sample during the HF and KOH treatments (Vinogradov *et al.* 1997).

3.2.1.1.2 NMR spectroscopic analysis of OS$_{KOH}$.

The ^{1}H-NMR spectrum confirmed that OS$_{KOH}$ was a complex oligosaccharides mixture. By comparing the ^{1}H-NMR anomeric region spectrum of OS$_{KOH}$ (Figure 3a) with previously published ^{1}H-NMR of the same fraction obtained from LPS$_{waaL}$ (Figure 3b, Reguè *et al.*, 2005 (b)) we can note the presence of a signal at 5.65 ppm, correlated to a carbon signal at 106.7 ppm in a HSQC-DEPT experiment, that was identified as the H-4 of a *threo*-hex-4-enuronopyranosyl unit.

This last residue could derive from a 4-substituted GalA after β-elimination that occur during the alkaline treatment. The composition and the NMR data suggested that the OS$_{KOH}$ is truncated by the terminal β-GalA respect to the alkaline product of *Klebsiella pneumoniae* Δ*waaL* mutant (Reguè *et al.*, 2005 (b)).

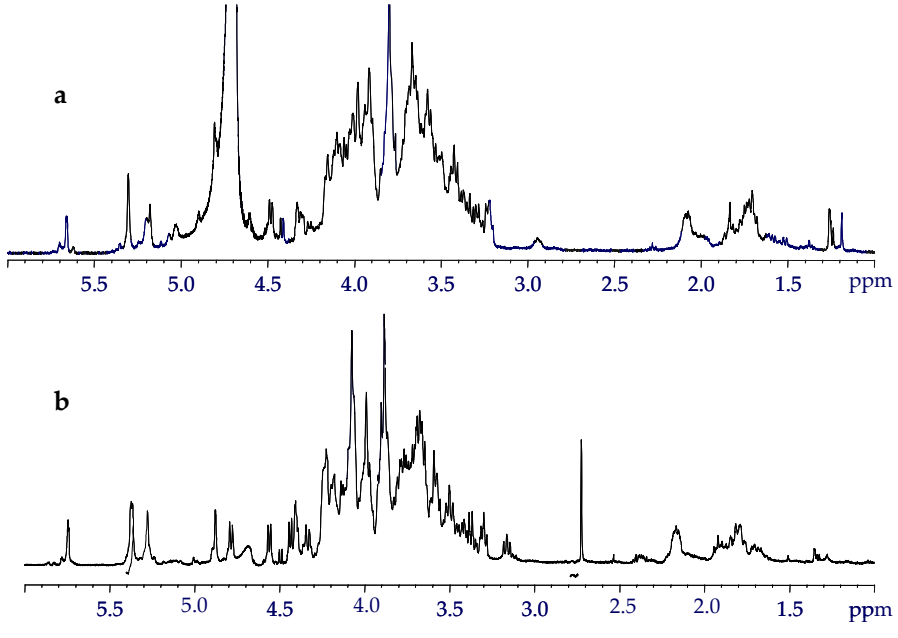

Fig 3.3. ^{1}H-NMR spectra of a) OS$_{KOH}$ obtained from Δ*waaL*-Δ*wabO* mutant and b) OS$_{KOH}$ from Δ*waaL* mutant.

3.2.1.2 OS_{AcOH} analysis.

In order to confirm this hypothesis and to check if alkaline treatment had removed base sensitive groups, the LPS was hydrolyzed in acidic conditions with AcOH 1% that cleaves the labile linkage between the Kdo and the glucosamine II of the lipid A. The OS_{AcOH} was then analysed both by mass spectrometry and NMR spectroscopy.

3.2.1.2.1 MALDI-TOF mass spectrometric analysis of OS_{AcOH}.

The positive ions MALDI-TOF mass spectrum of OS_{AcOH} (Figure 3.5) showed two main peaks at *m*/*z* 1661.36 and 1643.35, which correspond to the pseudomolecular ions $(M+Na)^+$ and $(M+Na-18)^+$, respectively. The signal at *m*/*z* 1661.36 corresponded to three hexose, three heptoses, one hexuronic acid, one hexosamine and one Kdo unit, and it was in agreement with the calculated average molecular mass 1661.40 Da. The signal at *m*/*z* 1643.35 was attributable to the same structure with the anhydro form of the terminal reducing end Kdo (Olsthoorn *et al.*, 1999).

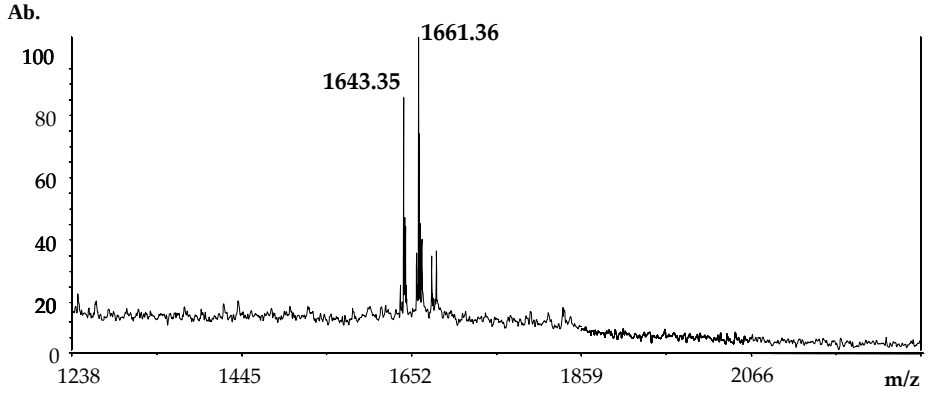

Fig. 3.5. MALDI-TOF spectrum of OS_{AcOH} performed in the reflectron positive ion mode.

The PSD MALDI-TOF experiment of the $(M+Na)^+$ ion at *m/z* 1661.36 is reported in Figure 3.6. This spectrum is dominated by fragment ions of B, Y and Z series (Table 3.1; Domon and Costello, 1998), besides to some double fragmentations.

The signal at *m/z* 1422.8 has been attributed to a B_6 ion ($[M+Na]^+$-220-18) followed by a B_3 ion at *m/z* 485.8, which indicated the presence of the fragment Glc-Glc-GlcN. The fragment ions Y_4 and Z_4 at *m/z* 1175.6 and 1157.7, respectively, confirmed the absence of the *t*-β-GalA in the inner core structure. In addition, further signals arising from these ions by multiple Y-type cleavages were also present in the spectrum. Starting from the B_6 signal at *m/z* 1422.8 there was a peak at *m/z* 938.3 which derived from the loss of two Glc and one GlcN. The signal at 600.9 m/z derived from a double fragmentation from the peak at 938 m/z, with simultaneous loss of a Glc and a GalA residues. Finally signals at *m/z* 323.9 (B_3-Glc) and *m/z* 162.1 (B_3-Glc-Glc) were also present.

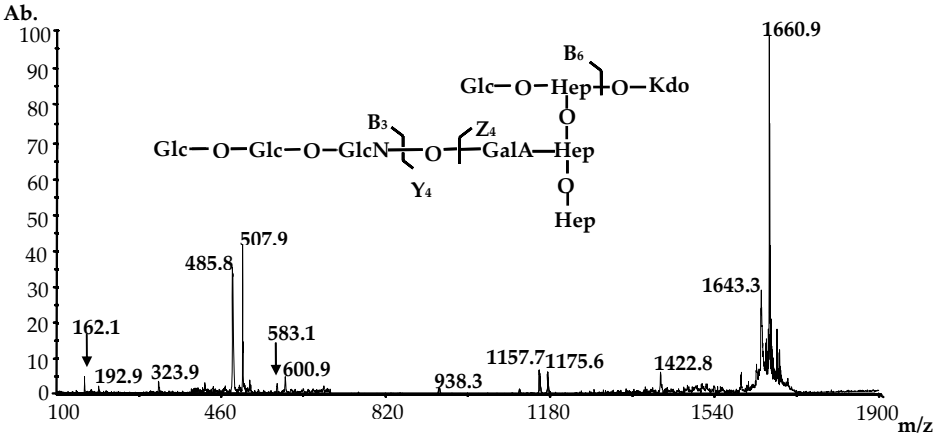

Fig. 3.6. MALDI-PSD experiment performed on OS_{AcOH}. Fragments composition is reported in Table 3.1

Table 3.1. List of the fragments observed in the MALDI-PSD spectrum performed on OS_{AcOH}.

Signals	Calculated mass (Da)	Observed mass (m/z)	Proposed compositions
1	1661.41	1660.9 ▲	**M (Glc_3 GalA Hep_3 GlcN Kdo)**
2	1423.21	1422.8 ▲	**B_6**
3	1175.96	1175.6 ▲	**Y_4**
4	1157.95	1157.7 ▲	**Z_4**
5	937.77	938.3 ▲	**B_6 -Glc-Glc-GlcN**
6	600.51	600.9 ▲	**B_6-$(Glc)_3$ -GlcN-GalA**
7	485.44	485.8	**B_3**
8	324.28	323.9	**B_3 -Glc**
9	162.14	162.1	**B_3 -Glc-Glc**

▲ sodiated fragments

3.2.1.2.2 NMR spectroscopic analysis of OS_{AcOH} .

The complete assignment of the protons and carbons chemical shift of OS_{AcOH} was obtained on the basis of the ^1H-^1H DQF-COSY, TOCSY, ROESY and ^1H-^{13}C HSQC–DEPT spectra (Table 3.2). For the Kdo spin system the assignment was not allowed due to the well known arrangements of this sugar in multiple forms, including 2,7-anhydro form (McNicholas *et al.*, 1987). The ^1H and ^1H-^{13}C HSQC-DEPT NMR spectra (Figure 3.7a and b, respectively), recorded for OS_{AcOH}, contained signals for 8 anomeric protons and carbons. In the 2D-NMR spectra it was possible to recognize some of the spin systems already observed in OS_{KOH} spectra. In addition other signals due to the saccharide moiety lost during alkaline degradation were present. In particular the residue **G** with H-1/C-1 signals at δ 5.42/99.8 ($^3J_{H\text{-}1,H\text{-}2}$ 3.9 Hz) was assigned to a α-glucose unit on the basis of the chemical shift of the carbons and the low value of the coupling constant between H-1 and H-2 protons. Moreover the downfield shift of C-6 of this unit at 68.6 ppm, respect to the value of 61.9 ppm for an

unsubstituted glucose (Lipkind *et al*., 1988), revealed that it was 6-linked. The residue **B** with H-1/C-1 signals at δ 4.59/102.6 was assigned to a β-glucose ($^3J_{H-1,H-2}$ 8.0 Hz). As all the protons and carbons chemical shift of this residue were in good agreement with that of an unsubstituted glucose this unit was deduced to be terminal.

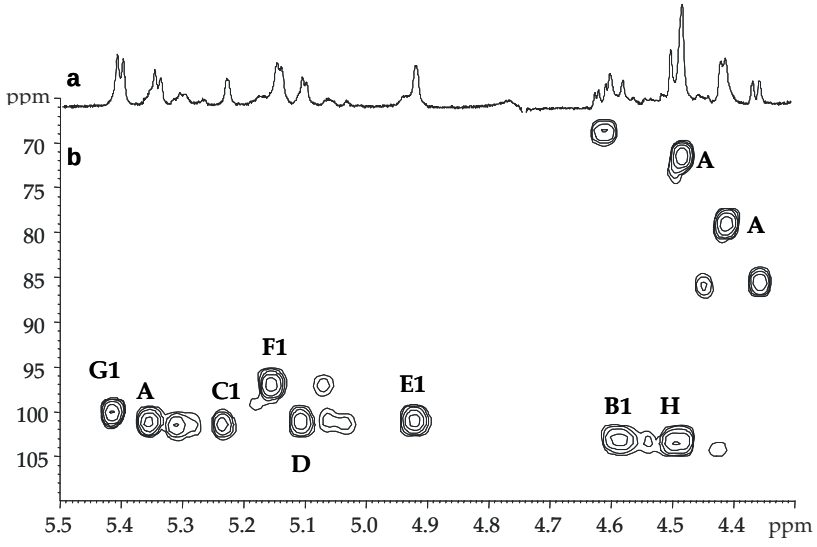

Fig. 3.7. HSQC-DEPT NMR spectrum recorded for OS_{AcOH}, Aceton was used as internal standard (2.225-31.45 ppm)

The residue **F** showed H-1/C-1 signals at δ 5.16/96.6 and it was assigned to an α-glucosamine ($^3J_{H-1,H-2}$ 3.1 Hz) on the basis of the chemical shift of C-2 at δ 54.6. For this unit the downfield shift of its C-4 revealed that it was 4-linked. The residue **A** with H-1/C-1 signals at δ 5.35/100.7 was assigned to an α-galacturonic acid on the basis of the small vicinal coupling constant ($^3J_{H-1,H-2}$ 4.1 Hz), of the five protons spin system and the value of the chemical shift of C-6 at 175.4 ppm. Finally the residue **E** with H-1/C-1 signals at δ 4.92/100.6 was assigned to an α-heptose on the basis of the low values of the $^3J_{H-1,H-2}$ and $^3J_{H-2,H3}$, which suggested, together with the carbons chemical shift, a *manno* configuration. In addition all the carbons and protons chemical shift values suggested a terminal residue. This data were in agreement with the methylation

analysis of *N*-acetylated and reduced OS_{AcOH} which revealed the presence of terminal glucose, 6-linked glucose, 4-linked glucosamine, 4-linked galacturonic acid, terminal heptose, 3,4-linked heptose and 3,7 linked heptose.

TABLE 3.2. ^{1}H and ^{13}C-NMR chemical shifts (δ) for OS_{AcOH} from *K. pneumoniae* 52145 Δ*waaL*-Δ*wabO* mutant LPS obtained by acid hydrolysis, in D_2O at 298 K, on a Bruker Avance spectrometer operating at 400 and 125 MHz, respectively.

Residue	H1 C1	H2 C2	H3 C3	H4 C4	H5 C5	H6a C6	H6b/7a C7	H7b
A 4-α-GalA	5.35 100.7	3.92 69.8	4.13 69.7	4.41 79.8	4.49 71.5	 175.4		
B *t*-β-Glc	4.59 102.6	3.30 75.2	3.52 76.0	3.37 69.8	3.40 76.2	3.90 61.4	3.75	
C 3,7-α-Hep	5.24 101.4	4.16 70.8	4.01 79.6	4.01 66.3	3.71 72.7	4.18 68.9	3.79 71.3	3.86
D 3,4-α-Hep	5.12 100	4.06 70.3	4.22 75.9	4.15 74.6	3.73 72.6	3.94 68.6	3.67 63.1	3.73
E *t*-α-Hep	4.92 100.6	4.00 70.1	3.86 72.2	3.86 66.3	3.62 71.7	4.04 66.9	3.84 63.7	3.87
F 4-α-GlcN	5.16 96.6	3.24 54.6	4.13 71.0	3.77 76.4	4.26 71.2	3.84 60.2	3.84	
G 6-α-Glc	5.42 99.8	3.61 71.7	3.70 72.7	3.51 69.4	3.88 71.9	4.18 68.6	3.92	
H *t*-β-Glc	4.49 102.8	3.32 73.3	3.51 75.6	3.36 69.9	3.40 76.3	3.74 62.2	3.93	

The sequence of residues in OS_{AcOH} was inferred by inter-residue nuclear Overhauser enhancements obtained by a ROESY experiment (Table 3.3).

By comparing the chemical shift data of OS_{AcOH} reported in Table 3.2 with those reported for acetic acid hydrolysis product obtained from *Klebsiella pneumoniae* Δ*waaL* mutant LPS (Reguè *et al*., 2005 (b)), it was possible to deduce the lack of a 7-substituted heptose together with the appearance of a terminal heptose unit.

Table 3.3. Nuclear Overhauser enhancements (ROESY) interresidue connectivities for the anomeric protons in OS_{AcOH}.

H-1 of sugar residue	NOE correlations
GalA **A**	**C** 3-H
Glc **B**	**D** 4-H, 3-H
Hep **C**	**D** 3-H
Hep **E**	**C** 7-H
GlcN **F**	**A** 4-H
Glc **G**	**F** 4-H
Glc **H**	**G** 6-H

Based on the data obtained from both the alkaline and acid degradation of LPS the products OS_{KOH} and OS_{AcOH} have structures **1** and **2** respectively, which allow us to conclude that the *wabO* gene codify for the transfer of the terminal-GalA.

1

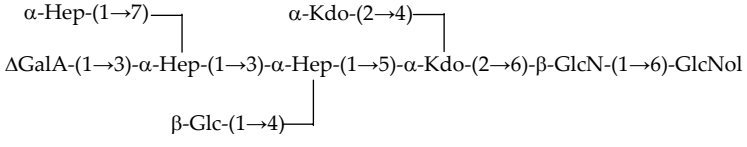

2

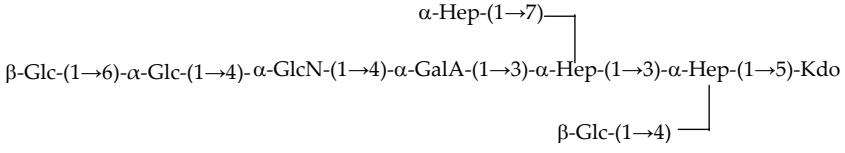

Moreover an *in vitro* assay (data not shown) demonstrates that the purified WabO is able to catalyze the transfer of GalA from UDP-GalA to the acceptor LPS isolated from the Δ*wabO* mutant, but not to the LPS isolated from Δ*waaQ* mutant (deficient in L,D-Hep III (residue **E**), see also Figure 1.10), in agreement with structural data.

3.2.2 Capsule association to the cell surface.

In order to correlate the GalA transferase enzymatic activity with the pathogen virulence and the amount of cell-bound capsule, transmission electron microscopy experiments were performed (Figure 3.8). The experiments were carried out in Spanish laboratories by using specific anti-K2 capsule serum with *Klebsiella pneumoniae* 52145 Δ*wabO* whole cells. It showed a drastic reduction in the amount of cell-bound capsule in comparison to wild type (Figure 3.8). A similar result was obtained using *Klebsiella pneumoniae* 52145 double mutant Δ*waaL*-Δ*wabO* cells versus Δ*waaL*. As expected, introduction of *wabO* restored wild type levels of cell surface associated K2 capsule (Figure 3.8).

The presence of an ionic interaction between the core and the capsular polysaccharide in of *Klebsiella pneumoniae* strain 52145 has been previously established (Fresno *et al*., 2006)

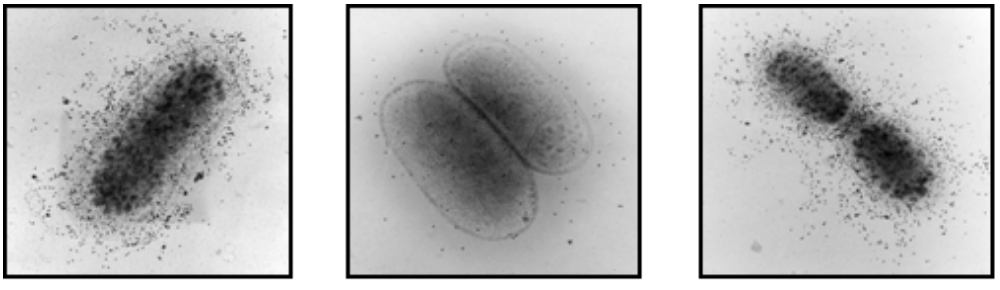

Fig. 3.8. Transmission electron microscopy experiments performed on the wild type (1), the Δ*wabO* mutant (2) and on the ΔwabO mutant after complementation(3).

In order to confirm this result the LPS extraction from *Klebsiella pneumoniae* Δ*waaL*-Δ*wabO* double mutant cells was repeated using a modified PW method. After ultracentrifugation the supernatant was freeze-dried and the sugar GC-MS analysis showed the presence of both LPS and K2 capsule monosaccharides. This fraction was

then purified on a sephacryl S-200 column using as eluent a buffer with an high ionic strength (10mM TRIS, 0.2M NaCl) containing the metal ion chelator EDTA and the dissociating detergent DOC, as previously reported (Fresno *et al*., 2006). The fractions were detected by SDS-PAGE. The electrophoresis analysis showed a separation of the two components after reiteration of the procedure.

Fig. 3.9. a) eletrophoresis profile of the sample obtained after ultracentrifugation of the extract. It shows the presence of both the LPS and of the CPS. b-c) electrophoresis profile of two fractions obtained after gel-filtration in denaturing conditions, containing the CPS and the LPS respectively.

3.2.3 Discussion.

The role of galacturonic acid in *Klebsiella pneumoniae* pathogenicity and in outer membrane stability has been well established (Fresno *et al*., 2006; Frirdich *et al*., 2005; Frirdich and Whitfield, 2005). In this work a new glycosyl transferase has been identified for the core LPS biosynthesis of *Klebsiella pneumoniae* 52145. NMR and MS analysis of LPS from the Δ*waaL*-Δ*wabO* mutant together with in vitro assay indicate that *wabO* encodes for a galacturonic acid transferase. This finding complete the characterization of the *Klebsiella pneumoniae* type 2 core gene cluster and confirmed the presence of an ionic interaction between core OS and K-antigen in *Klebsiella pneuomoniae*, providing a direct prove for the involvement of GalA residues in this interaction (Fresno *et al*., 2007).

Even if not all the capsulated strains in *Klebsiella pneumoniae* are virulent, the capsular polysaccharides are thought to be one of the major virulence determinants. Capsular polysaccharides in *Klebsiella pneumoniae* are classified in 77 serotypes. They are mostly constituted of repeating units consisting of four to six sugars, very often comprising uronic acids. Nevertheless, among clinical isolated strains, 25 of the 77 capsular types have been found.

Because of its role in virulence a CPS based vaccine was thought to be developed for *Klebsiella pneumoniae*. To be effective and of wide utility, a CPS based vaccine should contain at least 25 CPS types. Moreover it must be considered that CPS could cause autoimmunity, due to similarity between CPS and glycosidic groups present on the host cell surface.

Alternative approaches must be considered. For example the development of new antibiotics able to affect the amount of capsule retained on the cell surface of the bacteria.

With this work we provide a new target for drug development with the finding of a glycosyltransferase that is able to drastically reduce the cell bound K2 polysaccharide on the *Klebsiella pneumoniae* cell surface.

3.2.4 Experimental part.

3.2.4.1 Bacterial growth, LPS isolation and electrophoresis.

Bacteria were grown in LB broth and LB agar. LB media was supplemented with kanamycin (50 μg/ml), ampicillin (100 μg/ml), chloramphenicol (20 μg/ml), and tetracycline (25 μg/ml) when needed.

LPS was extracted from dry cells according to the phenol/chloroform/light petroleum ether method (Galanos *et al.*, 1969) and the yield resulted to 2.6%. LPS samples were separated by N-[2-hydroxy-1,1-bis(hydroxymethyl)ethyl]glycine (Tricine)-SDS-PAGE and visualized by silver staining as previously described (Tsai and Frasch, 1982)

3.2.4.2 Isolation of oligosaccharides OS_{KOH} and OS_{AcOH}.

An aliquot of LPS (50 mg) was suspended in 1M THF/anhydrous hydrazine (5 mL), stirred at 37 °C for 90 min and then cooled in a ice bath. Cold acetone was added to allow the *O*-deacylated LPS precipitation (Holst, 2000). The suspension was then centrifuged (4 °C, 3000 g, 30 min) and the precipitate was washed twice with cold acetone, dried, and then dissolved in water and lyophilized (35 mg). The sample was treated with 48% HF (1.2 mL, 4 °C, 48 h) and then reduced in 0.1 M NaOH with 6 mg of $NaBH_4$. Complete de-acylation was achieved by treatment with 4 mL of 4 M KOH for 16 h at 120 °C. The oligosaccharides were purified from salts by gel-filtration chromatography on a Sephadex G10 column (Pharmacia, 1.5 x 47 cm, H_2O as eluant, flow rate 22 mL h^{-1}), giving after lyophilization a residue of 9 mg (OS_{KOH}).

To obtain OS_{AcOH} another aliquot of LPS (20 mg) was hydrolyzed in 1% acetic acid (100 °C, 120 min) and the precipitate was removed by centrifugation (8000 x g, 30 min) and lyophilized to give Lipid A (10 mg). The supernatant was lyophilized (6 mg).

3.2.4.3 General and analytical methods.

Monosaccharides were analyzed as their methyl glycoside acetates. Briefly, a sample (1 mg) of LPS was dried over P_2O_5 overnight, treated with 1M HCl/CH_3OH (1 mL) at 80 °C for 20 h and the crude reaction was extracted twice with hexane. The methanol layer was then neutralized with Ag_2CO_3, dried and acetylated.

The absolute configuration of the residues was determined by the gas-chromatographic published method of the acetylated (*S*)-2-octyl glycosides (Leontein *et al.*, 1978).

For methylation analysis 1 mg of OS_{AcOH} was first reduced with $NaBH_4$ and then *N*-acetylated by treating it with acetic anhydride in dry methanol. After evaporation of the solvents, the sample was methylated using CH_3I in DMSO and NaOH (Ciucanu and Kerek, 1984). Briefly, the methylated sample was carboxymethyl reduced with $NaBD_4$ in ethanol, mild hydrolyzed (0.1 M TFA, 100°C, 30 min) to cleave ketosidic linkage, reduced by using $NaBD_4$, then totally hydrolyzed (2 M TFA, 120°C, 2h), reduced with $NaBD_4$ and finally acetylated (Ac_2O 50 µl, Py 100 µl).

Partially methylated alditol acetates and methyl glycoside acetates were analyzed on a Agilent Technologies gas chromatograph 6850A equipped with a mass selective detector 5973N and a Zebron ZB-5 capillary column (Phenomenex, 30 m x 0.25 mm i.d., flow rate 1 ml/min, He as carrier gas). Acetylated methyl glycosides analysis was performed with the following temperature program: 150° for 3 min, 150°→240° at 3° C/min. For partially methylated alditol acetates the temperature program was: 90 °C for 1 min, 90 °C →140 °C at 25 °C/min, 140 °C→200 °C at 5 °C/ min, 200 °C →280 °C at 10 °C/min, 280°C for 10 min. Analysis of acetylated octyl glycosides was performed as follows: 150 °C for 5 min, 150 °C→240 °C at 6 °C/min, 240 °C for 5 min.

3.2.4.4 LPS-CPS co-extraction and separation.

The cell were extracted by using a mixture of phenol and phosphate buffer (20mM Na_3PO_4, pH 7) in 1:1 (v/v) ratio at 68°C. The water phase, containing the sample was dyalized and lyophilized (100 mg).

LPS and CPS separation was performed by gel filtration with an S-200 column (1.76 x 850 mm) eluted with 10mM TRIS, 0.2M NaCl, 5 mM EDTA and 0.25% DOC buffered at pH 8, as reviously reported (Fresno *et al*., 2006). The fractions were detected by 15% SDS-PAGE.

3.2.4.5 NMR spectroscopy.

^{1}H-NMR spectra were recorded in D_2O at 400 MHz with a Bruker DRX 400 Avance spectrometer equipped with a reverse probe, in the FT mode at 303 K. ^{13}C and ^{1}H chemical shifts were measured in D_2O using acetone as internal standard (δ 2.225 and 31.45 for proton and carbon, respectively). Two-dimensional homo- and heteronuclear experiments (COSY, TOCSY, ROESY and HSQC-DEPT) were performed using standard pulse sequences available in the Bruker software.

3.2.4.6 Mass spectrometry analysis.

Positive and negative ions reflectron time-of-flight mass spectra (MALDI-TOF) were acquired on a Voyager DE-PRO instrument (Applied Biosystems) equipped with a delayed extraction ion source. Ion acceleration voltage was 25 kV, grid voltage was 17 kV, mirror voltage ratio 1.12 and delay time 150 ns. Samples were irradiated at a frequency of 5 Hz by 337 nm photons from a pulsed nitrogen laser. PSD was performed using an acceleration voltage of 20 kV. The reflectron voltage was decreased in 10 successive 25% steps. Mass calibration was obtained with a maltooligosaccharide mixture from corn syrup (Sigma). A solution of 2,5-

dihydroxybenzoic acid in 20% CH_3CN in water at a concentration of 25 mg/ml was used as the MALDI matrix. One μl of matrix solution was deposited on the target followed by loading of 1 μl of the sample. The droplets were allowed to dry at room temperature. Spectra were calibrated and processed under computer control using the Applied Biosystems Data Explorer software.

Chapter 4

Function Determination of the YibD Protein of *Escherichia coli* Responsible of Capsule Association to the Cell Membrane

4.1 Background of the work.

Once we determined the function of the Orf10 (WabO) in *Klebsiella pneumoniae,* we searched for similarities of the aminoacidic sequence in the database. YibD of *E. coli* showed high similarity with WabO. Furthermore the protein contained a conserved domain, typically presents in glycosyltransferases. The *yibD* gene is located upstream of the *waa* cluster of all *E. coli* core types. Nevertheless the high similarity with the WabO suggested that YibD could be involved in the transfer of a glycosidic residue to the core oligosaccharide.

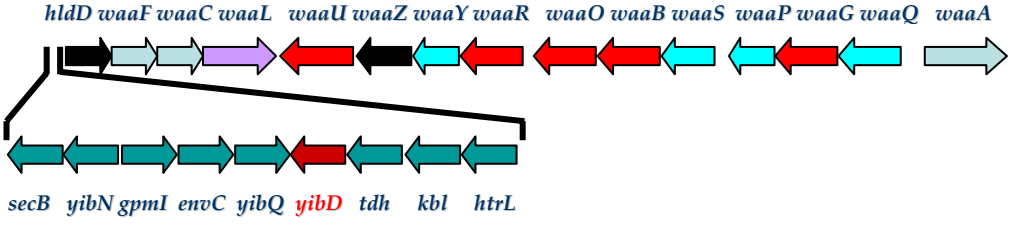

Fig. 4.1. Cluster *waa* of the genes involved in the core oligosaccharide biosynthesis of E.coli K-12. It is also shown the region upstream of that cluster, which contains the *yibD* gene.

Since in *Klebsiella pneumoniae* we found a strict relation between the *wabO* gene and the capsule association to the bacteria cell surface, some experiments were performed aiming at study the role of the *yibD* gene in capsule association to the cell membrane in *E. coli* O16:K1 (K-12 core type).

A mutant, which presented deletion in the *yibD* gene, showed a decrease in the amount of capsule attached to the cell surface, when analysed by E.L.I.S.A. with anti-K1 antibodies.

On the basis of these data, we decided to look for structural modification in the core oligosaccharide in the *yibD* mutant of *E. coli*.

In order to simplify this analysis two mutants were constructed for *E. coli* O16:K1 (K-12 core type). The Δ*waaL* mutant and the double non-polar Δ*waaL*-Δ*yibD* mutants. Since the function of the *waaL* gene is known to be involved in the O-antigen linkage to the core-lipid A, both the mutants possessed a rough type LPS.

4.2 Results.

4.2.1 Analysis of the LPS from Δ*waaL* and Δ*waaL*-Δ*yibD* mutants.

The dried cells in both cases were extracted by the PCP method (phenol: chloroform: light petroleum; Galanos, 1969). The recovered material was then analyzed by SDS-PAGE which confirmed the rough nature of the LPSs (Figure 4.2).

The sugar analysis on both samples was performed by GC-MS analysis of acetylated methyl glycosides derivatives. The chromatograms did not reveal any difference between the two mutants. In particular, in both cases, rhamnose, galactose, glucose, glucosamine, heptose and Kdo were present without significative differences in the relative amounts.

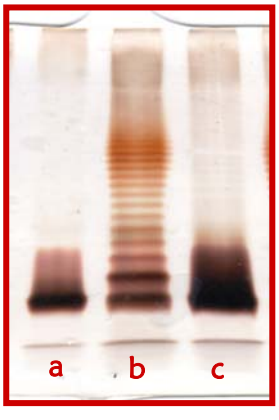

Fig. 4.2 12% SDS-PAGE analysis of the LPS from Δ*waaL* and Δ*waaL*-Δ*yibD* mutants (**c** and **a**, respectively), compared with the wild type LPS (**b**).

4.2.1.1 Analysis of the de-*O*-acylated LPS from Δ*waaL* and Δ*waaL*-Δ*yibD* mutants.

The LPS from the Δ*waaL* and Δ*waaL*-Δ*yibD* mutants were de-*O*-acylated with anhydrous hydrazine obtaining LPS-OH$_{waaL}$ and LPS-OH$_{waaL\text{-}yibD}$ respectively. The samples were freeze-dried and analyzed by ESI-MS.

The negative ions ESI-MS spectrum of the LPS-OH$_{waaL}$ (Figure 4.3) revealed the presence of a complex mixture of LPS-OH structures that had a composition as indicated in Table 4.1. The most abundant species, named M^3, M^6, M^8 and M^{10}, shared the same composition except for phosphates content. In addition, less abundant species, containing three Kdo units, were present, in agreement with the finding of only 10-15% of these species on the cell surface of *E. coli* K-12 (Frirdich *et al.*, 2003).

The ESI-MS spectrum (Figure 4.4; Table 4.2) of the LPS-OH$_{waaL\text{-}yibD}$ appeared as complex as that of the LPS-OH$_{waaL}$, but in the former the most abundant species contained only one Kdo unit. Moreover species containing three Kdo residues were completely absent.

These data suggested that the *yibD* gene is involved in the transfer of the Kdo III. To confirm this hypothesis, other *E. coli* K-12 mutants were constructed. In order to reduce the number of LPS structures to analyse, deep rough mutants were considered.

As stated above the gene responsible for core OS biosynthesis in *E. coli* are located in the *waa* locus (Figure 4.1). Since the WaaF is the heptosyl transferase responsible for the transfer of the second heptose in the inner core, a mutation in the *waaF* gene should provide highly truncated LPS structures (Figure 4.5). For this reason *E. coli* K-12 Δ*waaF* and Δ*waaF*-Δ*yibD* mutants were constructed and LPS structures of both mutants were determined.

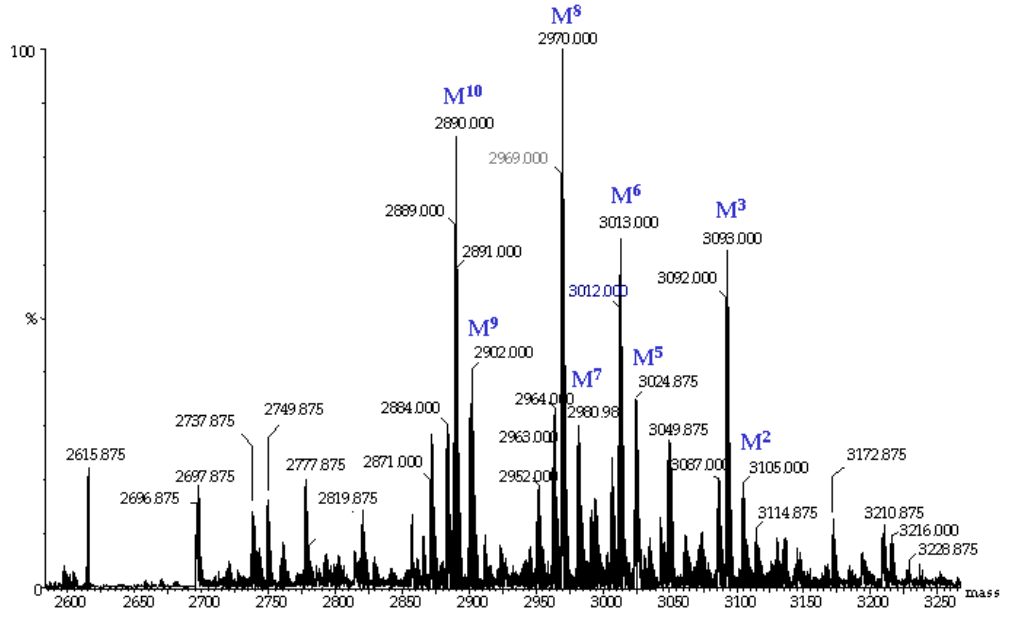

Fig. 4.3. Negative ions ESI-MS mass spectrum of LPS-OH*waaL*. For the species composition refer to the table 4.1.

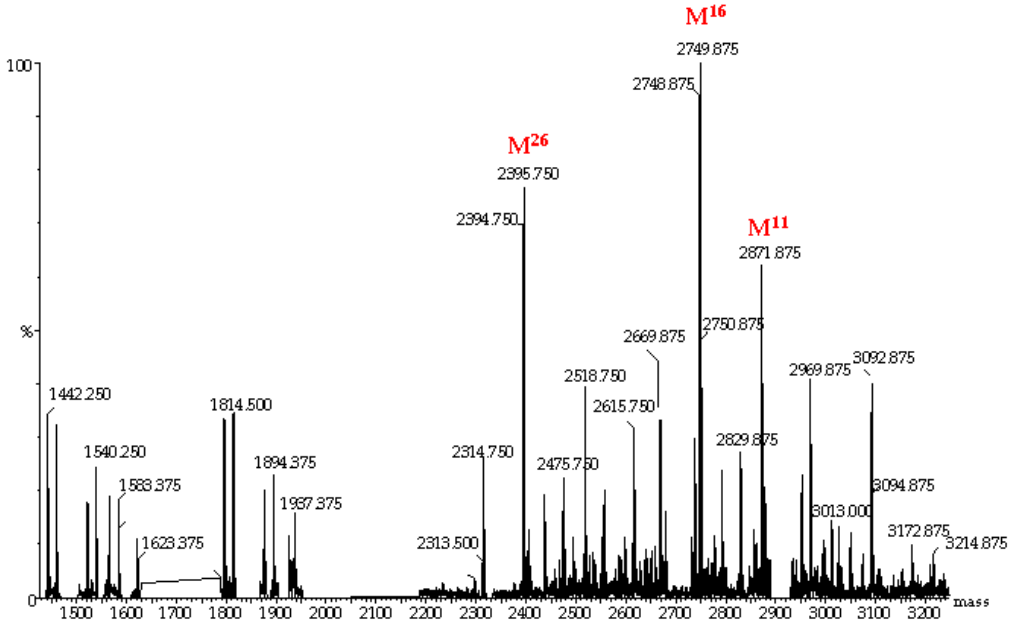

Fig. 4.4. Negative ions ESI-MS mass spectrum of LPS-OH*waaL-yibD*. For the species composition refer to the Table 4.2.

Table 4.1. *E. coli* LPS-OH$_{waaL}$ mass data. The spectrum was acquired in the negative ion mode. The most abundant species are indicated in blue.

Species	Observed mass (m/z)	Calculated mass (Da)	Composition
M^{1}	3171.93	3172.06	Gal$_1$Glc$_3$Hep$_4$Kdo$_2$GlcNAcGlcNAcyl$_2$P$_4$
M^{2}	3103.99	3103.99	Glc$_3$Hep$_3$Rha$_1$Kdo$_3$GlcNAcyl$_2$P$_5$EtN
M^{3}	**3091.92**	**3091.99**	**Gal$_1$Glc$_3$Hep$_4$Kdo$_2$GlcNAcyl$_2$P$_5$EtN**
M^{4}	3048.90	3048.94	Gal$_1$Glc$_3$Hep$_4$Kdo$_2$GlcNAcyl$_2$P$_5$
M^{5}	3023.97	3024.02	Gal$_1$Glc$_2$Hep$_3$Rha$_1$Kdo$_3$GlcNAcyl$_2$P$_4$EtN
M^{6}	**3011.99**	**3012.02**	**Gal$_1$Glc$_3$Hep$_4$Kdo$_2$GlcNAcyl$_2$P$_4$EtN**
M^{7}	2980.98	2980.98	Gal$_1$Glc$_2$Hep$_3$Rha$_1$Kdo$_3$GlcNAcyl$_2$P$_4$
M^{8}	**2968.98**	**2968.983**	**Gal$_1$Glc$_3$Hep$_4$Kdo$_2$GlcNAcyl$_2$P$_4$**
M^{9}	2900.95	2901.018	Gal$_1$Glc$_2$Hep$_3$Rha$_1$Kdo$_3$GlcNAcyl$_2$P$_3$
M^{10}	**2889.00**	**2889.017**	**Gal$_1$Glc$_3$Hep$_4$Kdo$_2$GlcNAcyl$_2$P$_3$**
M^{11}	2871.85	2871.93	Gal$_1$Glc$_3$Hep$_4$Kdo$_1$GlcNAcyl$_2$P$_5$ EtN
M^{12}	ND	2828.89	Gal$_1$Glc$_3$Hep$_4$Kdo$_1$GlcNAcyl$_2$P$_5$
M^{13}	2819.97	2819.962	Gal$_1$Glc$_3$Hep$_3$Kdo$_2$GlcNAcyl$_2$P$_4$EtN
M^{14}	ND	2791.967	Gal$_1$Glc$_3$Hep$_4$Kdo$_1$GlcNAcyl$_2$P$_4$EtN
M^{15}	2776.88	2776.92	Gal$_1$Glc$_3$Hep$_3$Kdo$_2$GlcNAcyl$_2$P$_4$
M^{16}	2748.90	2748.92	Gal$_1$Glc$_3$Hep$_4$Kdo$_1$GlcNAcyl$_2$P$_4$
M^{17}	2737.89	2737.87	Gal$_1$Glc$_2$Hep$_3$Kdo$_2$GlcNAcyl$_2$P$_5$EtN
M^{18}	2696.92	2696.95	Gal$_1$Glc$_3$Hep$_3$Kdo$_2$GlcNAcyl$_2$P$_3$
M^{19}	2679.90	2679.87	Gal$_1$Glc$_3$Hep$_3$Kdo$_1$GlcNAcyl$_2$P$_5$EtN
M^{20}	2668.94	2668.96	Gal$_1$Glc$_3$Hep$_4$Kdo$_1$GlcNAcyl$_2$P$_3$
M^{21}	2614.86	2614.87	Gal$_1$Glc$_2$Hep$_3$Kdo$_2$GlcNAcyl$_2$P$_4$
M^{22}	2556.86	2556.86	Gal$_1$Glc$_3$Hep$_3$Kdo$_1$GlcNAcyl$_2$P$_4$
M^{23}	2517.85	2517.82	Gal$_1$Glc$_2$Hep$_3$Kdo$_1$GlcNAcyl$_2$P$_5$EtN
M^{24}	2474.76	2474.77	Gal$_1$Glc$_2$Hep$_3$Kdo$_1$GlcNAcyl$_2$P$_5$
M^{25}	2437.81	2437.852	Gal$_1$Glc$_2$Hep$_3$Kdo$_1$GlcNAcyl$_2$P$_4$EtN
M^{26}	2394.79	2394.81	Gal$_1$Glc$_2$Hep$_3$Kdo$_1$GlcNAcyl$_2$P$_4$
M^{27}	2314.82	2314.843	Gal$_1$Glc$_2$Hep$_3$Kdo$_1$GlcNAcyl$_2$P$_3$

ND= not detected

Table 4.2. *E. coli* LPS-OH$_{waaL\text{-}yibD}$ mass data. The spectrum was acquired in the negative ion mode. The most abundant species are indicated in red.

Species	Observed mass (m/z)	Calculated mass (Da)	Composition
M^{1}	3171.93	3172.06	Gal$_1$Glc$_3$Hep$_4$Kdo$_2$GlcNAcGlcNAcyl$_2$P$_4$
M^{2}	ND	3103.99	Glc$_3$Hep$_3$Rha$_1$Kdo$_3$GlcNAcyl$_2$P$_5$EtN
M^{3}	3091.92	3091.99	Gal$_1$Glc$_3$Hep$_4$Kdo$_2$GlcNAcyl$_2$P$_5$EtN
M^{4}	3048.90	3048.94	Gal$_1$Glc$_3$Hep$_4$Kdo$_2$GlcNAcyl$_2$P$_5$
M^{5}	ND	3024.02	Gal$_1$Glc$_2$Hep$_3$Rha$_1$Kdo$_3$GlcNAcyl$_2$P$_4$EtN
M^{6}	3011.99	3012.02	Gal$_1$Glc$_3$Hep$_4$Kdo$_2$GlcNAcyl$_2$P$_4$EtN
M^{7}	ND	2980.98	Gal$_1$Glc$_2$Hep$_3$Rha$_1$Kdo$_3$GlcNAcyl$_2$P$_4$
M^{8}	2968.98	2968.983	Gal$_1$Glc$_3$Hep$_4$Kdo$_2$GlcNAcyl$_2$P$_4$
M^{9}	ND	2901.018	Gal$_1$Glc$_2$Hep$_3$Rha$_1$Kdo$_3$GlcNAcyl$_2$P$_3$
M^{10}	2889.00	2889.017	Gal$_1$Glc$_3$Hep$_4$Kdo$_2$GlcNAcyl$_2$P$_3$
M^{11}	**2871.85**	**2871.93**	**Gal$_1$Glc$_3$Hep$_4$Kdo$_1$GlcNAcyl$_2$P$_5$ EtN**
M^{12}	2828.87	2828.89	Gal$_1$Glc$_3$Hep$_4$Kdo$_1$GlcNAcyl$_2$P$_5$
M^{13}	ND	2819.96	Gal$_1$Glc$_3$Hep$_3$Kdo$_2$GlcNAcyl$_2$P$_4$EtN
M^{14}	2791.87	2791.96	Gal$_1$Glc$_3$Hep$_4$Kdo$_1$GlcNAcyl$_2$P$_4$EtN
M^{15}	*2776.88*	*2776.92*	*Gal$_1$Glc$_3$Hep$_3$Kdo$_2$GlcNAcyl$_2$P$_4$*
M^{16}	**2748.90**	**2748.92**	**Gal$_1$Glc$_3$Hep$_4$Kdo$_1$GlcNAcyl$_2$P$_4$**
M^{17}	2737.89	2737.87	Gal$_1$Glc$_2$Hep$_3$Kdo$_2$GlcNAcyl$_2$P$_5$EtN
M^{18}	ND	2696.95	Gal$_1$Glc$_3$Hep$_3$Kdo$_2$GlcNAcyl$_2$P$_3$
M^{19}	2679.90	2679.87	Gal$_1$Glc$_3$Hep$_3$Kdo$_1$GlcNAcyl$_2$P$_5$EtN
M^{20}	2668.94	2668.96	Gal$_1$Glc$_3$Hep$_4$Kdo$_1$GlcNAcyl$_2$P$_3$
M^{21}	2614.86	2614.87	Gal$_1$Glc$_2$Hep$_3$Kdo$_2$GlcNAcyl$_2$P$_4$
M^{22}	2556.86	2556.86	Gal$_1$Glc$_3$Hep$_3$Kdo$_1$GlcNAcyl$_2$P$_4$
M^{23}	2517.85	2517.82	Gal$_1$Glc$_2$Hep$_3$Kdo$_1$GlcNAcyl$_2$P$_5$EtN
M^{24}	2474.76	2474.77	Gal$_1$Glc$_2$Hep$_3$Kdo$_1$GlcNAcyl$_2$P$_5$
M^{25}	2437.81	2437.852	Gal$_1$Glc$_2$Hep$_3$Kdo$_1$GlcNAcyl$_2$P$_4$EtN
M^{26}	**2394.79**	**2394.81**	**Gal$_1$Glc$_2$Hep$_3$Kdo$_1$GlcNAcyl$_2$P$_4$**
M^{27}	2314.82	2314.843	Gal$_1$Glc$_2$Hep$_3$Kdo$_1$GlcNAcyl$_2$P$_3$

ND= not detected

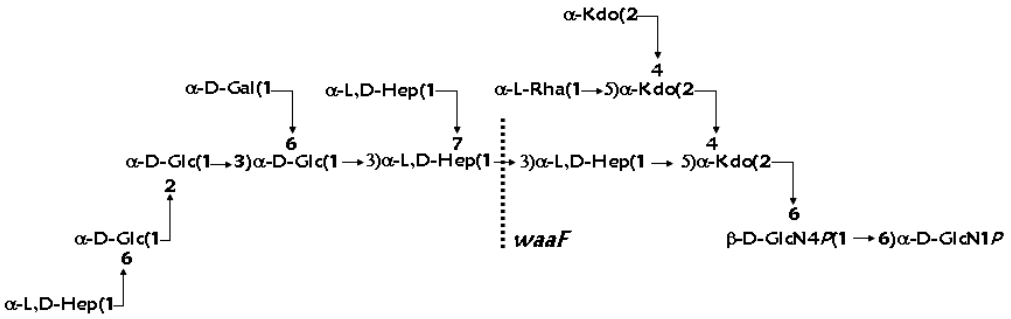

Fig. 4.5. K-12 core type structure of *E. coli*. WaaF is responsible for the transfer of the heptose II to heptose I.

4.2.2 Analysis of the LPS from Δ*waaF* and Δ*waaF*-Δ*yibD* mutants.

The LPSs were isolated from the dried cells by the PCP method (phenol: chloroform: light petroleum). The recovered material was then analyzed by SDS-PAGE which confirmed a high truncation of the core oligosaccharide in this mutants (Figure 4.6).

The sugar analysis revealed for both samples the presence of glucosamine, heptose and Kdo.

Fig. 4.6. 12% SDS-PAGE analysis of the LPS from the Δ*waaF* and the Δ*waaL* mutants (**a** and **b**, respectively). LPS_{waaF} run slightly faster that the LPS_{waaL}

4.2.2.1 Analysis of the de-*O*-acylated LPS from Δ*waaF* and Δ*waaF*-Δ*yibD* mutants.

The lipopolysaccharides from Δ*waaF* and Δ*waaF*-Δ*yibD* mutants were de-*O*-acylated with anhydrous hydrazine obtaining LPS-OH$_{waaF}$ and LPS-OH$_{waaF\text{-}yibD}$, respectively. The samples were analysed by ESI-MS in the negative-ion mode. As expected the LPS-OH$_{waaF}$ mass spectrum showed a reduced number of molecular species, and all the signals were identified as reported in Table 4.3. The most abundant species, named M^4 and M^7, resulted to be monophosphorylated and containing two and one Kdo residues, respectively. Nevertheless an other specie (M^1) at *m*/*z* 1724.61, which contained three Kdo residues, was present in lower amount.

Table 4.3. *E. coli* LPS-OH$_{waaF}$ mass data The spectrum was acquired in the negative ion mode. The reported masses refer to the charge deconvoluted spectrum and the main species are indicated in blue.

Specie	Observed mass (Da)	Calculated mass (Da)	Composition
M^1	1724.61	1724.75	$HepKdo_3GlcNAcyl_2P$
M^2	ND	1707.66	$HepKdo_2GlcNAcyl_2P_2PEtN$
M^3	1584.52	1584.65	$HepKdo_2GlcNAcyl_2P_2$
M^4	**1504.45**	**1504.69**	**$HepKdo_2GlcNAcyl_2P$**
M^6	1364.47	1364.59	$HepKdoGlcNAcyl_2P_2$
M^7	**1284.45**	**1284.63**	**$HepKdoGlcNAcyl_2P$**
M^8	952.37	952.47	$GlcNAcyl_2P_2$
M^9	872.35	872.51	$GlcNAcyl_2P$
M^{10}	632.08	632.18	$HepKdo_2$

ND: not detected

The mass spectrum of LPS-OH$_{waaF\text{-}yibD}$ showed the presence of several peaks, the composition of which have been identified and reported in Table 4.4. In particular the spectrum clearly showed the lack of the M^1 specie. The highest molecular weight peak, named M^2, was consistent with the presence of only two Kdo residues (Table 4.4). Moreover the main signal, named M^3, shared the same sugar backbone of M^2, but

with the loss of a phosphoryl ethanolamine. This results indicated once more that the *yibD* gene is involved in the transfer of the third Kdo residue.

Table 4.4. *E. coli* LPS-OH$_{waaF\text{-}yibD}$ mass data. The spectrum was acquired in the negative ion mode. The reported masses refer to the charge deconvoluted spectrum and the main species are indicated in red.

Specie	Observed mass (Da)	Calculated mass (Da)	Composition
M^1	ND	1724.75	HepKdo$_3$GlcNAcyl$_2$P
M^2	1707.50	1707.66	HepKdo$_2$GlcNAcyl$_2$P$_2$PEtN
M^3	**1584.52**	**1584.65**	**HepKdo$_2$GlcNAcyl$_2$P$_2$**
M^4	1504.45	1504.69	HepKdo$_2$GlcNAcyl$_2$P
M^6	1364.47	1364.59	HepKdoGlcNAcyl$_2$P$_2$
M^7	1284.45	1284.63	HepKdoGlcNAcyl$_2$P
M^8	952.32	952.47	GlcNAcyl$_2$P$_2$
M^9	872.38	872.51	GlcNAcyl$_2$P
M^{10}	632.08	632.18	HepKdo$_2$

ND: not detected

A slight difference in the phosphates content could be found between LPS-OH$_{waaF}$ and LPS-OH$_{waaF\text{-}yibD}$. This difference is anyway not relevant because phosphate groups are sensistive to the reaction alkaline conditions.

For a further confirmation about the attributed compositions, MS-MS experiments were performed on the two species M^1 and M^2 (Figure 4.7 and 4.8; Table 4.5 and 4.6). The fragmentation spectrum of M^1 showed the loss of two Kdo units from the parent ion signal at *m/z* 1723.829 giving the Y$_4$ and Y$_3$ ions at 1503.752 and 1283.678 *m/z* respectively. The presence of the signal at 1091.605 *m/z* indicated the loss of one heptose from the Y$_3$ ion, while the signal at 871.520 m/z was attributed to a Y$_2$ ion corresponding to the de-*O*-acylated lipid A. A type B ion was also found at *m/z* 851.258, whose composition is reported in Table 4.5. This signal was subjected to

secondary fragmentation with loss of one Kdo, giving the signal at 631.184 *m/z*. This data confirmed the composition of the M^1 species of the LPS-OH_{waaF}.

Table 4.5. MS-MS data of the M^1 specie belonging to LPS-OH_{waaF}

signal	Observed mass (m/z)	Calculated mass (Da)	Composition
M	1723.829	1724.745	$Kdo_3HepGlcNAcyl_2P$
Y_4	1503.752	1504.687	$Kdo_2HepGlcNAcyl_2P$
Y_3	1283.678	1284.628	$KdoHepGlcNAcyl_2P$
Y_3 - Hep	1091.605	1092.565	$KdoGlcNAcyl_2P$
Y_2	871.520	872.507	$GlcNAcyl_2P$
B_3	851.258	852.238	Kdo_3Hep
B_3 -Kdo	631.184	632.180	Kdo_2Hep

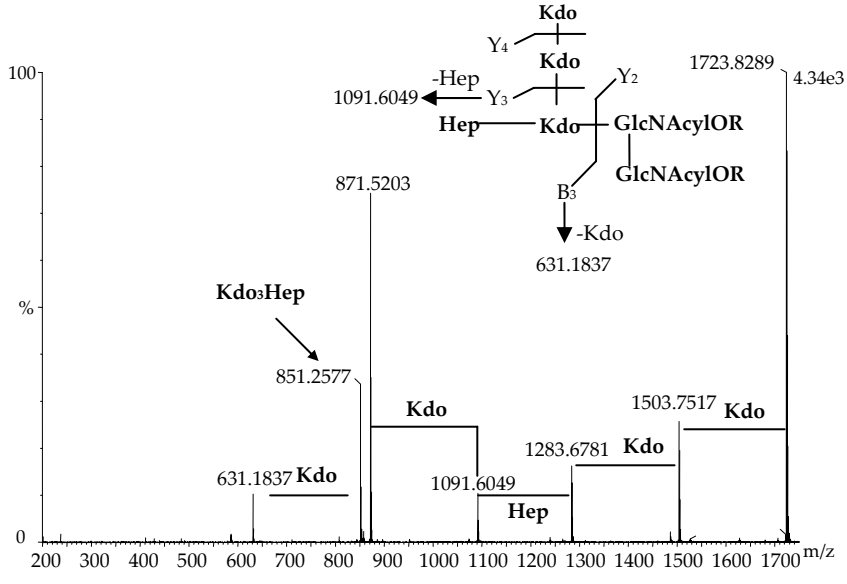

Fig. 4.7. MS-MS mass spectrum of M^1 specie belonging to LPS-OH_{waaF}

The MS-MS experiment was performed on the LPS-$OH_{waaF\text{-}yibD}$ starting from the specie M^2 (Figure 4.8, Table 4.6). The spectrum showed the loss of both Kdo and PEtN, which

Table 4.6. MS-MS data of the M^2 specie belonging to LPS-$OH_{waaF\text{-}yibD}$

signal	Observed mass (m/z)	Calculated mass(Da)	Composition
$[M-H]^-$	1706.427	1707.661	$Kdo_2HepGlcNAcyl_2P_3EtN$
M-P	1608.488	1609.685	$Kdo_2HepGlcNAcyl_2P_2EtN$
Y_3	1363.403	1364.595	$KdoHepGlcNAcyl_2P_2$
Y_2	951.320	952.473	$GlcNAcyl_2P_2$

lead to the formation of a Y_3 ion at *m*/*z* 1363.403. Moreover a Y_2 ion at *m*/*z* 951.320 was present, which was attributed to the de-*O*-acylated lipid A.

In the *E. coli* K-12 core type, the PEtN had been found as non stoichiometric substituent both in position 7 of the Kdo II and in position 4 of the Hep I. In this case, the simultaneous loss of Kdo and PEtN suggested that it is located on the Kdo residue. In conclusion, the mass spectrometric analysis confirmed that the LPS-$OH_{waaF\text{-}yibD}$ did not contain the third Kdo residue.

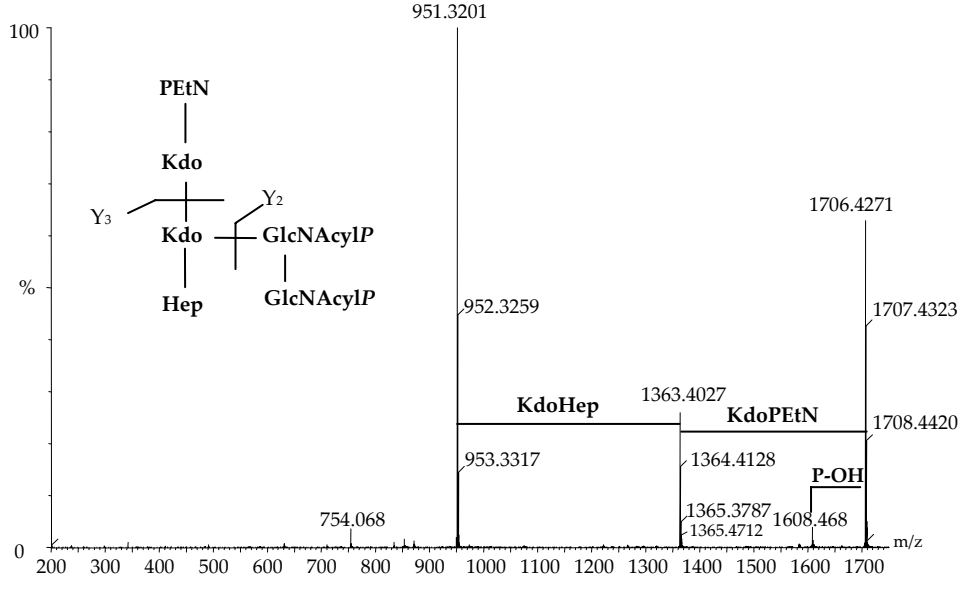

Fig. 4.8. MS-MS spectrum of the species M^2 belonging to LPS-$OH_{waaF\text{-}yibD}$. The fragments compositions is reported in Table 4.6

4.3 Discussion.

The *yibD* gene is located upstream of the *waa* cluster of *E. coli* and the corresponding YibD protein showed high similarity with the WabO glycosyltransferase, which is involved in the core biosynthesis and in the K2 CPS association to the cell surface in *Klebsiella pneumoniae* 52145 (Fresno *et al*., 2007).

The *E. coli* Δ*yibD* mutant showed a decrease in the amount of cell bound capsule suggesting for YibD a function similar to that of the *Klebsiella pneumoniae* WabO glycosyltransferase.

To verify this hypothesis the LPS from various *E. coli* K-12 mutants were analysed. First the LPS from Δ*waaL* and Δ*waaL*-Δ*yibD* mutants were compared. The *O*-deacylated LPS were analysed by ESI mass spectrometry. The analysis of the spectra suggested that the difference between the LPS-OH$_{waaL}$ and LPS-OH$_{waaL\text{-}yibD}$ resides in the inner core and in particular in the third Kdo residue, which was absent in the LPS$_{waaL\text{-}yibD}$. To confirm these results, ESI-MS analysis was performed on mutants with an high truncated core too (LPS$_{waaF}$ and LPS$_{waaF\text{-}yibD}$).

Thus we determined the function of the *yibD* gene which resulted to be responsible of the transfer of the third Kdo residue in the inner core of *E. coli* O16:K1 (K-12 core type). The lack of the negatively charged Kdo residue leads to a decrease in the cell bound capsule. These data suggested that also in this case, as for *Klebsiella pneumoniae*, an ionic interaction could contribute to the association of the negatively charged K-1 CPS to the cell wall. Nevertheless the small amount of CPS produced by this strain of *E. coli* made not possible to directly prove it.

4.4 Experimental part.

4.4.1 Bacterial growth and LPS isolation.

All the analyzed mutants were grown in LB medium at 37°C. LPS was extracted from dry cells of *E. coli* mutants Δ*waaL* (3,6 g), Δ*waaL*-Δ*yibD* (5,2 g), Δ*waaF* (2,7 g) and Δ*waaF*-Δ*yibD* (4,1 g), according to the phenol/chloroform/light petroleum ether method (Galanos *et al.*, 1969) and the yield resulted to 3.52, 2.7, 1.75 and 4,6% respectively.

4.4.2 General and analytical methods.

Monosaccharides were analyzed as their methyl glycoside acetates. Briefly, a sample (1 mg) of LPS was dried over P_2O_5 overnight, treated with 1M HCl/CH_3OH (1 mL) at 80 °C for 20 h and the crude reaction was extracted twice with hexane. The methanol layer was then neutralized with Ag_2CO_3, dried and acetylated.

Methyl glycoside acetates were analyzed on a Agilent Technologies 6850A Gas Chromatograph equipped with a 5973N MS instrument and a Zebron ZB-5 capillary column (Phenomenex, 30 m x 0.25 mm i.d., flow rate 1 ml/min, He as carrier gas). The analysis was performed with the following temperature program: 150° for 3 min, 150°→240° at 3° C/min.

4.4.3 Preparation of LPS-OH$_{waaL}$, LPS-OH$_{waaL\text{-}yibD}$, LPS-OH$_{waaF}$ and LPS-OH$_{waaF\text{-}yibD}$.

An aliquot of each LPS (50, 50, 21 and 80 mg, respectively) was suspended in anhydrous hydrazine ([LPS]=25 mg-mL), stirred at 37 °C for 90 min and then cooled in a ice bath. Cold acetone was added to allow the *O*-deacylated LPS precipitation (Holst, 2000). The precipitate was then centrifuged (4 °C, 7000 g, 30 min), washed

twice with cold acetone, dried, and then dissolved in water and lyophilized. The yield resulted to 70%.

4.4.4 Mass spectrometric analysis.

High resolution ESI-MS and MS-MS spectra were acquired on a Q-TOF premier instrument (WATERS).

The capillary voltage was set at 3.5-4.0 kV and a capillary temperature of 180 °C was employed; All the analyzed molecules were dissolved in CH_3OH and then diluted in CH_3OH/H_2O (1:1). Samples were injected into the spectrometer at a flow rate of 5 mL/min using an external syringe pump.

Chapter 5

Structural Characterization of the Core Region from the Lipopolysaccharide of the Haloalkaliphilic Bacterium *Halomonas pantelleriensis*

5.1 Introduction.

5.1.1 Extremophile bacteria.

An extremophile is an organism that thrives in and may even require physically or geochemically extreme conditions that are detrimental to the majority of life on Earth. Extremophile microorganisms are found in all three domains of life: *Archaea*, *Bacteria*, and *Eucarya* and they are grouped in many different classes, each corresponding to the way its environmental niche differs from mesophilic conditions (Table 5.1).

The interest towards these microorganisms is due mainly to the production of biocatalysts that are functional under extreme conditions (van den Burg, 2003).

Table. 5.1 Some classes of extremophiles and the corresponding characteristics.

Type	Characteristics
Acidophile	optimum pH level at or below pH 3 for growth
Alkaliphile	optimal growth at pH levels of 9 or above
Halophile	requiring at least 2M of salt, NaCl, for growth
Metalotolerant	tolerating high levels of dissolved heavy metals in solution, such as copper, cadmium, arsenic, and zinc.
Psychrophile/Cryophile	grows better at temperatures of 15 °C or lower
Thermophile	can thrive at temperatures between 60-80 °C

5.1.1.1 Halophiles.

Halophile bacteria are able to optimally grow in environments with high concentration of salt. Halophiles can be classified into three groups on the basis of their response to NaCl: (i) the slight halophiles (most rapid growth at 2 to 5% NaCl [0.34 to 0.85 M]), (ii) the moderate halophiles (most rapid growth at 5 to 20% NaCl [0.85 to 3.4 M]), and (iii) the estreme halophiles (most rapid growth at 20 to 30% NaCl [3.4 to 5.1 M]) (Ollivier *et al.*, 1994).

Halophiles are submitted to osmotic stress due to the high concentration of salt outside of the cell. Two different strategies enable these microorganisms to survive in such conditions. One requires the maintainement of high salt concentration within the cell, osmotically equivalent to the outer cell salt concentration. This implies that all the intracellular system has to be adapted to such conditions. The other one consist in the balance of the osmotic pressure from the environment using organic compatible solutes, which range from sugars, polyols, amino acids and their respective derivatives, ectoines and betaines. The advantage, in this case, is that the cell does not

need special adaptation of the intracellular system (da Costa, 1998; Oren, 1999; Oren, 2002).

Moreover, it has been reported that salt-tolerant bacteria possess a more compact cell wall, tightly bound to the cytoplasmic membrane. At the same time they showed an increased amount of negatively charged lipids (Vreeland *et al*., 1984; Russel N. J., 1989; Adams and Russel, 1992; Romano *et al.*, 2001, Giordano *et al*., 2007).

5.1.1.2 Alkaliphiles.

The alkaliphile, uses Na+/H+ antiporters in pH regulation which result in an extraordinary capacity for pH homeostasis. Above pH 9.5, aerobic alkaliphiles maintain a cytoplasmic pH that is two or more units below the external pH.

This chemiosmotically adverse delta pH is bypassed by use of an electrochemical gradient of Na+ rather than of protons to energize solute uptake and motility (Krulwich, 1995). In this way the cytoplasm does not reach very high values of pH and the intracellular enzymes from these microorganisms do not need to be adapted to estreme growth conditions (van den Burg, 2003).

The cell surface may play a key role in keeping the intracellular pH value in the range between 7 and 8.5, allowing alkaliphiles to thrive in alkaline environments, although adaptation mechanisms have not yet been clarified.

5.1.2 *Halomonas pantelleriensis.*

Halomonas pantelleriensis is a Gram-negative haloalkaliphilic bacterium isolated from the sand of the volcanic Venus mirror lake, closed to seashore in the Pantelleria island in the south of Italy. It is able to optimally grow in media containing 3-15% (w/v) total salt and at pH between 9-10 (Romano *et al*., 1996; Romano *et al*., 2001). It accumulates osmoprotectants such as glycine betaine, ectoine, hydroxyectoine and glutamate, whose relative proportion depends on growth conditions. The main lipids produced by the bacterium were 1,2 diacylglycero-3-phosphorylethanolamine (PEA), 1,2 diacylglycero-3-phosphoryl-glycerol (GPG) and cardiolipin (DPG). The predominant fatty acids were C16:0 and C18:1, minor fatty acids were C16:1 and C18:0. The relative percentage of polar lipids and fatty acids were affected by growth conditions (Romano *et al*., 2001).

Several haloalkaliphilic bacteria are able to thrive in alkaline hyper-saline environments thanks to their ability to maintain a lower salt concentration and a lower pH inside the cell. The mechanisms on the basis of this phenomenon are far from being elucidated.

The main research in this field is aimed at the study of the cell wall components and differences in the outer membrane lipid composition have been found.

The lipopolysaccharides, which constitute the 75% of the outer membrane of Gram-negative bacteria, are supposed to play a crucial role in the outer membrane permeability properties. Nevertheless, few data are available about LPS structure from haloalkaliphilic microorganisms (de Castro *et al.*, 2003), even if the determination of the LPS primary structure is the mandatory starting point for the comprehension of the biological role played by these molecules.

Recently it was determined the O-chain repeating unit structure of the LPS of *Halomonas pantelleriensis* which is constituted by the highly charged tetrasaccharidic

repeating unit →4)-β-D-Glc*p*A-(1→4)-α-D-Gal*p*NAcA-(1→3)-β-L-Qui*p*NAc-(1→2)-β-D-[4-*O*-(*S*)-1-carboxyethyl]-Glc*p*A-(1→ (Corsaro *et al.*, 2006).

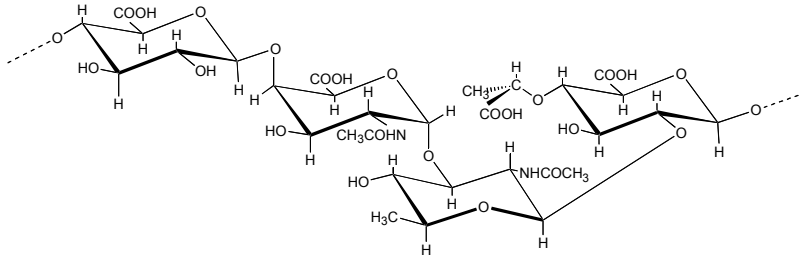

Here is reported the complete core oligosaccharide structure of *Halomonas pantelleriensis* LPS (Pieretti *et al*., 2007), which to my knowledge represents the first core structure described for a LPS of an extremophile bacterium. In addition, the sugar that linked the O-chain to the core oligosaccharide was identified.

5.2 Results.

5.2.1 LPS isolation and preliminary data.

The LPS was recovered from dried bacteria by extraction with phenol/chloroform/light petroleum as described (Galanos *et al.*, 1969). The sample was free from nucleic acids as confirmed by sugar analysis and UV spectroscopy, after DNase and RNase treatment. DOC-PAGE electrophoresis of the purified LPS showed a ladder banding pattern typical for smooth LPS, as compared to a standard LPS from *Escherichia coli* O55:B5 serotype (Figure 5.1).

A *Halomonas pantelleriensis* LPS

B *Escherichia coli* O55:B5 serotype LPS

Fig. 5.1. 16% DOC-PAGE on the LPS recovered after PCP extraction from *Halomonas pantelleriensis* dried bacterial cells.

The electrophoresis profile confirmed the presence of few O-chain repeating units for the LPS of *H. pantelleriensis*, as previously reported (Corsaro *et al.*, 2006).

The LPS, after reduction of the carboxylic groups with $NaBD_4$, was hydrolyzed and acetylated to give alditol acetates, the analysis of which by GC-MS revealed the presence of the sugars D-Glc, D-GlcN, L,D- and D,D-Hep, in addition to L-QuiN, D-

GlcA, D-GalNA, 4-*O*-(1-carboxyethyl)-D-GlcA belonging to the O-chain repeating unit (Corsaro *et al.*, 2006). All sugar derivatives were identified by EI-MS and GC retention times in comparison to those of authentic standards.

Methanolysis of the LPS was performed, followed by extraction with hexan in order to separate the lipidic from the saccharidic portion. The former fraction was analyzed by GC-MS revealing the presence of decanoic, dodecanoic, and 3-hydroxy-dodecanoic acids. The latter fraction was dried and acetylated to give the acetylated methyl glycosides, the analysis of which, by GC-MS, confirmed the above data.

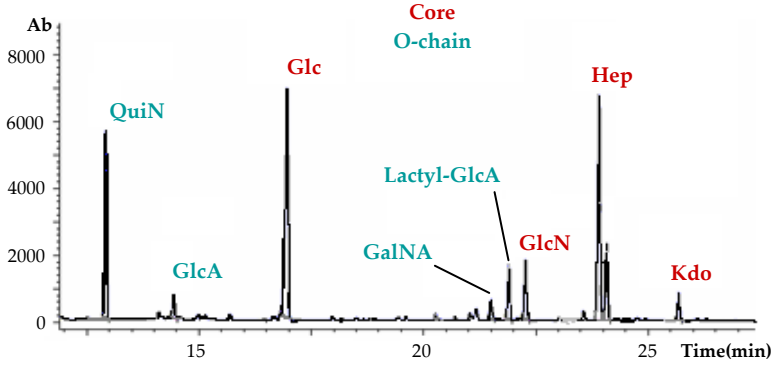

Fig.5.2 GC-MS chromatogram of the acetylated methyl glycosides derivatives

Since in untreated LPS Kdo could not be found, the LPS was first dephosphorylated with 48% aqueous HF and then subjected to methanolysis and acetylation. The thus identified Kdo suggested its phosphorylation in native LPS. In Figure 5.2 is reported the GC profile of the acetylated methyl glycosides derivatives.

5.2.2 Acid hydrolysis of the LPS.

The LPS was hydrolyzed with 1% aqueous AcOH (100°C, 6 h). The supernatant containing the oligosaccharidic portion of the LPS was fractionated on a column of Sephadex G-50 (Pharmacia). Six fractions were collected (Figure 5.3), each one containing a different number of O-chain repeating units (O-chain RU).

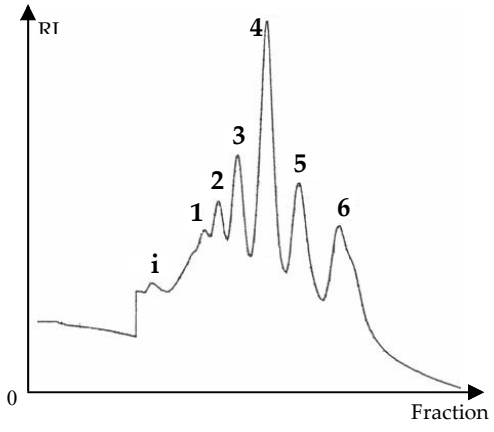

Fig. 5.3. Sephadex G50 chromatogram of the polysaccharide portion obtained after mild acid hydrolysis of the LPS from *Halomonas pantelleriensis*. Letter i indicates impurities.

The most abundant fraction was analyzed by electrospray ionization Fourier-transform ion cyclotron resonance mass spectrometry (ESI FT-ICR MS). The spectrum (Figure 5.4) showed the presence of two main peaks differing for one heptose residue at *m/z* 2506.798 and 2314.724.

Based on sugar analysis, the following composition for the oligosaccharide corresponding to the signal at *m/z* 2506.798 was deduced: (O-ChainRU)$_1$(Glc)$_3$(Hep)$_4$(GlcNAc)$_1$(Kdo)-18. The long hydrolysis time required to cleave the Kdo-lipid A linkage and the almost exclusive presence of the anhydro form of Kdo, suggested that the LPS contained Kdo4*P* (Banoub *et al*., 2004; Kondo *et al*., 1992).

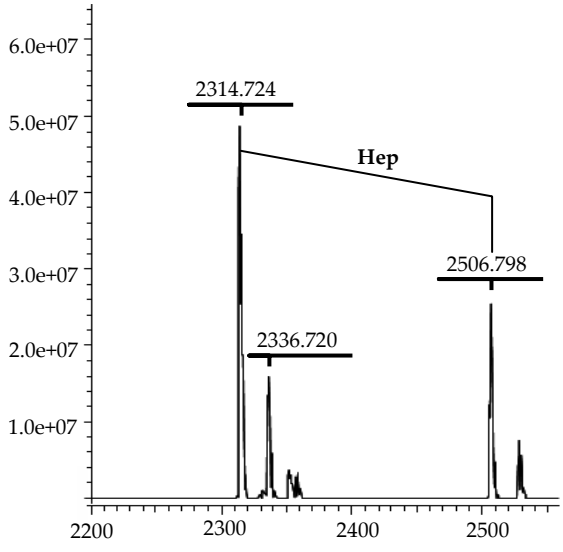

Fig. 5.4. Charge deconvoluted ESI FT-ICR mass spectrum of the main fraction isolated after Sephadex G-50 of the oligosaccharides mixture obtained after mild acid hydrolysis of the LPS from *Halomonas pantelleriensis* bacterium. The spectrum was acquired in negative ion mode.

Methylation analysis on this sample identified the substitution pattern of the core region, i.e. terminal Glc, 4-linked Glc, 6-linked Glc, terminal Hep, 2-linked Hep, 2,6-linked Hep, 7-linked Hep, 3,4-linked Hep, 4-linked GlcNAc and 3-linked QuiNAc. (Figure 5.5)

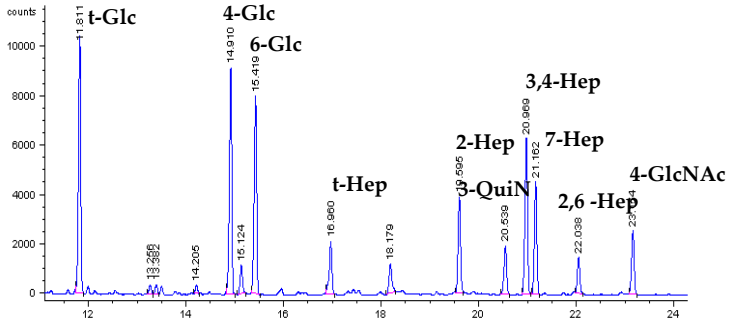

Fig. 5.5. GC-MS analysis of the partially methylated alditol acetates.

Since the ^{1}H-NMR spectrum of this fraction appeared to be very complex, the LPS was deacylated in alkaline conditions.

5.2.3 *O*-deacylation of the LPS.

O-deacylation was performed with anhydrous hydrazine, and the negative ion mode ESI FT-ICR mass spectrum of the product (LPS-OH) identified five main species (Figure 5.6). The signal at *m/z* 896.410 was attributed to the *O*-deacylated lipid A (lipid A-OH) containing two *N*-linked 3-hydroxy-dodecanoic fatty acids.

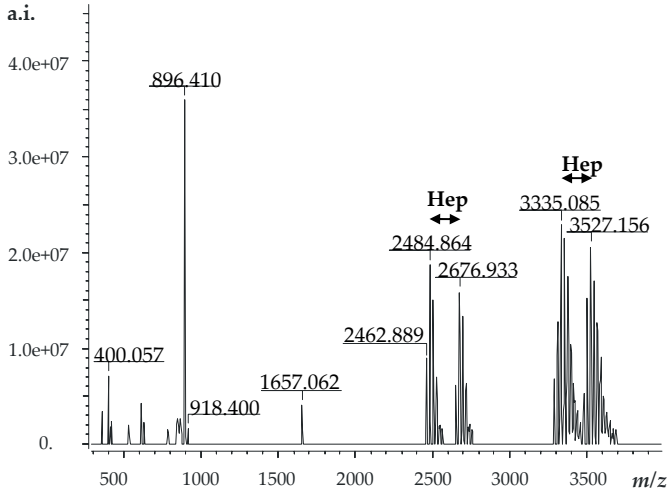

Fig. 5.6. Charge deconvoluted ESI FT-ICR mass spectrum of the de-*O*-acylated LPS from *Halomonas pantelleriensis*. The spectrum was acquired in negative ion mode.

The mass peaks with higher mass units were attributed to LPS-OH, according to the sugar composition. In particular the signal at *m/z* 2676.933 could be attributed to the mono-sodiated molecular species $(Glc)_3(Hep)_4GlcNAc(GlcN)_2KdoP_3(C12{:}3OH)_2$, according to the calculated mass of 2676.913 Da. Moreover, the signal at *m/z* 3527.156 was consistent with a LPS-OH species containing one O-chain repeating unit, as the difference to the ion at *m/z* 2676.933 corresponded to the mass of the repeating unit (828.228 Da; Corsaro *et al*., 2006). Finally the signals at *m/z* 2484.864 and 3335.085 confirmed the presence of two core glycoforms differing for one heptose unit.

The presence of 4-substituted uronic acids in the O-chain repeating units allowed the isolation of a phosphorylated core structure lacking most of the O-chain

repeating units, due to β-degradation occurring during *N*-deacylation under strong alkaline conditions with 4 M KOH.

The ESI-FT-ICR mass spectrum of deacylated LPS identified six oligosaccharides termed M^1 - M^6 (Figure 5.7), the compositions of which are summarized in Table 5.2.

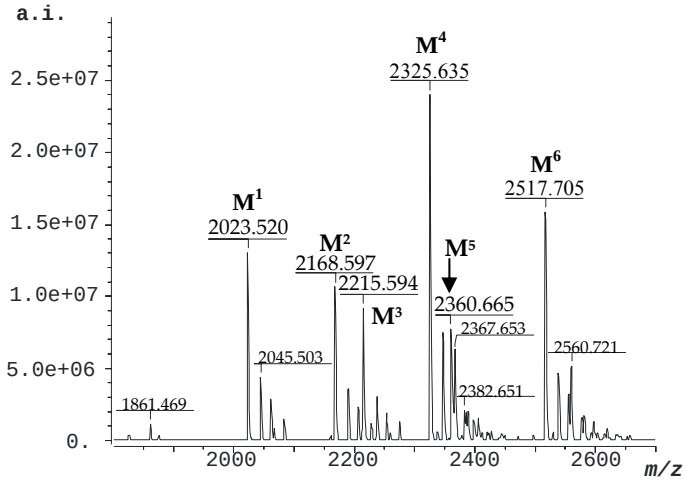

Fig. 5.7. Charge deconvoluted ESI FT-ICR mass spectrum of the fully de-acylated LPS from *Halomonas pantelleriensis*. The glycosyl composition of M^1-M^6 are reported in Table 5.2. The spectrum was acquired in negative ion mode.

Table 5.2. Composition of the main species present in the ESI FT-ICR mass spectrum of deacylated LPS from *Halomonas pantelleriensis* (Figure 5.7).

Glycoform	Observed Mass (Da)	Calculated Mass (Da)	Oligosaccaride composition
M^1	2023.520	2023.520	$(Glc)_3$ $(GlcN)_3$ $(Hep)_3$ Kdo P_3
M^2	2168.597	2168.594	QuiN $(Glc)_3$ $(GlcN)_3$ $(Hep)_3$ Kdo P_3
M^3	2215.594	2215.583	$(Glc)_3$ $(GlcN)_3$ $(Hep)_4$ Kdo P_3
M^4	2325.635	2325.631	ΔHexNA QuiN $(Glc)_3$ $(GlcN)_3$ $(Hep)_3$ Kdo P_3
M^5	2360.665	2360.657	QuiN $(Glc)_3$ $(GlcN)_3$ $(Hep)_4$ Kdo P_3
M^6	2517.705	2517.694	ΔHexNA QuiN $(Glc)_3$ $(GlcN)_3$ $(Hep)_4$ Kdo P_3

Since oligosaccharides M^4 and M^6 still possessed QuiN and a ΔHexNA, QuiN was unambiguously identified as the sugar that links the O-chain to the core region.

The oligosaccharides mixture was then partially purified by HPAEC, and the chromatogram obtained under alkaline conditions identified three fractions (Figure 5.8). ESI–FT-ICR mass spectra of these fractions (data not shown) showed that each contained two molecular species differing for one heptose, i.e. fraction A contained the two core oligosaccharides M^1 and M^3, fraction B contained M^2 and M^5 and fraction C M^4 and M^6 (Figure 5.9).

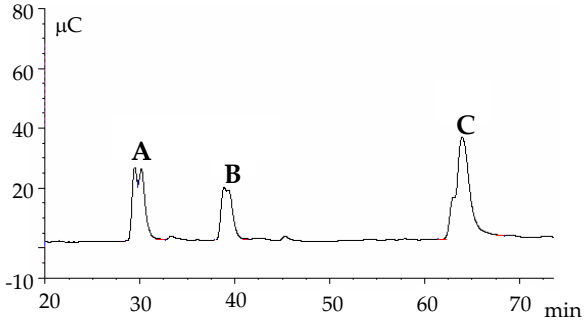

Fig. 5.8. HPAEC chromatogram of the fully de-acylated LPS from *Halomonas pantelleriensis*. Each fraction contained two specie. In particular fraction A contained M^1 and M^3, fraction B contained M^2 and M^5 and fraction C contained M^4 and M^6.

5.2.3.1 MS and NMR analysis of fraction C.

The ^{1}H-NMR spectrum of fraction C was recorded at two different temperatures in order to reduce overlapping peaks. The anomeric regions of the spectra recorded at 300 and 313 K are depicted in Figure 5.10a and 5.10b, respectively.

Besides a very minor component, there were two major species as suggested by the non-stoichiometric intensities of residues **E**, **F** and **G,** compared to the other anomeric signals. It turned out that singlet **E** was diagnostic for the amount of OS1 whereas the intensities of **F** and **G** were diagnostic for that of OS2.

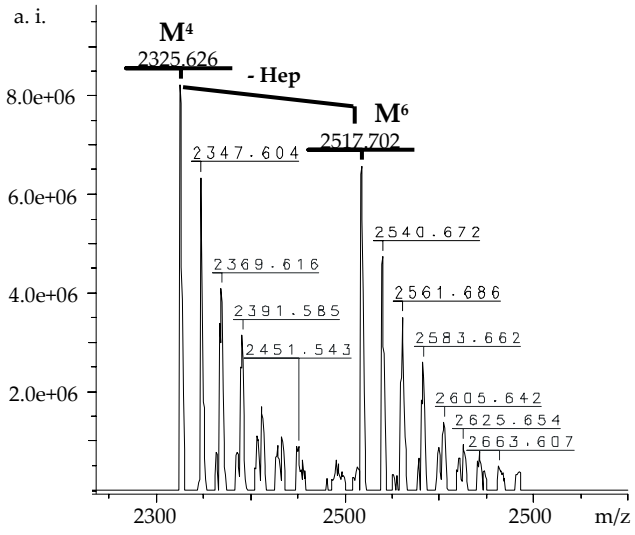

Fig. 5.9. Charge deconvoluted ESI FT-ICR mass spectrum of the fraction C. The spectrum was acquired in negative ion mode.

The anomeric regions of the proton spectra also included a downfield shifted signal at 5.86 ppm diagnostic for H-4 of a *threo*-hex-4-enuronoaminopyranose residue. 2 D-NMR spectroscopy experiments (COSY, TOCSY, ROESY, HSQC, HMBC, HSQC-TOCSY and 2D *F2*-coupled HSQC) (Tables 5.2 and 5.3) determined the complete structure of the two core oligosaccharides OS1 and OS2 as showed in figure 5.11, in which all sugars were pyranoses. Residue **A** was attributed to the 6-substituted α-Glc*p*N-1*P* residue of lipid A, based on the multiplicity of the anomeric proton signal due to its phosphorylation ($^3J_{H,P}$= 6.6 Hz), on the C-2 chemical shift at 55.4 ppm, indicating a nitrogen bearing carbon, and on the C-6 chemical shift, downfield shifted at 70.1 ppm due to its glycosylation.

Residue **B** with C-1/H-1 signals at 100.6/4.98 ppm ($J_{H-1,H-2}$ 8.4 Hz) was attributed to the 6-substituted β–Glc*p*N-4*P* residue, due to its C-2 chemical shift at 56.5 ppm and

its linkage to C-6 of **A**. This structural feature was inferred by the inter-residual connectivity between H-1 of **B** and both, C-6 and H-$6_{a,b}$ of **A** identified in the HMBC

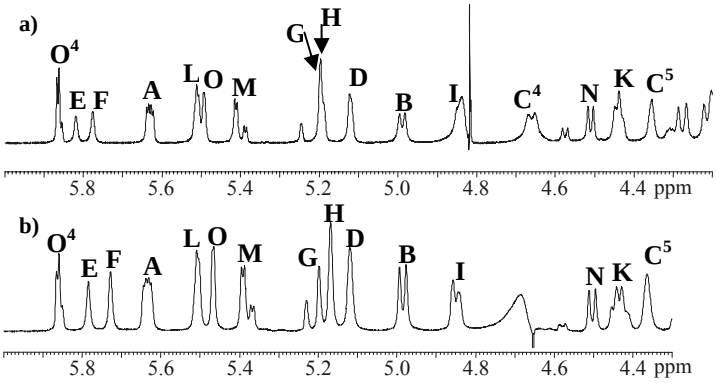

Fig. 5.10. ^{1}H-NMR anomeric region of the fully de-acylated LPS from *Halomonas pantelleriensis* performed at 300 K (a) and 313 K (b). The spectra were recorded in D_2O at 500 MHz. The letters refer to the residues as described in Table 5.3.

and ROESY experiments. Moreover the H-4 and C-4 down field shifts are diagnostic for the presence of a phosphate group linked to O-4.

Residues **D**, **E**, **F**, **G** and **H** were identified as five *manno*-configured α-heptopyranoses due to their small $^{3}J_{H\text{-}1,H\text{-}2}$, $^{3}J_{H\text{-}2,H\text{-}3}$ and $^{1}J_{C\text{-}1,H\text{-}1}$values. Downfield shifted carbon signals indicated substitutions at O-3 and O-4 of residue **D** (C-3 at 76.3 and C4 at 73.6 ppm), at O-2 of **E** (C-2 at 80.8 ppm), at O-2 and O-6 of residue **F** (C-2 at 80.8 and C-6 at 74.8 ppm), and at O-7 of **H** (C-7 at 71.3 ppm). Residue **G** was assigned to a terminal heptose unit as none of its carbons was shifted downfield. All these residues were found to be L,D-configured except **H**. For this residue, the chemical shift of its C-6 at 69.9 ppm suggested a D,D-configuration (Brisson *et al.*, 2002).

Residue **O** with C-1/H-1 signals at 99.1/5.46 ppm ($^3J_{H-1,H-2}$ 2.0 Hz) was identified as Δ-α-Hex*p*NA, according to H-4/C-4 chemical shift values in the sp^2 region at 5.86 and 108.3 ppm, respectively, and H-2/C-2 chemical shifts at 3.34/55.6 ppm.

Residue **N** with C-1/H-1 signals at 103.4/4.49 ppm ($^3J_{H-1,H-2}$ 8.8 Hz) was assigned to a 3-substituted β–L-Qui*p*N based on the TOCSY spectrum, possessing a methyl proton signal at 1.33 ppm, H-2/C-2 chemical shifts at 2.92/57.4 ppm, and a strongly downfield shifted C-3 resonance at 84.6 ppm. The other four residues, i.e. **M**, **K**, **L** and **I**, were attributed to 6-substituted α-Glc (**M**), 4-substituted α-GlcN (**L**), 4-substituted β-Glc (**K**) and terminal α-Glc (**I**), on the basis of their protons and carbons chemical shifts and their $^3J_{H-1,H-2}$ coupling constants.

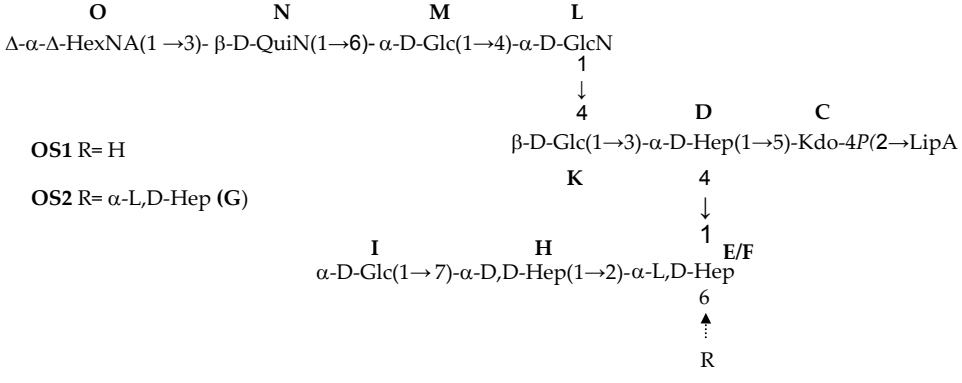

Fig 5.11. Schematic representation of OS1 and OS2 obtained from deacylation of the LPS from *Halomonas pantelleriensis*. Letters refers to residues as reported in Table 5.3

Table 5.3. ^{1}H-^{13}C NMR assignments of OS1 and OS2. All the chemical shifts values are referred to acetone as internal standard (^{1}H, 2.225 ppm;^{13}C, 31.45 ppm). Spectra were recorded at 313 K.

Residue	1	2	3	4	5	6	7	8
α-GlcN*1P*	5.63	3.36	3.89	3.43	4.17	4.26,3.89		
A	91.8	55.6	72.9	71.06	73.8	70.1		
6-β-GlcN*4P*	4.98	3.07	3.87	4.04	3.72	3.61,3.61		
B	100.6	56.5	73.8	74.0	75.3	62.5		
5-α-Kdo*4P*	-	-	1.92,2.25	4.69	4.37	3.91	3.70	3.75,3.95
C			35.9	69.3	72.6	72.9	70.6	64.9
3,4-α-Hep	5.12	4.14	4.11	3.99	nd-nd	nd-nd	3.69,3.79	nd
D	100.4	71.3	76.3	73.6			64.2	
2-α-Hep	5.72	4.14	3.91	3.92	nd-nd	4.09	nd-nd	nd
E	99.5	80.8	71.1	67.5/67.0		69.7		
2,6-α-Hep[a]	5.78	4.13	3.92	3.92	nd-nd	4.15	3.75	nd
F	99.0	80.8	71.1	67.5/67.0		74.8	62.5	
t-α-Hep[a]	5.20	3.87	4.01	3.82	3.68	nd-nd	nd-nd	nd
G	100.3	72.0	70.3	67.1	73.9			
7-α-Hep	5.17	3.98	3.68	3.77	3.77	4.22	3.80,3.84	
H	102.9	71.6	73.3	67.0	73.6	69.9	71.3	
t-α-Glc	4.85	3.72	3.61	3.49	nd-nd	nd-nd	nd	
I	100.3	73.9	70.7	70.9				
4-β-Glc	4.44	3.55	3.72	3.61	3.60	3.97,3.82		
K	103.9	74.4	71.9	79.0	76.1	62.1		
4-α-GlcN	5.50	3.31	4.08	3.71	nd-nd	nd-nd	nd	
L	98.97	55.4	71.9	78.1				
6-α-Glc	5.39	3.62	3.90	3.69	3.46	4.17,3.85		
M	101.1	72.7	73.1	70.6	70.6	69.8		
3-β-QuiN	4.49	2.92	3.75	3.34	3.54	1.33		
N	103.4	57.4	84.6	74.5	73.03	18.0		
α–ΔHexA	5.46	3.34	4.39	5.86				
O	99.1	55.6	65.9	108.3	146.0			

[a] Monosaccharides belonging to OS2
Nd: not determined

In the ^{1}H-NMR spectrum recorded at 313 K (Figure 5.10b) an additional resonance was present under the water signal which was resolved in the spectrum recorded at 300 K, and assigned to H-4 of Kdo-4*P* (residue **C**), based on the downfield shift of both, H-4 and C-4 signals at 4.69 and 69.3 ppm, respectively (Figure 5.11).

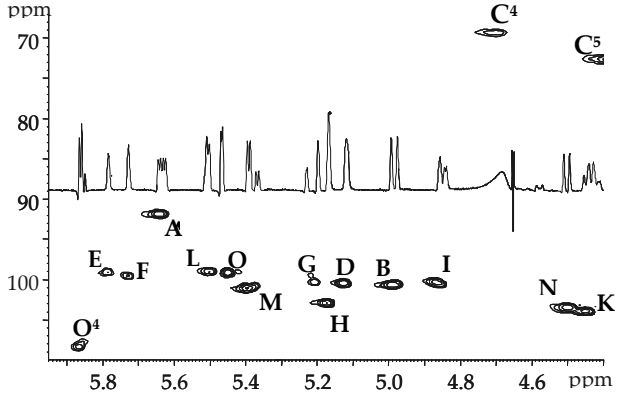

Fig. 5.11. Carbinolic region of the DEPT-HSQC spectrum of the fully de-acylated LPS from *Halomonas pantelleriensis* performed at 500 MHz in D_2O at 313 K. The letters refer to the residues as described in Table 5.3.

The monosaccharides sequences in OS1 and OS2 were deduced from ROESY (Table 5.3) and ^{1}H,^{13}C HMBC NMR experiments. Heptose **D** was linked to O-5 of Kdo unit as revealed by a strong NOE between H-1 of **D** and H-5 of **C**. Both residues **E** in OS1 and **F** in OS2 were linked to O-4 of **D** as both their anomeric proton signals gave a NOE contact with H-4 **D** at 3.99 ppm. Strong NOE contacts between H-1 **H** and both H-1 and H-2 of **E**/**F**, together with a long-range correlation between H-1 **H**/C-2 **E**/**F**, and the NOE contact H-1 **I**/H-7 **H** indicated the sequence α-Glc*p*-(1→7)-α-Hep*p*-(1→2)-α-Hep*p*. Long range scalar connectivities H-1 **K**/C-3 **D**, H-1 **L**/C-4 **K**, H-1 **M**/C-4 **L** and NOE contacts reported in Table 5.4 (Figure 5.12) allowed to assign for these residues the sequence indicated for both OS1 and OS2. Noteworthy was the NOE

contact H-1 **N**/H-6$_a$ **M** and the HMBC correlation H-1 **N**/C-6 **M** which identified the linkage between the O-chain and the core region.

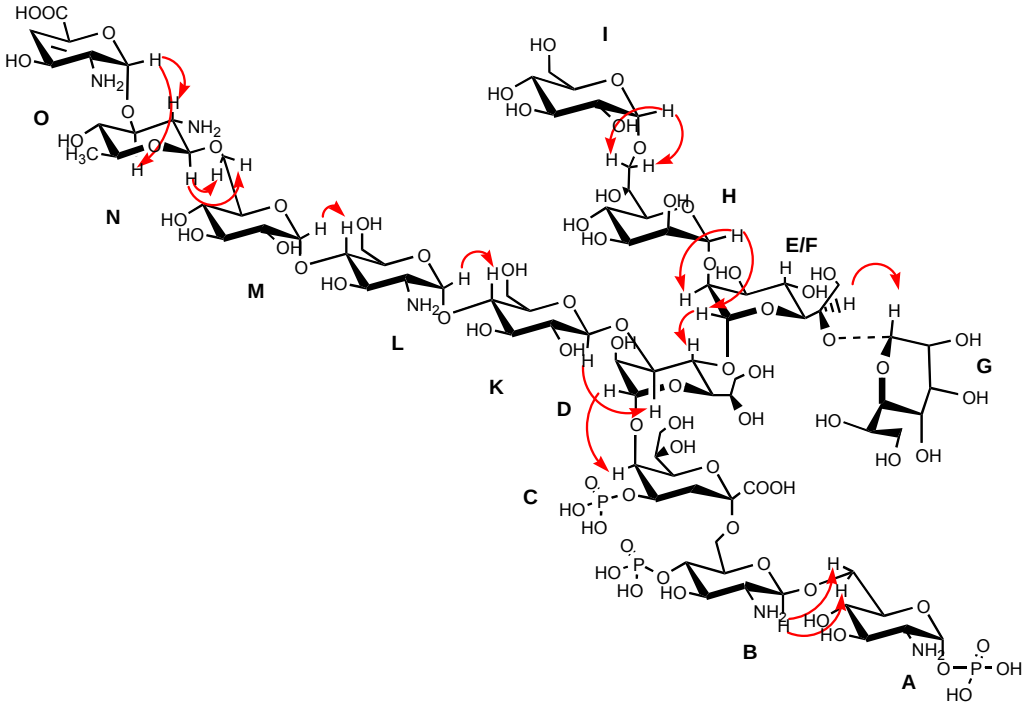

Fig. 5.12. Core oligosaccaride from *Halomonas pantelleriensis.* The NOE contacts are indicated with red arrows.

TABLE 5.4. Nuclear Overhauser enhancement inter-residual connectivities (ROESY) for the anomeric protons of OS1 and OS2.

H-1 of sugar residue	NOE correlations
GlcN **B**	**A** H-6a,b
Hep **D**	**C** H-5, H-6
Hep **E**	**D** H-4
Hep **F**	**D** H-4
Hep **G**	**F** H-6
Hep **H**	**F/E** H-1, H-2, H-3
Glc **I**	**H** H-7a,b
Glc **K**	**D** H-3, H-4
GlcN **L**	**K** H-3, H-4
Glc **M**	**L** H-3**,** H-4
QuiN **N**	**M** H-6a,b
ΔHexNA **O**	**N** H-2, H-3

5.3 Conclusions.

In conclusion, two main core oligosaccharides structures were established for *Halomonas pantelleriensis* bacterium (OS**1** and OS**2**) that differ in one heptose residue. When present, this sugar was linked to O-6 of the 2-substituted α-L,D-Hep*p*. This was proved by chemical shift values of residues **E** and **F** and from the fact that H-1 of the 7-substituted α-D,D-Hep*p* gave an intense NOE correlation with both, H-2 of the 2-substituted and the 2,6-substituted α-L,D-Hep*p* residues. Consistent with these data were the long-range scalar connectivities and the results of the methylation analysis. It is noteworthy that this investigation allowed the determination of the biological O-chain repeating unit by identifying Qui*p*NAc linked to the outer core. Finally, the occurrence in deacylated LPS of a species containing only the Qui*p*N suggested that the O-chain polysaccharide biosynthesis occurs by sequential addition of a single monosaccharide unit.

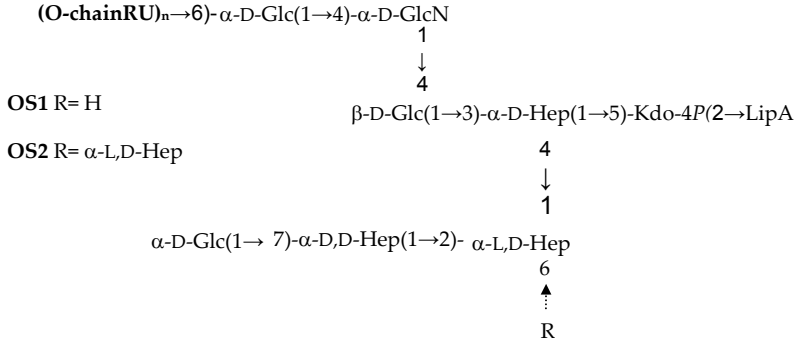

5.4 Experimental section.

5.4.1 Growth of bacteria and isolation of LPS.

Halomonas pantelleriensis (DSM 9661) was isolated from the sand of the lake Venere on the Pantelleria island in Italy (Romano *et al*., 1996) and was cultivated as reported previously (Corsaro et al., 2007).

Bacterial dried cells (11 g) were extracted using phenol/chloroform/light petroleum (2:5:8, by vol.) as described (Corsaro et al., 2006). The product (240 mg) was then incubated in 30 ml of phosphate buffer (pH 8) with RNAse and DNAse for two hours at 37°C and then with Protease K for 1 hour at 68°C, in order to purify the LPS from nucleic acids. The reaction mixture was then dyalized and lyophilyzed to yield 200 mg of crude LPS (yield 1.8% of dried cells). DOC-PAGE was performed as already reported (Galanos *et al*., 1969; Corsaro *et al*., 2006).

5.4.2 Sugar analysis.

Monosaccharides were analyzed as alditol acetates as well as acetylated methyl glycosides. Acetylated alditols were obtained from the LPS (1 mg). Briefly, LPS was treated with 0.5 M MeOH/HCl (0.5 ml, 85°C, 45 min.), and after the usual work up the methanol layer was dried and reduced with $NaBD_4$. The reaction mixture was then hydrolyzed with 2 M trifluoroacetic acid (120°C, 2 h), reduced with $NaBD_4$ and acetylated. Acetylated methyl glycosides were obtained from the crude LPS (0.5 mg). The LPS was dephosphorylated with 48% aqueous HF (4°C, 16 h) then dried under vacuum over NaOH. Methanolysis was performed in 0.5 M MeOH/HCl (0.5 ml, 85°C, 45 min) and the sample was extracted twice with hexan. The methanol layer was then dried and acetylated.

The linkage positions of the monosaccharides were determined by methylation analysis. Briefly the product obtained from acid hydrolysis of the LPS (1 mg) was reduced with $NaBH_4$. Methylation was performed with CH_3I in DMSO and NaOH (2.5 h; Ciucanu and Kerek 1984). The product was then hydrolyzed with 4 M trifluoroacetic acid (100°C, 4 h), reduced with $NaBD_4$ and then acetylated.

The absolute configuration of the sugars was determined by gas-chromatography of the acetylated (*S*)-2-octyl glycosides (Leontein *et al*., 1978).

Derivatyzed monosaccharides were analyzed on a Agilent Technologies 5973N MS instrument equipped with a 6850A gas chromatograph and a Zebron ZB-5 capillary column (Phenomenex, 30 m x 0.25 mm i.d., flow rate 1 ml/min, He as carrier gas). Acetylated methyl glycosides and alditolacetates were analysed accordingly, with the following temperature programs: 150°C for 3 min, 150°C→240°C at 3°C/min and 150°C for 3 min, 150°C→310°C at 3°C/min. For partially methylated alditol acetates the temperature program was: 90°C for 1 min, 90°C →140°C at 25°C/min, 140°C→200°C at 5°C/ min, 200°C →280°C at 10°C/min, 280°C for 10 min. Analysis of acetylated octyl glycosides was performed at 150°C for 5 min, then 150°C→240°C at 6°C/min, 240°C for 5 min.

5.4.3 Mild acid hydrolysis of the LPS.

The LPS (50 mg) was hydrolyzed with 1% aqueous CH_3COOH (5 ml, 100°C, 6 h). The obtained suspension was then centrifuged (10.000 *g*, 4°C, 30 min.). The pellet was washed twice with water and the supernatant layers were combined and lyophilized (polysaccharide, 34 mg). The precipitate (lipid A) was also lyophilized (13 mg). The polysaccharide portion was then fractionated on a column (4.9 x 700 mm) of Sephadex G-50 (superfine, flow rate 36 ml/h, fraction volume 4 ml), eluted with 0.4% pyridine-1% sodium acetate in water (v/v, pH 4.3).

5.4.4 De-acylation of the LPS.

The LPS (60 mg) was first dried over phosphorus anhydride under vacuum and then it was incubated with hydrazine (2 ml, 37°C, 1.5 h). Cold acetone was then added to precipitate the *O*-deacylated LPS. The pellet was recovered after centrifugation (4°C, 8.000 *g*, 30 min), washed 3 times with acetone and finally dissolved in water and lyophilized (35 mg).

The *O*-deacylated LPS was dissolved in 4 M KOH (1.5 ml), kept at 20-22°C under nitrogen for 15 min and then incubated at 120°C for 16 h. KOH was neutralized with 4 M HCl until pH 6 and the mixture was extracted three times with CH_2Cl_2. The water phase was recovered and then desalted on a column (1.5 x 800 mm) of Sephadex G-10 (30 ml/h, fraction volume 1 ml) eluted with 10 mM ammonium bicarbonate. The eluted oligosaccharide mixture was then lyophilized (12 mg).

5.4.5 HPAEC Analysis.

Separation of the oligosaccharides mixture obtained after deacylation of the LPS (7 mg) was performed by HPAEC-PAD on a semi-preparative column (9×250mm) of Carbopac PA-100 eluted with a gradient of 30-45% 1 M NaOAc/ 0.1 M NaOH) at 2 ml/min over 90 min to yield fraction A (0.5 mg), B (1 mg) and C (3 mg). Fractions were desalted on a column (1.5 x 800 mm) of Sephadex G-10 (30 ml/h, fraction volume 1 ml, eluent 10 mM NH_4HCO_3).

5.4.6 NMR spectroscopy.

For structural assignments 1D and 2D ^{1}H- and ^{13}C-NMR spectra were recorded at 313 K using a Varian Inova 500 spectrometer. Chemical shifts were measured in D_2O using acetone (δ 2.225 and 31.45 for proton and carbon, respectively) as internal standard. All two-dimensional homo- and heteronuclear experiments (COSY, TOCSY,

ROESY, HSQC-DEPT, HMBC, HSQC-TOCSY and 2D *F2*-coupled HSQC) were performed using standard pulse sequences available in the Varian software.

5.4.7 Mass spectrometry analysis.

FT-MS was performed in the negative ion mode using an APEX II – Instrument (Bruker Daltonics, Billerica, MA, USA) equipped with an actively shielded 7 Tesla magnet and an Apollo II ESI ion source. Mass spectra were acquired using standard experimental sequences as provided by the manufacturer. Samples (~ 10 $ng \cdot \mu l^{-1}$) were dissolved in a 50:50:0.001 (v/v/v) mixture of 2-propanol, water, and triethylamine (TEA). The latter was added step by step to exclude that pH 9 was exceeded since higher concentration of TEA might otherwise cause the cleavage of O-linked fatty acid residues. The samples were sprayed at a flow rate of 2 $\mu L \cdot min^{-1}$. Capillary entrance voltage was set to 3.8 kV, and drying gas temperature to 180°C. The spectra, which showed several charge states for each component, were charge-deconvoluted, using the xmass-6.1 software, and mass numbers given refer to the monoisotopic molecular masses. Each spectrum is an average of at least 20 transients composed of 1M data points.

References:

Adams R. L. and Russell N. J. **1992** "Interactive effects of salt concentration and temperature on growth and lipid composition in the moderately halophilic bacterium *Vibrio costicola*" *Can. J. Microbiol*. 38: 823-827.

Adinolfi M., Corsaro M. M., De Castro C., Evidente A., Lanzetta R., Mangoni L., Parrilli M. **1995** "The relative and absolute configurations of stereocenters in caryophyllose" *Carbohydr. Res.* 274: 223-232.

Alexander C. and Rietschel E. T. **2001 "**Bacterial lipopolysaccharides and innate immunity**"** *J. Endotoxin Res.* 7: 167-202.

Amor K., Heinrichs D. E., Frirdich E., Ziebell K., Jonson R. P., Whitfield C. **2000** "Distribution of core oligosaccharide types in lipopolysaccharides from *Escherichia coli*" *Infect. Immun.* 68(3): 1116-1124.

Banoub J., El Aneed A., Cohen A., Martin P. **2004** "Characterization of the O-4 phosphorylated and O-5 substituted Kdo reducing end group and sequencing of the core oligosaccharide of *Aeromonas salmonicida ssp salmonicida* lipopolysaccharide using tandem mass spectrometry" *Eur. J. Mass Spectrom.* 10(5): 715-730.

Belunis C. J., Clementz T., Carty S. M., Raetz C. R. **1995** "Inhibition of lipopolysaccharide biosynthesis and cell growth following inactivation of the kdtA gene in *Escherichia coli*" *J. Biol. Chem.* 270(46): 27646–27652.

Beveridge T. J. and Graham L. L. **1991** "Surface layers of bacteria" *Microbiol. Rev.* 55(4): 684-705.

Brisson J. R., Crawford E., Uhrín D., Khieu N. H., Perry M. B., Severn W. B., Richards J. C. **2002** "The core oligosaccharide component from *Mannheimia (Pasteurella) haemolytica* serotype Al lipopolysaccharide contains L-*glycero*-D-*manno*- and D-*glycero*-D-*manno*-heptoses: Analysis of the structure and conformation by high-resolution NMR spectroscopy" *Can. J. Chem.* 80: 949-963.

Cabeen M. and Jacobs-Wagner C. **2005** "Bacterial cell shape" *Nat. Rev. Microbiol.* 3(8): 601–610.

Caroff M. and Karibian D. **2003 "**Structure of bacterial lipopolysaccharides" *Carbohydr. Res.* 2431-2447.

Ciucanu I. and Kerek F. **1984** "A simple and rapid method for the permethylation of carbohydrates" *Carbohydr.Res.* 131: 209-217.

Corsaro M. M., Evidente A., Lanzetta R., Lavermicocca P., Parrilli M., Ummarino S. **2002 "**5,7-Diamino-5,7,9-trideoxynon-2-ulosonic acid: a novel sugar from a phytopathogenic *Pseudomonas lipopolysaccharide*" *Carbohydr. Res.* 337: 955–959.

Corsaro M. M., De Castro C., Naldi T., Parrilli M., Tomás J. M., Regué M. **2005** "^{1}H and ^{13}C NMR characterization and secondary structure of the K2 polysaccharide of *Klebsiella pneumoniae* strain 52145" *Carbohydr. Res.* 340(13): 2212-2217.

Corsaro M. M., Gambacorta A., Iadonisi A., Lanzetta R., Naldi T., Nicolaus B., Romano I., Ummarino S., Parrilli M. **2006 "**Structural determination of the O-chain polysaccharide from the lipopolysaccharide of the haloalkaliphilic *Halomonas pantelleriensis* bacterium" *Eur. J. Org. Chem.* 1801–1808.

Corsaro M. M., Gambacorta A., Lanzetta R., Nicolaus B., Pieretti G., Romano I., Parrilli M., **2007** "O-allyl decoration on alpha-glucan isolated from the haloalkaliphilic *Halomonas pantelleriensis* bacterium**"** *Carbohydr. Res.* 342: 1271–1274.

de Castro C., Lanzetta R., Molinaro A., Parrilli M., Piscopo V. **2001** "Acetyl substitution of the O-specific polysaccharide caryophyllan from the phenol phase of *Pseudomonas (Burkholderia) caryophylli*" *Carbohydr. Res.* 335(3): 205-211.

de Castro C., Molinaro A., Nunziata R., Grant W., Wallace A., Parrilli M. **2003** "The O-specific chain structure of the major component from the lipopolysaccharide fraction of *Halomonas magadii* strain 21 MI (NCIMB 13595)" *Carbohydr. Res.* 338(6): 567-570.

da Costa M. S., Santos H., Galinski E. A. **1998** "An overview of the role and diversity of compatible solutes in Bacteria and Archaea" *Adv. Biochem. Eng. Biotechnol*. 61: 117-153.

Demchick P. and Koch A. L. **1996** "The permeability of the wall fabric of *Escherichia coli* and *Bacillus subtilis*" *J. Bacteriol.* 178(3): 768-773.

Domon B. and Costello C. E. **1988** "A systematic nomenclature for carbohydrate fragmentations in FABMS/MS of glycoconjugates" *Glycoconj. J.* 5: 397-409.

Fresno S., Jiménez N., Izquierdo L., Merino S., Corsaro M. M., De Castro C., Parrilli M., Naldi T., Regué M., Tomás J. M. **2006** "The ionic interaction of *Klebsiella pneumoniae* K2 capsule and core lipopolysaccharide" *Microbiology* 152(6): 1807-1818.

Fresno S., Jiménez N., Canals R., Merino S., Corsaro M. M., Lanzetta R., Parrilli M., Pieretti G., Regué M., Tomás J.M. **2007** "A second galacturonic acid transferase is required for core lipopolysaccharide biosynthesis and complete capsule association with the cell surface in *Klebsiella pneumoniae*" *J. Bacteriol.* 189(3): 1128-1137**.**

Frirdrich E., Lindner B., Holst O., Whitfield C., **2003** "Overexpression of the *waaZ* gene leads to modification of the structure of the inner core region of *Escherichia coli* lipopolysaccharides, truncation of the outer core, and reduction of the amount of O polysaccharide on the cell surface" *J. Bacteriol.* 185(5): 1659-1671.

Frirdich E. and Whitfield C. **2005 "**Lipopolysaccharide inner core oligosaccharide structure and outer membrane stability in human pathogens belonging to the *Enterobacteriaceae*" *J. Endotoxin Res.* 11(3): 133-144.

Frirdich E., Bouwman C., Vinogradov E., Whitfield C. **2005** "The Role of Galacturonic Acid in Outer Membrane Stability in *Klebsiella pneumoniae*" *J. Biol. Chem*. 280(30): 27604–27612.

Galanos C., Lüderitz O., Westphal O. **1969** "A new method for the extraction of R lipopolysaccharides" *Eur. J. Biochem.* 9: 245-249.

Giordano A., Vella F. M., Romano I., Gambacorta A. **2007** "Structural elucidation of a novel phosphoglycolipid isolated from six species of *Halomonas* genus" *J. Lipid Res.* 48(8):1825-1831.

Gotschlich E. C., Fraserg B. A., Nishimurag O., Robbinsg J. B. and Liug T.-Y. **1981** "Lipid on capsular polysaccharides of gram-negative bacteria" *J. Biol. Chem.* 256(17): 8915-21.

Helander I. M., Vaara M., Sukupolvi S., Rhen M., Saarela S., Zähringer U., Mäkelä P.H. **1989** "rfaP mutants of *Salmonella typhimurium*" *Eur. J. Biochem.* 185(3):541-6.

Holst O. **2000** In *Bacterial Toxins: Methods and Protocols, Methods in Molecular Biology*; Ed., Humana Press: Totowa, NJ; pp.345-353.

Izquierdo L., Abitiu N., Coderch N., Hita, B., Merino S., Gavin R., Tomàs J. M., Regue M. **2002** "The inner-core lipopolysaccharide biosynthetic *waaE* gene: function and genetic distribution among some *Enterobacteriaceae*" *Microbiology* 148(11): 3485-3496.

Izquierdo L., Coderch N., Piqué N., Bedini E., Corsaro M. M., Merino S., Fresno S., Tomás J. M., Regué M. **2003** "The *Klebsiella pneumoniae wabG* gene: role in biosynthesis of the core lipopolysaccharide and virulence" *J. Bacteriol*. 185(24): 7213-7221.

Jann K., Dengler T., Jann B. **1992** "Core-lipid A on the K40 polysaccharide of *Escherichia coli* O8:K40:H9, a representative of group I capsular polysaccharides" *Zentralbl. Bakteriol.* 276 (2): 196-204.

Kaper J. B., Nataro J. P., Mobley H. L. **2004** "Pathogenic *Escherichia coli*" *Nat. Rev. Microbiol.* 2(2): 123-140.

Komuro T. and Galanos C. **1988** "Analysis of *Salmonella* lipopolysaccharides by sodium deoxycholate-polyacrylamide gel electrophoresis" *J. Chromatogr.* 450: 381-387.

Kondakov A. and Lindner B. **2005** "Structural characterization of complex bacterial glycolipids by Fourier transform mass spectrometry" *Eur. J. Mass Spectrom.* 11: 535-546.

Kondo S., Haishima Y., Hisatsune K. **1992** "Taxonomic implication of the apparent undetectability of 3-deoxy-D-manno-2-octulosonate (Kdo) in lipopolysaccharides of the representatives of the family *Vibrionaceae* and the occurrence of Kdo 4-phosphate in their inner-core regions" *Carbohydr. Res.* 231: 55-64.

Krulwich T. A. **1995** "Alkaliphiles: 'basic' molecular problems of pH tolerance and bioenergetics" *Mol. Microbiol.* 15(3): 403-410.

Leontein K., Lindberg B., Lönngren J. **1978** "Assignment of absolute configuration of sugars acetylated glycosides formed from chiral alcohols" *Carbohydr. Res.* 62*:* 359-362.

Lipkind G. M., Shashkov A. S., Knirel Y. A., Vinogradov E. V., Kochetkov N. K. **1988** "A computer-assisted structural analysis of regular polysaccharides on the basis of ^{13}C-n.m.r. data." *Carbohydr. Res.* 175: 59-75

MacLachlan P. R., Keenleyside W. J., Dodgson C., Whitfield C. **1993** "Formation of the K30 (group I) capsule in *Escherichia coli* O9:K30 does not require attachment to lipopolysaccharide lipid A-core" *J. Bacteriol.* 175(23): 7515-22.

Mayer H., Bhat R., Masoud H., Radziejewska-Lebrecht J., Widemann C., Krauss J. H. **1989** "Bacterial lipopolysaccharides" *Pure and Appl. Chem.* 61(7): 1271-1282.

McNicholas P. A., Batley M., Redmond J. W. **1987** "The reactions of 3-deoxy-D-manno-oct-2-ulosonlc acid (KDO) in dilute acid" *Carbohydr. Res.* 165: 17-22.

Münstermann M., Wiese A., Brandenburg K., Zähringer U., Brade L., Kawahara K., Seydel U.J. **1999** "Complement activation by bacterial surface glycolipids: a study with planar bilayer membranes" *Membr. Biol.* 167(3): 223-232.

Mushtaq N., Redpath M. B., Luzio J. P., Taylor. P. W. **2004** "Prevention and cure of systemic *Escherichia coli* K1 infection by modification of the bacterial phenotype" *Antimicrob. Agents Chemother*. 48: 1503-1508.

Nataro J. P. and Kaper J. B. **1998** "Diarrheagenic *Escherichia coli***"** *Clinical Microbiol. Rev.* 11: 142–201.

Nikaido H. **2003** "Molecular basis of bacterial outer membrane permeability revisited" *Microbiol. Mol. Biol. Rev*. 67: 593-656.

Ollivier B., Caumette P., Garcia J. L., Mah R. A. **1994** "Anaerobic Bacteria from Hypersaline Environments" *Microbiol. Rev.* 58(1): 27-38.

Olsthoorn M. M. A., Haverkamp J., Thomas-Oates J. E. **1999 "**Mass spectrometric analysis of *Klebsiella pneumoniae* ssp. *pneumoniae* rough strain R20 (O1-: K20-) lipopolysaccharide preparations: identification of novel core oligosaccharide components and three 3-deoxy-D-manno-oct-2-ulopyranosonic artifacts" *J. Mass Spctrom.* 34: 622-636.

Oren A. **1999** "Bioenergetic Aspects of Halophilism" *Microbiol. Mol. Biol. Rev.* 63(2): 334–348

Oren A. **2002** In *Halophilic microorganisms and their environments,* Kluwer Academic Publishers, Dordrecht.

Parker C. T., Kloser A. W., Schnaitman C. A., Stein M. A., Gottesman S., Gibson, B. W. **1992** "Role of the rfaG and rfaP genes in determining the lipopolysaccharide core structure and cell surface properties of *Escherichia coli* K-12." *J. Bacteriol*. 174(8): 2525-2538.

Pieretti G., Corsaro M. M., Lanzetta R., Parrilli M., Nicolaus B., Gambacorta A., Lindner B., Holst O. **2007** "Structural characterization of the core region from the lipopolysaccharide of the

haloalkaliphilic bacterium *Halomonas Pantelleriensis.* identification of the biological o-antigen repeating unit" *Eur. J. Org. Chem.* in press.

Pink D., Moeller J., Quinn B., Jericho M., Beveridge T. **2000** "On the architecture of the gram-negative bacterial murein sacculus" *J. Bacteriol.* 182(20): 5925-5930.

Raetz C. R. H. and Whitfield C. **2002** "Lipopolysaccharide endotoxins" *Annu. Rev. Biochem.* 71: 635-700.

Regué M., Izquierdo L., Fresno S., Jimenez N., Pique N., Corsaro M. M., Parrilli M., Naldi T., Merino S., Tomas J. M. **2005** "The incorporation of glucosamine into enterobacterial core lipopolysaccharide: two enzymatic steps are required" *J. Biol. Chem.* 280(44): 36648-36656. **(a)**

Regué M., Izquierdo L., Fresno S., Piqué N., Corsaro M. M., Naldi T., De Castro C., Waidelich D., Merino S., Tomás J. M. **2005** "A second outer-core region in *Klebsiella pneumoniae* lipopolysaccharide" *J. Bacteriol.* 187(12): 4198-4206. **(b)**

Roberts I. S. **1996** "The biochemistry and genetics of capsular polysaccharide production in bacteria" *Annu. Rev. Microbiol.* 50: 285-315.

Romano I., Nicolaus B., Lama L., Manca M. C., Gambacorta A., **1996** "Characterization of haloalkalophilic strictly aerobic bacterium isolated from Pantelleria island" *Syst. Appl. Microbiol.* 19: 326-333.

Romano I., Nicolaus B., Lama L., Travaso D., Caracciolo G., Gambacorta A. **2001** "Accumulation of osmoprotectants and lipid pattern modulation in response to growth conditions by *Halomonas pantelleriense*" *Syst. Appl. Microbiol.* 24: 342-352.

Russell N. J. **1989** "Adaptive modifications in membranes of halotolerant and halophilic microorganisms" *J. Bioenerg. Biomembr*. 21: 93-113.

Spengler B. **1997** "Post-source decay analysis in matrix-assisted laser desorption/ionization mass spectrometry of biomolecules" *J. Mass Spec.* 32: 1019-1036.

Spina E., Sturiale L., Romeo D., Impallomeni G., Garozzo D., Waidelich D., Glueckmann M. **2004** "New fragmentation mechanisms in matrix-assisted laser desorption/ionization time-of-flight/time-of-flight tandem mass spectrometry of carbohydrates" *Rapid Comm. Mass Spec.* 18: 392-398.

Straus D. C. **1987** "Production of an extracellular toxic complex by various strains of *Klebsiella pneumoniae*" *Infect. Immun.* 55(1): 44-48.

Trent M. S. **2004** "Biosynthesis, transport, and modification of lipid A" *Biochem. Cell Biol.* 82(1): 71-86.

Troy F. A. **1992** "Polysialylation: from bacteria to brains" *Glycobiology* 2: 5-23.

Tsai C. M. and Frasch C. E. **1982 "**A sensitive silver stain for detecting lipopolysaccharides in polyacrylamide gels" *Anal. Biochem.* 119(1): 115-119.

van den Burg B. **2003** "Extremophiles as a source for novel enzymes" *Current Opinion Microbiol.* 6: 213–218.

Vinogradov E. V., Müller-Loennies S., Petersen B. O., Meshkov S., Thomas-Oates J. E., Holst O., Brade H. **1997** "Structural investigation of the lipopolysaccharide from *Acinetobacter haemolyticus* strain NCTC 10305 (ATCC 17906, DNA group 4)" *Eur. J. Biochem*. 247(1): 82-90.

Vinogradov E., Cedzynski M., Ziolkowski A., Swierzko A. **2001** "The structure of the core region of the lipopolysaccharide from *Klebsiella pneumoniae* O3. 3-deoxy-alpha-D-*manno*-octulosonic acid (alpha-Kdo) residue in the outer part of the core, a common structural element of *Klebsiella pneumoniae* O1, O2, O3, O4, O5, O8, and O12 lipopolysaccharides." *Eur. J. Biochem.* 268(6): 1722–1729.

Vinogradov E., Frirdich E., MacLean L. L., Perry M. B., Petersen B. O., Duus J. O., Whitfield C. **2002** "Structures of lipopolysaccharides from *Klebsiella pneumoniae*. Eluicidation of the structure of the linkage region between core and polysaccharide O chain and identification of the residues at the non-reducing termini of the O chains" *J. Biol. Chem.* 277(28): 25070–25081.

Volk W. A., Salomonsky N. L., Hunt D. **1972** "Isolation of 4,7-anhydro- and 4,8-anhydro-3-deoxy-octulosonic acid followixg acid hydrolysis of *Xanthomonas sinensis* Lipopolysaccharide" *J. Biol. Chem.* 247(12): 3881-3887.

Vreeland R. H., Anderson R., Murray R. G. **1984** "Cell wall and phospholipid composition and their contribution to the salt tolerance of *Halomonas elongata*" *J. Bacteriol.* 160: 879-883.

Westphal O. and Jann K. **1965** "Bacterial lipopolysaccharides: extraction with phenol-water and further application of the procedure" *Methods Carbohydr. Chem.* 5: 83-91.

Whitfield C. **2006** "Biosynthesis and assembly of capsular polysaccharides in *Escherichia coli*" *Annu. Rev. Biochem.* 75: 39–68.

Williams P. and Tomàs J. M. **1990** "The pathogenicity of *Klebsiella pneumoniae*" *Rev. Med. Microbiol.* 1: 196-204.

Yethon J. A., Heinrichs D. E., Monteiro M. A., Perry M. B., Whitfield C. **1998** "Involvement of *waaY, waaQ* and *waaP* in the Modification of *Escherichia coli* Lipopolysaccharide and Their Role in the Formation of a Stable Outer Membrane" *J. Biol. Chem.* 273(41): 26310-26316.

Yethon J. A., Gunn J. S., Ernst R. K., Miller S. I., Laroche L., Malo D., Whitfield C. **2000** "*Salmonella enterica* Serovar *Typhimurium waaP* Mutants Show Increased Susceptibility to Polymyxin and Loss of Virulence in Vivo" *Infec. and Immun.* 68(8): 4485-4491.

Yethon J. A. and Whitfield C. **2001 "**Lipopolysaccharide as a target for the development of novel therapeutics in gram-negative bacteria" *Curr Drug Targets Infect Disord***.** 1(2): 91-106**.**

Young K ., **2006**. "The selective value of bacterial shape" *Microbiol. Mol. Biol. Rev.* 70(3): 660–703.